Dissertation

submitted to the

Combined Faculty of the Natural Sciences and Mathematics

of the Ruperto Carola University of Heidelberg, Germany

for the degree of

Doctor of Natural Sciences

Presented by

Eleonore Holzwart, Master of Science

born in Charvak, Uzbekistan

Oral-examination: 16th November 2018

The role of RLP44 in cell wall signalling integration and vascular cell fate determination in *Arabidopsis thaliana*

Referees: Prof. Dr. Karin Schumacher

Dr. Sebastian Wolf

# Table of contents

## Contribution to this work

The author explains that this work was written independently and only with the specified sources. The work of others has always been marked and quoted with the appropriate reference.

Indicated results are part of the manuscript, which has been submitted to PNAS with the title: "**BRI1 Controls Vascular Cell Fate in the *Arabidopsis* Root through RLP44 and Phytosulfokine Signalling**" and tracking number 2018-14434. The manuscript was provisionally accepted with minor revisions on September 8th, 2018 (Holzwart et al., in revision at PNAS).

A previous version of the publication is online available at https://www.biorxiv.org/ with the title "Integration of Brassinosteroid and Phytosulfokine Signalling Controls Vascular Cell Fate in the *Arabidopsis* Root". https://doi.org/10.1101/244749 (Holzwart et al., 2018).

Next to the author and the supervisor, the following people contributed to this work:

FRET-FLIM analysis were performed by Dr. Friederike Wanke and Nina Glöckner in the laboratory of Prof. Klaus Harter in Tübingen. The author of this thesis was involved in the cloning of the constructs, but experiments were performed in the laboratory of Prof. Klaus Harter.

Recombinant protein expression was provided by Dr. Ulrich Hohmann in the laboratory of Prof. Michael Hothorn, Geneva.
Prediction for amino acids clusters of RLP44 that could be involved in pectate binding were performed by Prof. Michael Hothorn.

## Abstract

Plants are characterized by a highly plastic development governed by the interaction with the environment. The determination of plant cell fate depends of the integration on intrinsic and extrinsic stimuli, such as clonal cell identity and positional information obtained by non-cell autonomous signals. The aim of this work is to understand how plant cells integrate signals from the cell wall with intracellular growth-regulation processes and, as a consequence, how cell behaviour is influenced. We identified the receptor-like protein 44 (RLP44) of the model organism *Arabidopsis thaliana* as a putative sensor of cell wall pectate. RLP44 balances two crucial plant developmental signalling pathways: BRASSINOSTEROID (BR) signalling, a well-characterized pathway regulating plant growth, and the PHYTOSULFOKINE (PSK) signalling pathway. Genetic and biochemical analysis reveal a connection between the three receptors RLP44, BR INSENSITIVE 1 (BRI1), and PSK RECEPTOR 1 (PSKR1). Our data supports a model in which BRI1 controls vascular cell fate through transcriptional regulation of RLP44, independent of known BR signalling outputs. In addition, we describe a new role for RLP44, balancing two signalling pathways through direct interaction with the RLKs and modulation of their interaction with the respective co-receptor. We hypothesize that the PSK pathway is crucial for determination of procambial identity. Therefore, dynamic balancing of PSK and BR signalling may be a key regulatory step of vascular development in *Arabidopsis thaliana*.

## Kurzdarstellung

Pflanzen zeichnen sich durch ihre hohe Anpassungsfähigkeit aus, die vor allem durch die Interaktion mit ihrer Umwelt bestimmt wird. Welche Art von Zellen wo in der Pflanze entsteht, hängt sowohl von intrinsischen als auch extrinsischen Signalen ab, wie zum Beispiel der Abstammung und Position der Zelle. Ziel dieser Arbeit war es herauszufinden, wie Pflanzenzellen Signale von der Zellwand mit intrazellulären Wachstumsregulationsprozessen integrieren und somit das Zellverhalten bestimmen.

Wir haben das Rezeptor-ähnliche Protein 44 (RLP44) des Modellorganismus *Arabidopsis thaliana* als möglichen Sensor für Zellwandpektat identifiziert. Darüber hinaus reguliert RLP44 zwei wichtige pflanzliche Signalwege. Einerseits den gut beschriebenen, BRASSINOSTEROID (BR) Signalweg, der das Wachstum der Pflanze reguliert, und andererseits den PHYTOSULFOKIN (PSK) Signalweg. Genetische und biochemische Analysen lassen auf eine Verbindung zwischen den drei Rezeptoren: RLP44, BR INSENSITIVE 1 (BRI1) und PSK RECEPTOR 1 (PSKR1) schließen. Unsere Daten sind kompatibel mit einem Modell, in dem BRI1 das vaskuläre Zellschicksal durch transkriptionelle Regulation von RLP44 unabhängig von dem BR-Signalweg steuert. Darüber hinaus beschreiben wir eine neue Rolle für RLP44, welches in der Lage ist, durch direkte Interaktion mit den RLKs und der Modulation ihrer Interaktion mit dem jeweiligen Co-Rezeptor, die zwei erwähnten Signalwege im Gleichgewicht zu halten. Wir vermuten, dass der PSK-Signalweg entscheidend für die Bestimmung der prokambialen Identität ist. Des Weiteren nehmen wir an, dass das Gleichgewicht zwischen der PSK- und BR-Signalkaskade ein wichtiger regulatorischer Schritt der Vaskulaturentwicklung in *Arabidopsis thaliana* ist.

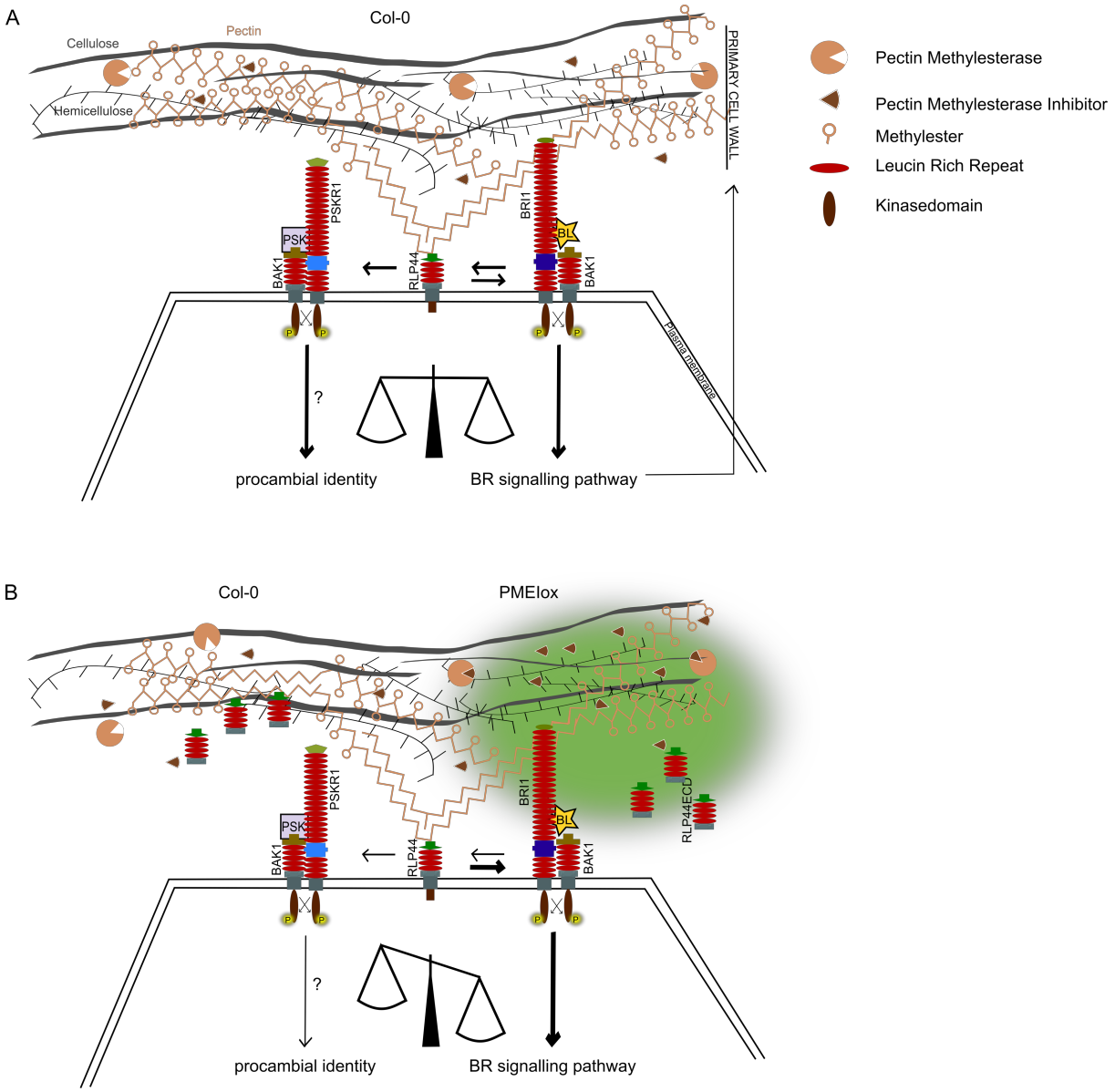


**Graphical abstract I. RLP44 balances PSK and BR signalling pathways.**
(A) The receptor like protein 44 (RLP44) is a plasma membrane (PM) localized protein and presumably senses demethylesterified pectin in the cell wall surrounding the plant cell. The BR signalling pathway is a well described signalling pathway in plants. Upon activation of the BRASSINOSTEROID INSENSITIVE 1 (BRI1) by BL, a canonical signalling cascade is initiated, and leads to the transcriptional activation of developmental processes including primary cell wall regulating enzymes. So far, the components of the PHYTOSULFOKINE (PSK) signalling pathway are unknown, apart from the PSK receptor (PSKR1), a leucine-rich repeat RLK closely related to BRI1. We show that the PSK signalling pathway regulates procambial identity. The BR and PSK pathways have in common, that both RLKs can interact with the co-receptor BRI1-ASSOCIATED KINASE 1 (BAK1). Our model suggests that RLP44 has the role of a mediator of the two signalling pathways and acts as a scaffolding protein, strengthening the respective complex formation – either BRI1-BAK1-RLP44 or PSKR1-BAK1-RLP44. Depending on cell wall changes, RLP44 maintains a balance between both pathways to secure the growth and development of the plants' vasculature. As a readout for the balance of the pathways, we identified a shift in the development of metaxylem cells.
(B) When pectin methylesterase inhibitor is overexpressed (PMEIox) RLP44ECD cannot bind. For the full length protein this could mean it is free and leads to a compensatory effect by binding to the BRI1-BAK1 complex, overactivating BR signalling (Wolf et al., 2014) and, as consequence, shifting the balance between PSK and BR signalling.

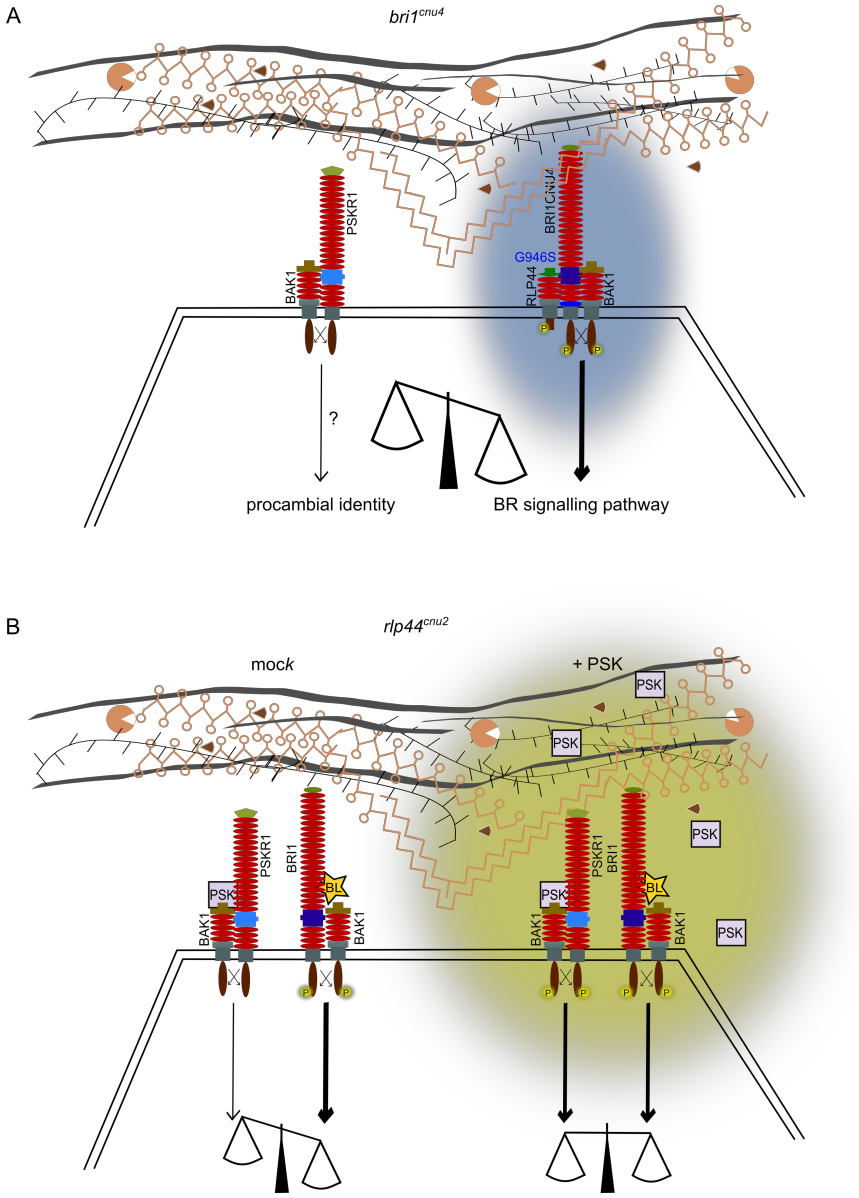


**Graphical abstract II. RLP44 balances PSK and BR signalling pathways**.
**(**A) The *bri1*$^{cnu4}$ mutant has an amino acid exchange caused by a point mutation at position 746 from glycine to serine in the BRI1 receptor. Our results indicate a sequestration of RLP44 by BRI1cnu4, caused by a stronger complex formation of BRI1cnu4-BAK1-RLP44. Therefore, RLP44 is not able to form a complex with PSKR1-BAK1, hence the BR signalling is elevated compared to PSK signalling. As a result of the imbalance between the two signalling pathways, the procambial cell identity cannot be maintained. This is evident in a disrupted xylem phenotype in about 50% of the analysed *bri1*$^{cnu4}$ seedlings with four metaxylem cells, and with some of them having a metaxylem cell in a procambial position.
(B) The *rlp44*$^{cnu2}$ mutant lacks the RLP44 receptor due to a premature STOP codon caused by a point mutation. Absence of RLP44 leads to an imbalance between PSK and BR signalling, as the mediator RLP44 between the two complexes is missing to adapt to a changing environment. As the vasculature of *rlp44*$^{cnu2}$ seedlings exhibits the same pattern in increase of metaxylem cell incidences, we conclude that PSK signalling is not able to maintain the procambial identity without RLP44. However, the exogenous application of PSK was sufficient to activate the PSKR1-BAK1 complexes to rescue the vasculature phenotype to a wildtype-like appearance.

# 1 Introduction

All organisms face the same fundamental challenges; they are constantly exposed to an ever-changing environment and therefore need to monitor these changes to be able to sense the need for adaptation. As sessile organisms, plants especially are forced to adapt to environmental changes to survive. Plant cells are surrounded by cell walls, which permit the plant, together with the inner turgor or hydrostatic pressure, to grow upright, and are also the first barrier against pathogens (Cosgrove 2005).

## 1.1 The plant cell wall

The cell wall is a chemically complex and unique extracellular matrix. It is mainly composed of polysaccharides and provides strength and rigidity while it is also dynamic and flexible, ensuring plant growth (Wolf et al., 2012). These properties have evolved conjointly with specific features to allow signal transduction to pass this flexible wall. This is on display, for example, during the finely-tuned growth process. Further complexity is added by the fact that two adjacent cells always share the same cell wall and growth has to be highly synchronized. Plant growth is based on cell wall loosening and the turgor displaces cell wall polymers. This needs to be tightly controlled, as too much loosening can lead to a burst of the cell. Thus, cell growth itself is a challenge to cell wall integrity.

### *1.1.1 Cell wall composition*

The cell wall and its extracellular surroundings, together known as the apoplast, define the extracellular space of a plant cell (Sattelmacher 2001). For a long time, the role of the apoplast was scientifically neglected. However, in the past decades, it was revealed to be a significant source for enzymes and ions, and additionally, a structural prerequisite for the survival of the plant cell. In order to accomplish these diverse tasks, the cell wall consists of multiple layers, whose composition further differs depending on developmental stage and cell type. The middle lamella is the outermost layer, followed by the primary cell wall and the secondary cell wall, which arise only in some cells, e.g. xylem, once the cell has finished growing (Cosgrove 2005). The middle lamella is deposited between two adjacent cells during cell division and essential for adhesion (Zamil and Geitmann 2017). The

primary cell wall envelops the growing cells and contributes to wall structural integrity, cell adhesion and signal transduction (Cosgrove 2005).

Pectins provide up to one third of primary cell wall dry mass (Xiao and Anderson 2013) and are a chemically heterogeneous group. They consist of four different classes of polysaccharides: homogalacturonans (HGs), rhamnogalacturonans type I (RG-I), rhamnogalacturonans type II (RG-II), and substituted galacturonans like apiogalacturonan and xyclogalacturonan (Caffall and Mohnen 2009). HG, the most prevalent pectin, is a polymer of α-1,4-linked-D-galacturonic acid residues (GalA). HG is synthesized in the Golgi apparatus and subsequently transported to the cell wall in a highly methylesterified status via secretory vesicles (Atmodjo et al., 2013). PECTIN METHYLESTERASES (PMEs) are cell wall-based enzymes and catalyse the demethylesterification of HG within the cell wall. In this chemical process, methanol and protons are released and the remaining demethylesterified HG can establish $Ca^{2+}$ bonds, which enable the formation of an egg-box structure, thus manipulating cell wall rigidity. Methylesterification is a dynamic and strictly regulated process, due to the fact that PMEs themselves are further regulated by PME INHIBITORS (PMEIs) (Pelloux et al., 2007).

Hemicellulose is a diverse mix of β-1-4-linked xylose, glucose or mannose (Scheller and Ulvskov 2010). Xyloglucans (XG) are the most common group of hemicelluloses in *Arabidopsis* primary cell walls and are synthesized in Golgi apparatus by XYLOSYLTRANSFERASES (XXT1/XXT2), precursor XGs are subsequently transported to the cell wall. In the apoplast, glycoside hydrolases modify XGs and which finally are embedded in the matrix by XG endo-transglycosyles. The *xxt1/xxt2* double mutant plant lacks XG completely, and displays a relatively mild phenotype with slightly smaller plants compared to wildtype (Cavalier et al., 2008). Depending on the chain length, XGs can bind to cellulose or be cross-linked to microfibrils to strengthen the cell wall (Hanus and Mazeau 2006; Pauly et al., 1999; Takeda et al., 2002). Pectins and hemicellulose are both soluble polysaccharides, which perfectly fit into gaps of cellulose microfibrils and further cross-link them (McFarlane et al., 2014).

Finally, cellulose, which accounts for the largest fraction of the planetary biomass, is a linear polymer of β-1-4-linked glucose and is synthesized in the plasma membrane by CELLULOSE SYNTHASE (CESA) (Somerville 2006). Pectins and Hemicellulose form

the basis of the matrix in which cellulose is embedded. For the organization of cellulose, the cortical microtubule cytoskeleton is crucial, as it guides CESA complexes (CSC) to the PM (Gutierrez et al., 2009). CSC are hexameric rosette-formed complexes composed of different CESAs. CESA1, mutants of which are embryo-lethal, and CESA3 are essential, while other CESAs are partially redundant (Gillmor et al., 2002; Somerville 2006).

The secondary cell wall (SCW) has a greater relative content of cellulose and less pectin than the primary cell wall (Caffall and Mohnen 2009). Whereas each plant cell includes a primary cell wall, SCWs are built in-between the primary cell wall and the PM only in cells which have reached their final cell size and serve a special function (Kumar et al., 2016). The main components of SCWs are cellulose, hemicellulose, lignin, and cell wall proteins. Lignin is a complex polymer consisting of phenolic monomers covalently linked to the other components in the SCW, providing strength and rigidity to the cell wall. Lignin is highly hydrophobic and thus makes the cells waterproof, which is an important characteristic of tracheary element cells, which provide the water and nutrient supply of the plant (Schuetz et al., 2012). Biosynthesis of lignin has been intensively been studied and presumably takes place after cell death (Turner et al., 2007; Liu et al., 2018).

### *1.1.2 Pectin - a supplier of cell wall state information*

Plant growth is a highly regulated process and controlled by the characteristics of the cell wall (Cosgrove 2005).

Pectins can interact with cellulose and hemicellulose, creating a complex network which is modified during the controlled growth process (Cosgrove 2005). Changes in the methylesterification go along with drastic conformational changes catalysed by PECTIN METHYLESTERASES (PMEs) directly in the cell wall. Congruent with this, various physiological processes have been reported to be dependent on HG modifications by PMEs. PMEs are under the control of PME inhibitors (PMEIs) (Pelloux et al., 2007). This fine-tuning of the pectin methylesterification state is the primary supplier to convey information of the mechanical properties of the cell wall, and thus enable adaptation to changes (Levesque-Tremblay et al., 2015). Methylesterification is important in diverse biological functions, such as shoot apical meristem pattern formation (Peaucelle et al., 2008), fruit development (Wakabayashi et al., 2003), hypocotyl growth (Derbyshire et al.,

2007; Pelletier et al., 2010), and pollen formation (Francis et al., 2006). The release of methanol and protons enable the generation of HG-$Ca^{2+}$ cross-links which, according to reports leads to increase of cell wall elasticity (Peaucelle et al., 2015; Peaucelle et al., 2011; Qi et al., 2017). Interestingly, changes of the cell wall properties are not only essential for growth processes and organ formation, but it has also been suggested that ectopic PME expression promotes patterning processes (Peaucelle et al., 2008). Furthermore, HGs, or more specifically the degradation products of HGs, can also serve as signal molecules in response to pathogen attack or auxin signals (Ridley et al., 2001; Wolf et al., 2009).

## 1.2 Cell wall signalling

Communication processes are crucial for the adaption of an organism to its surroundings and plants have implemented different strategies to arrange with the ever-changing external conditions. Cell wall signalling is required to adapt to environmental changes, in particular for sessile organisms like plants. These pathways are well described in yeast, another cell walled organism encounter difficulties to adapt to environmental changes. Fungal cell walls are essential structures to maintain shape and function, and enable environmental perception *via* various receptors. Hence, cell wall signalling in *Saccharomyces cerevisiae* (*S. cerevisiae)* is well studied, and particularly noteworthy are five cell wall-associated transmembrane sensor proteins, such as Wsc1, Wsc2, Wsc3, Mid2 and Mtl1 (Rodicio and Heinisch 2010). Developmental signals and environmental effects on the cell wall integrity activate the corresponding receptor, which then in turn induces a signal cascade. This function most likely arises from the ability to sense mechanical changes happening during cell wall deformation (Kock et al., 2015). However, in plants, this is more complex; being multicellular organisms, plant cells are tightly connected *via* their cell walls and depend on receptors to perceive information from adjacent cells as well as from the environment to coordinate growth (Cosgrove 2005). In the *Arabidopsis* genome, more than 600 Receptor-like kinases (RLK) and Receptor-like proteins (RLP) are encoded, and the largest group is composed of more than 200 members of RLKs and RLPs containing an extracellular domain with a leucine-rich repeat (LRR) (Shiu and Bleecker 2001). Other organisms with cell walls, e.g. fungi, additionally include integrity sensors, which can trigger compensatory effects based on cell wall property changes (Jendretzki et al., 2011).

### *1.2.1 Receptor-like kinases*

Receptor-like kinases (RLKs) are typically composed of an N-terminal signal peptide, an extracellular domain (ECD), a single-pass transmembrane domain (TMD), and a cytosolic protein kinase domain (Shiu and Bleecker 2001). Activation of the RLK triggers a phosphorylation cascade including phosphorylation of serine, threonine and tyrosine, leading to conformational changes (Jaillais et al., 2011; Bojar et al., 2014; Oh et al., 2009). Most RLKs form heterodimers with their co-receptors, enabling transphosphorylating and –activation (Song et al., 2017). Depending on the extracellular domain, three different classes of RLKs can be distinguished: leucine-rich repeat (LRR)-like kinase, *Cantharanthus roseus* receptor-like kinase 1-like proteins (CrRLK1L), and wall-associated kinase 1 (WAK1).

LRR-RLKs participate in numerous signalling processes, such as pathogen attack-related defence reactions or in the response to developmental cues. In most cases, RLKs seem to form heterodimers with SOMATIC EMBRYOGENESIS RECEPTOS KINASEs (SERKs) family members, fostered by ligand binding (Ma et al., 2016).

Two of the best studied LRR-RLKs are FLAGELLING-SENSING 2 (FLS2) and ELONGATION FACTOR-TU RECEPTOR (EFR); involved in detection of the bacterial elicitors flagellin and EF-TU, respectively, and initiation of the according immune response (Gómez-Gómez et al., 1999; Zipfel et al., 2006). In addition to plant defence, LRR-RLKs are also reported to sense hormones and peptides, and subsequently integrate this information enabling the plant to adapt (Ma et al., 2016). In this context some examples are important to list, like the BRASSINOSTEROID INSENSITIVE 1 (BRI1), first time described in a screen insensitive to the steroid hormone brassinosteroid, which later on was assigned as the ligand for BRI1 (Li and Chory 1997). Moreover, the signalling peptide CLAVATA 3 (CLV3) is perceived by the RLK CLAVATA 1, this interaction regulates the shoot apical meristem development (Clark et a., 1997; Brand et al., 2000). Another example is the signalling peptide PHYTOSULFOKINE (PSK) associated PSK receptor (PSKR1), described to regulate plant growth by cell elongation (Ladwig et al., 2015). In addition, organ abscission is controlled by a peptide, the RLK HAESA (HAE) perceives the peptide hormone INLFORESCENCE DEFFICIENT IN ABCISSION (IDA) as a signal to mediate floral organ abscission (Santiago et al., 2016). It is remarkable that for all

mentioned LRR-RLKs, the co-receptor SOMATIC EMBRYOGENESIS RECEPTOR KINASES (SERKs) haven been shown to be involved in receptor complex formation. There are in total five members in the SERK family and share high structural similarities (Chinchilla et al., 2009). Ligand binding of the receptor creates an interface for interaction with the co-receptor (Ma et al., 2016).

CrRLK1L is the best characterized subfamily of RLKs so far. Their ectodomain contains regions sharing homology with animal malectin, which is able to interact with diglucose motifs of N-linked oligoglycans, leading to the idea that CrRLK1L may bind to the cell wall in plants via this domain (Boisson-Dernier et al., 2011; Thomas et al., 2010). Recently, support for this hypothesis has accumulated. The PM-localized CrRLKs were described as being able to sense the cell wall state THESEUS (THE1) and FERONIA (FER) (Feng et al., 2018; Lin et al., 2018). A mutation in *THE1* can rescue a growth defect in the cellulose-deficient mutant *procuste1-1* (*prc1-1)* (Hématy et al., 2007). Interestingly, the cellulose content in the double mutant *prc1-1/the1* is comparable to the *prc1-1* single mutant, therefore, it is reasonable to suggest that the dwarf *prc1-1* phenotype is not caused by the low cellulose content, but rather dependent on a defective THE1 response to cellulose synthesis (Hématy et al., 2007). The mutation in THE1 restores growth but not the cellulose deficiency, this implies the ability of THE1 of monitoring cell wall integrity, and without this sensor no feedback is transmitted from the cell wall (Hématy et al., 2007). By now, RAPID ALKALINIZATION FACTOR (RALF) 34 has been identified as THE1 ligand (Gonneau et al., 2018).

FER is part of several different pathways, e.g. it is crucial for fertilization (Huck 2003), and interconnects with several hormonal pathways such as abscisic acid, ethylene and BR signalling (Chen et al., 2016; Deslauriers and Larsen 2010; Mao et al., 2015). Furthermore, RALF was found to bind to the ectodomain of FER and trigger phosphorylation cascades within the cell (Haruta et al., 2014). Meanwhile also the direct binding of FER to PGA was shown to maintain cell wall integrity during salt stress (Feng et al., 2018; Lin et al., 2018). ANXUR1 and 2 are the closest homologs to FER and were reported to be involved in maintaining pollen tube cell wall integrity (Boisson-Dernier et al., 2013; Miyazaki et al., 2009). There are first hints that the kinase domain of FER is not crucial to rescue the *fer*

mutant, it suggests that the cytoplasmic domain is sufficient as a kind of scaffold protein to perform the task for this specific pathway (Kessler et al., 2015).

Another class of receptors are wall associated kinases (WAKs) with having epidermal growth factor (EGF) like repeats, similar to vertebrates, in their extracellular domain. The intracellular domain has a serine/threonine kinase activity. WAKs prefer cross-linked configuration of pectate mediated by Ca2+ ions and have critical roles in overall plant developmental processes (Wagner 2001). WAK1 was shown to bind to insoluble cell wall fraction (He et al., 1996) this was confirmed 10 years later and the pectin –binding subdomain of the extracellular domain was identified and shown to interact with pectin via noncovalent binding (Decreux and Messiaen 2005).

### *1.2.2 Receptor-like proteins*

### *1.2.3 Receptor-like proteins*

As briefly mentioned above, Receptor-like proteins (RLP) are PM-localized proteins, but lack, in contrast to RLKs, kinase domains. There are 57 genes encoding for *RLPs* in the genome of *Arabidopsis* described, some of which are shown to be central in plant development. They mainly differ in their cytoplasmic domain and the number of LRR repeats in the ECD (Wang et al., 2008). It is widely accepted and supported by literature, that RLPs require complex formation with a kinase protein to trigger downstream signalling (Gust and Felix 2014).

Various RLPs take part in defence (Liebrand et al., 2014). Cf-9 and Ve1, two RLPs identified in *Solanum lycopersicum*, recognize pathogen elicitors and subsequently interact with a RLK to induce defence reactions (Jones et al., 1994; Liebrand et al., 2013). Furthermore, in *Arabidopsis*, pathogen attack triggers downstream effects transmitted through RLP3, RLP23 or RLP30 (Albert et al., 2015, Shen and Diener, 2013, Zhang et al., 2013). Similar to RLKs, RLPs can interact with SERKs, as it has been shown for RLP30 and RLP23, which form heterodimers with BAK1/SERK3 to relay the corresponding signal (Albert et al., 2015; Zhang et al., 2013). SUPPRESSOR OF BIR1-1 (SOBIR1) is a positive regulator of defence signalling and was shown to interact with several RLPs (RLP23 and RLP30) (Albert et al., 2015; Zhang et al., 2013). Interestingly, interactions

with SOBIR are constitutive, RLP-BAK1 interactions, however, is ligand-induced (Gust and Felix 2014; Liebrand et al., 2013).

In addition to pathogen response reactions, RLPs have also been described to be involved in plant development. One representative is RLP10 or CLAVATA2 (CLV2), which forms a functional unit with CORYNE (CRN), a receptor kinase able to recognize the signal peptide CLV3 (Müller et al., 2008). Furthermore, RLP17 or TOO MANY MOUTHS (TMM) forms active heteromers with an RLK of the ERECTA family to ensure correct stomatal development (Lee et al., 2012).

### *1.2.4 Receptor like protein 44*

Recently, we identified RLP44 as a suppressor of the severe phenotype caused by overexpression of *PECTIN METHYLESTERASE INHIBITOR 5* (PMEIox) (Wolf et al., 2014). PMEI5 is inhibiting PMEs, which hydrolyse the methylester groups of pectins. PMEIox plants compensate the effect on cell integrity by over-activation of BR-signalling, presumable mediated through RLP44, since with loss of RLP44, the pectin state cannot be sensed and the phenotype is rescued back to the wildtype phenotype. The suppressor mutant was named *comfortably numb 2* (*cnu2*). RLP44 at first seems like a typical member of its family, its cytoplasmic domain (CD) is only 25 AAs long and very well conserved when compared to orthologous plant proteins (Borja Garnelo Gómez 2017). However, the CD AA composition of RLP44 is predominantly basic and therefore stands out from the in general more acidic AA composition of the CD in other RLPs (Gust and Felix 2014). *In silico* analysis suggests four putative phosphorylation sites within the CD and degradation is most likely based on ubiquitination (Borja Garnelo Gómez 2017).

Presumably, phosphorylation of RLP44 occurs in a cell wall-responsive manner; however, it is not completely understood how RLP44 is regulated or which kinases are responsible. Previous research has shown that RLP44 can activate BR-signalling independent of BL-availability *via* interaction with BAK1 (Wolf et al., 2014). Overexpression of RLP44 alone induces a phenotype reminiscent of the BRI1-overexpressing phenotype such as long petioles (Wolf et al., 2014; Friedrichsen et al., 2000). However, neither the loss-of-function mutant *rlp44*$^{cnu2}$, nor the overexpression mutant RLP44ox show an altered BL-sensitivity

(Wolf et al., 2014). In conclusion, RLP44 is not part of the BR-signalling pathway itself but interacts with BAK1 to mediate the integration of the cell wall and BR signalling.

## 1.3 Brassinosteroid signalling

Brassinosteroids (BRs), as indicated by the name, were discovered in *Brassica napus*, specifically in pollen, as growth-promoting steroids. Today, the BR-signalling pathway is one of the best characterized pathways in plants (Grove et al., 1979; Mandava 1988, Belkhadir and Jaillais 2015). Many cell wall-modifying enzymes are described to be regulated by BRs, highlighting their role in cell expansion (Goda 2004). BRs occur ubiquitously in the plant, and Brassinolide (BL) is the most active form. The biosynthetic pathway of BL uses campesterol as a starting point and contains a sequence of oxidations and reductions resulting in BL (Yokota 1997). A number of enzymes involved in the BL biosynthesis have been identified, e.g. steroid hydroxylases as DWF4 (Asami et al., 2001), CONSTITUTUVE PHOTPMOHOGENIC DWAF (CPD) (Szekeres et al., 1996), and steroid reductase DE-ETIOLATED 2 (DET2) (Li et al., 1996). Interestingly, BR biosynthesis seems to be rather flexible, with the reaction catalysed by each enzyme being more important than the sequence of the reactions. Knockout of any of the enzymes leads to a BR-deficient phenotype displayed by dwarfism, darker green leaves and infertile flowers (Friedrichsen et al., 2000). With the application of propiconazole (PPZ), the endogenous BR-biosynthesis can be completely blocked, as this compound effectively inhibits the function of DWF4 (Hartwig et al., 2012). The BRASSINOSTEORID INSENSITIVE 1 (BRI1) receptor was identified in a screen for BRs-insensitive plants (Clouse 1996). BRI1 is a plasma membrane receptor-like kinase (RLK) (see chapter 1.2.1 for details). There are three BRI1 homologs, BRI1-LIKE1, BRI1-LIKE2 and BRI1-LIKE3 (BRL), however only BRI1, BRL1, and BRL3 are able to bind to BL and rescue the *bri1* mutant phenotype when expressed under control of the BRI1 promoter (Caño-Delgado et al., 2004). BRI1 consists of typical RLK domains, an ECD (built of 21 tandem amino-terminal LRRs, an island domain and four additional LRRs N-terminal of the TMD), a single-pass TMD, and a cytoplasmic kinase domain, which is essential for its function (Friedrichsen et al., 2000). Interference with BR-signalling, whether caused by deficient BL-biosynthesis or a mutation of the BRI1 receptor, leads to severe morphological, so

called BR-deficient phenotypes, such as dwarfism, male infertility, changed vascular development to mention a few (Belkhadir and Jaillais 2015). BL binds to a pocket formed by the island domain (ID) an approximately 70 AAs long stretch in the ECD of BRI1, inducing its activation. Subsequently, BRI1 KINASE INHIBITOR 1 (BKI1), which binds to the C-terminus of BRI1, is phosphorylated and released (Wang and Chory 2006; Wang et al., 2014), enabling BRI1 to interact with the co-receptor BRI-ASSOCIATED KINASE 1/SOMATIC EMRYOGENESIS RECEPTOR KINASE 3 (BAK1)/(SERK3) (Santiago et al., 2013; Sun et al., 2013). BAK1, another positive regulator of BR-signalling, is a RLK and heterodimerization of BRI1 and BAK1 leads to trans- and autophosphorylation reactions. BAK1 is described to be a co-receptor in different roles and can interact with several RLKs (Chinchilla et al., 2007; Ladwig et al., 2015). Subsequently, the activated heterodimer BRI1-BAK1 phosphorylates proteins of the receptor-like cytoplasmic kinase (RLCK) superfamily, e.g. the BRI1 SUBSTRATE KINASES (BSKs) and/or the CONSTITUTIVE DIFFERENTIAL GROWTH1/CDG-LIKE (CDG1/CDL) families (Tang et al., 2008; Kim et al., 2011; Sreeramulu et al., 2013). Thereupon, phosphorylated BSKs and CDGs are able to activate the phosphatase BRI1 SUPPRESSOR (BSU1) (Kim et al., 2009) which in turn dephosphorylates and deactivates BRI1 INSENSITIVE 2 (BIN2). BIN2 is a glycogen synthase kinase 3-like (GSK3) family member and can negatively regulate BR-signalling by phosphorylating the transcription factors (TFs) BRASSINAZOLE-RESISTANT 1 (BZR1) and BRI1-EMS-SUPPRESSOR 1 (BES1). Phosphorylated TFs are sequestered by 14-3-3 proteins in the cytosol preventing DNA-binding (Vert and Chory 2006) and targeting for degradation by the 26S-proteasome (He et al., 2002). Once Brassinosteroids are present, BIN2 is inactivated BZR1/BES1 are dephosphorylated by PROTEIN PHOSPHATASE 2A (PP2A) (Gampala et al., 2007), and can enter the nucleus to regulate BR-dependent genes (Sun et al., 2010) (Figure 1). Bikinin is a specific inhibitor of GSK3 proteins leading to activation of BR-signalling independent of BL-ligand availability downstream of the BRI1 receptor (De Rybel et al., 2009).

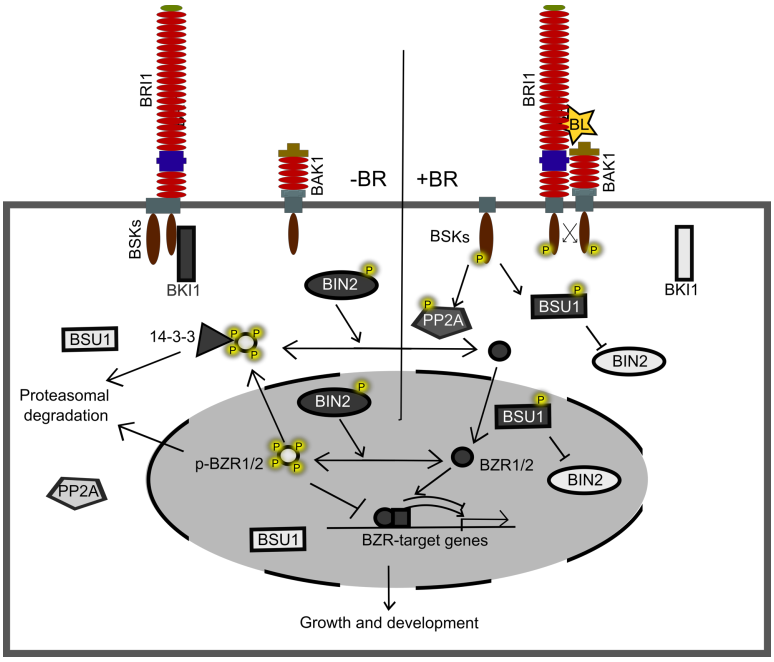


**Figure 1. Model of Brassinosteroid signalling.**
The left site of the model depicts the absence of the ligand BRASSINOLID (BL). BRASSINOSTEROID INSENITIVE 1 (BRI1) is inhibited by BRI1 SUBSTRAT KINASES (BSKs) and BRI1 KINASE INHIBITOR 1 (BKI1). THE GSK3-like kinase BRASSINOSTEROID INSENSITIVE 2 (BIN2) is phosphorylated and thereby in an active state and inactivates BRASSINAZOLE-RESISTENT 1 (BZR1) and BR-INSENSITIVE-EMS-SUPPRESSOR 1 (BES1), subsequently inhibiting the BL-signalling pathway. The phosphatase BRI1 SUPPRESSOR 1 (BSU1) is inactive and the protein 14-3-3 retains the phosphorylated TF BZR1/BES1 in the cytoplasm.
Right site shows that presence of BL activates BRI1 and leads to a trans-and autophosphorylation cascade with the co-receptor BRI1-ASSOCIATED KINASE 1 (BAK1). Activated PP2A dephosphorylates BZR1/BES1 which can then move to the nucleus to promote the BL-dependent gene transcription. Simultaneously the activated BSU1 protein inhibits BIN2 by dephosphorylation. Adapted from Kim et al., 2010.

## 1.4 Phytosulfokine signalling

More than 1000 potential plant signal peptides are thought to exist, however, only a few have been described in detail. The existing data suggest that these peptides are crucial for the coordination and securing cellular functions in multicellular organisms (Murphy, Smith, and De Smet 2012, Czyzewicz et al., 2013). Plant peptides are classified in two main groups, they either can be secreted or non-secreted. Secreted peptides again can be divided based on their structure in posttranslationally modified or cysteine-rich peptides (Matsubayashi 2014). Typical posttranslational modifications are e.g. tyrosine sulfation, proline hydroxylation, or hydroxyproline arabinosylation, and are important for the biological function of the peptide (Matsubayashi 2011). In general, posttranscriptionally modified peptides are shorter than 20 AA and the product of proteolytically processed polypeptide precursors. There are at least four classes sulfated peptides in plants –

phytosulfokine (PSK) (Matsubayashi and Sakagami 1996), plant peptide containing sulfated tyrosine (PSY) (Amano et al., 2007), root growth factor (RGF) (Matsuzaki et al., 2010), casparian strip formation integrity factor 1 (CIF1), and CIF2 (Doblas et al., 2017; Nakayama et al., 2017). Preliminary results point to interdependency of BR and PSK signalling, presenting peptides as an important tool to decipher communication processes in plants (Hartmann et al., 2013; Murphy et al., 2012). PSK is a peptide of only five AAs ($Y(SO_3H)$-I-$Y(SO_3H)$-T-Q) with two sulfated tyrosine residues and was first described as a secreted peptide in *Asparagus officinalis* cell culture, where it induces cell proliferation (Matsubayashi and Sakagami 1996). In *Arabidopsis*, all sulfation reactions are catalysed by TYROSYLPROTEIN SULFOTRANSFERASE (TPST) in the Golgi, which is involved in a variety of processes (Komori et al., 2009). The proteolytic processing of the sulfated preproteins in the apoplast is believed to involve subtilases and other, unknown proteases (Srivastava et al., 2008). Subsequently, the mature PSK peptide is perceived by PHYTOSULFOKINE RECEPTOR 1 and 2 (PSKR1/PSKR2). PSKR1/2 are LRR-RLKs, with 21 LRRs in which a 36 AAs long island domain is at position LRR18, the binding site of PSK (Shinohara et al., 2007). PSK stabilizes the interaction of PSKR1 with SERKs, reminiscent of the interaction between BRI1 and BAK1 supported by BL (Wang et al., 2015). However, subsequent to receptor activation, no information regarding the downstream signalling pathway is published yet. The current literature provides data concerning PSKR1 binding to calmodulin, which is as essential as the kinase activity for the functionality of the protein (Hartmann et al., 2014). Additionally, PSKR1 has been described to be co-expressed with the cyclic nucleotide-GATED channel gene (CNGC17), however, they are not directly interacting. Instead, CNGC17 can interact with BAK1, indicating a cGMP-depending downstream effect (Ladwig et al., 2015).

Until now, the effect of PSK on root elongation based on promotion cell expansion, on tracheary differentiation, and on defence responses has been described (Kutschmar et al., 2009; Matsubayashi et al., 1999; Igarashi et al., 2012). Exogenously applied PSK promotes root growth by around 10% compared to mock-treated control plants (Hartmann et al., 2013). Mutants affected in either PSK receptors or in TPST exhibit phenotypical growth defects (shorter roots and smaller plants) (Hartmann et al., 2013). PSK receptor mutants cannot sense PSK supply (Kutschmar et al., 2009), whereas the *tpst-1* mutant phenotype

can be partially restored by the addition of PSK, and completely restored by simultaneous application of PSK, PSY and RGF (Matsuzaki et al., 2010).

Overexpression of PSKR1 leads to longer roots and hypocotyls compared to the wildtype and expression of the PSKR1 transgene in the epidermis was sufficient to rescue the mutant phenotype, arguing for a non cell-autonomous mode of action (Hartmann et al., 2013).

The BR-regulated TF ETHYLEN RESPONSE FACTOR 115 (ERF115) is present in the quiescent centre (QC) and regulates the QC cell division. ERF115 was shown to transcriptionally regulate PSK5, one of the five PSK precursor-encoding genes in *Arabidopsis.* Transcription of both, *ERF115* and *PSK5* is elevated upon BL treatment (Heyman et al., 2013; Ladwig et al., 2015). Beyond that and the structural similarities between BRI1 and PSKR1, PSKR1 is also able to interact with the same co-receptor BAK1, suggesting once more a possible crosstalk between BR- and PSK-signalling (Ladwig et al., 2015; Wang et al., 2015).

## 1.5 Xylem development and the influence of plant peptides

The *Arabidopsis* root is characterized by precisely determined and structured tissues. The vascular tissue in the centre of the root is crucial for the survival of the plant and is a prerequisite for the evolutionary success of vascular plants. It provides the plant with water and nutrients, and mechanically supports vertical growth (Lucas et al., 2013). In *Arabidopsis* primary roots the composition of the vascular tissue is set precisely with five metaxylem cells in one axis, surrounded by the procambium in which the phloem cells are arranged on both sides, and finally surrounded by one layer of pericycle cells (Figure 2) (De Rybel et al., 2015).

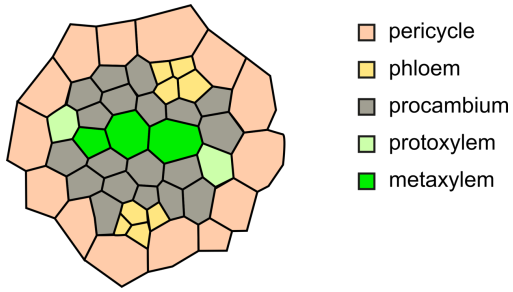


**Figure 2. Cross section of a differentiated *Arabidopsis thaliana* root.**

Xylem tracheary elements have lignified secondary cell wall thickenings, which enable the distinction between protoxylem and metaxylem. Metaxylem cells are characterized by pitted thickenings, while protoxylem can be distinguished by circular and spiral thickenings. Xylem is responsible for the water transport, phloem for nutrient distribution, and the procambium serves as a source for phloem and xylem cells during secondary (lateral) growth.

Secondary growth derived cells produced in the cambial meristem obtain the xylem cell fate dependent on positional information, but primary xylem cell fate is formed in the early embryo (Baum et al., 2002). How is this specific pattern formed?

The formation of the vascular tissue is highly organized and is already set up early in the globular stage of the embryo and determines vascular pattern for the postembryonic growth. Xylem, phloem and procambium of the root and hypocotyls arise from several periclinal divisions of four initial provascular cells (Scheres et al., 1994). PIN-FORMED (PIN) family auxin transporters are enriched in two provascular initial cells, leading to a local increase of auxin which activates AUXIN RESPONSE FACTORS (ARFs) (Friml et al., 2003). MONOPTEROS (MP/ARF5) is a crucial transcription factor (TF) for initiation of the vascular formation in the embryo, as *mp* mutants exhibit a phenotype in the early embryo (Hardtke and Berleth 1998). TARGET OF MONOPTEROS 5 (TMO5) and LONSESOME HIGHWAY (LHW), two basic helix-loop-helix transcription factors are expressed in the two mentioned provascular initial cells, which receive more auxin. (Ohashi-Ito and Bergmann 2007; Schlereth et al., 2010). TMO5-LHW heterodimers cause periclinal cell divisions during embryogenesis (Ohashi-Ito et al., 2013; De Rybel et al., 2013). LONELY GUY 4 (LOG4), a direct transcriptional target of the TMO5/LHW dimer, is a biosynthetic enzyme in Cytokinin (CK) biosynthesis. CK channels auxin to the xylem precursor cells via regulation of the PIN proteins. Furthermore, auxin induces ARABIDOPSIS HISIDINE PHOSPHATRANSFERASE PROTEIN 6 (AHP6), another MP target gene, and also a CK signalling inhibitor (Bishopp et al., 2011), leading to protoxylem differentiation (Figure 3A). Is the perception of cytokinin inhibited, for instance through a mutation of the cytokinin receptor ARABIDOPSIS HISTIDINE KINASE (AHK4) in *wooden leg* (*wol*) and has reduced periclinal divisions and all cell files differentiate to protoxylem cells (Mähönen et al., 2006). Taken together CK is a critical

hormone, and the mutual antagonism of auxin and cytokinin signalling sets the boundaries for vascular patterning. CK inhibits protoxylem formation, but promotes periclinal divisions. Two TF AT-HOOK MOTIF NUCLEAR LOCALIZED 3 (AHL3) and AHL4 regulate the vascular tissue boundaries between xylem and procambium, as mutants show ectopic expression of xylem cell within the procambium. Their expression overlaps with high CK levels and AHLs were shown to be CK-inducible (Zhou et al., 2013), but mutants are still CK-responsive (Figure 3B). Auxin also induces class III homeodomain leucine zipper (HD-ZIP III) genes as *ATHB8*, *PHABULOSA* (*PHB*), *PHAVOLUTA* (*PHV*), *REVOLUTA* (*REV*) and *ATHB15* (Donner et al., 2009; Ursache et al., 2014). HD-ZIP III are also targeted by miR165 and miR166, which are mobile small miRNAs (Carlsbecker et al., 2010). miRNA165/166 expression it initiated in the endodermis by SCARECROW (SCR), once SHORTROOT (SHR) is available, since it is only expressed in the in the stele. miR165/166 move into the stele and consequently a gradient of HD-ZIPIIIs is induced. High levels in HD-ZIPIII lead to metaxylem cells, whereas low levels of HD-ZIPIII promote protoxylem cell formation (Figure 3C) (Carlsbecker et al. 2010; Helariutta et al. 2000; Laurenzio et al. 1996).

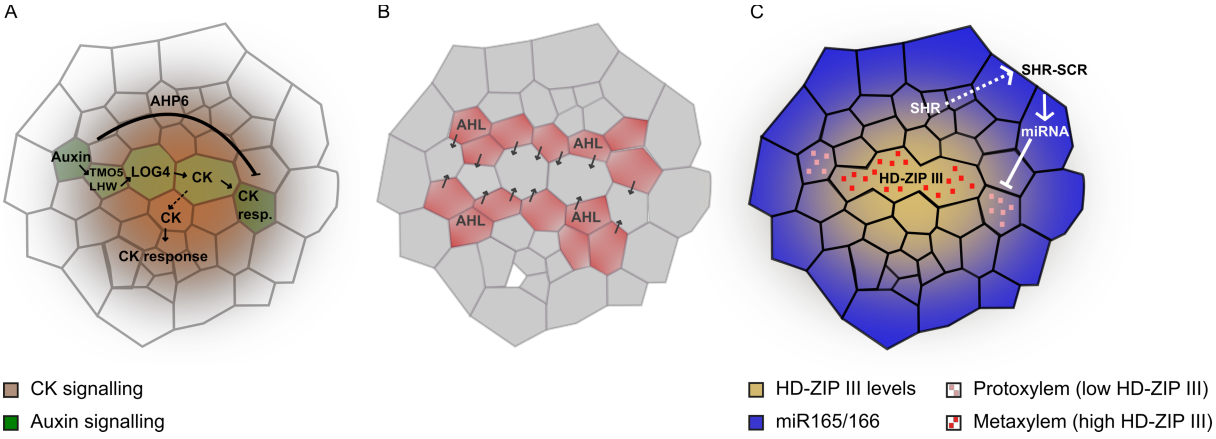


**Figure 3. Model for early vascular development.**
(A) Induced by auxin (green), TAGET OF MONOPTEROS 5 (TMO5) and LONESOME HIGHWAY (LHW) form a dimer and activate LONELY GUY 4 (LOG4) to control growth and vascular development. Local production of CK (brown) initiates periclinal divisions in the procambial cells. ARABIDOPSIS HISTIDINE PHOSPHOTRANSFER PROTEIN 6 (AHP6) is an auxin induced negative regulator of CK-signalling.
(B) A strict boundary between procambial and xylem cells is maintained by the expression of AT-HOOK MOTIF NUCLEAR LOCALIZED (AHL) in the procambial cells which then move towards the xylem axis. (C) Metaxylem and protoxylem cell identity is conducted by different HD-ZIP III TF levels. SHORTROOT (SHR) – SCARECROW (SCR) dimer induces miR165/miR166 production which regulates xylem identity by inhibiting the HD-ZIP III TF family leading to different TF levels. Adapted from De Rybel et al. 2015

Moreover, in the hypocotyl, CLAVATA3/ EMBRYO SURROUNDING REGION (CLE) peptide signalling is involved in vascular differentiation. *CLE41* and *CLE44,* encoding TRACHEARY ELEMENT DIFFERENTIATION INHIBITORY FACTOR (TDIF) are expressed in the phloem to repress xylem differentiation. Peptides are perceived in the procambium through LRR PHLOEM INTERCALATED WITH XYLEM (PXY) (Hirakawa et al., 2008) and actives the GSK3 family proteins to repress BES1/BZR2 TF and subsequently inhibit xylem differentiation (Kondo et al., 2014). However, relevance has not been shown in roots, so far.

An essential part of the vascular differentiation is the deposition of the SCW, a highly regulated process. VASCULAR-RELATED NAC DOMAIN (VND) proteins are involved in the SCW biosynthesis and programmed cell death to consequently initiate xylem differentiation (Kubo et al., 2005). VND6 expression defines metaxylem and VND7 protoxylem formation. MYBs are direct targets of VND6/7 and promote expression of biosynthetic genes, necessary for SCW construction (Ohashi-Ito et al., 2010; Yamaguchi et al., 2011). Additionally, it was shown in *Zinnia* cell culture that BRs can promote xylem differentiation, suggesting a physiological connection (Yamamoto et al., 1997). Thus, inhibitors of BR biosynthesis such as uniconazole and brassinazole inhibit xylem differentiation, which in turn can be rescued by exogenous application of BL (Iwasaki and Shibaok 1991). Supporting information for the impact of BRs on vasculature development is provided by the increased levels of five different BRs during transition from undifferentiated cells to tracheary elements (Yamamoto et al., 2001). In addition, it has been described that BR-signalling influences the formation of vascular bundles in *Arabidopsis* (Caño-Delgado et al., 2004; Ibañes et al., 2009). Furthermore, it was reported that PSK promotes the differentiation of mesophyll to tracheary cells in asparagus cell cultures (Matsubayashi et al., 1999). BR- and PSK- signalling have already been studied for interdependency, and these and further data suggest that PSK-signalling is BR-dependent (Hartmann et al., 2013).

## 1.6 Final destination: how a cell gets is identity

Plants grow throughout their whole life and permanently develop new organs. Therefore, for longitudinal growth, two primary meristems, the root apical meristem (RAM) and the

shoot apical meristem (SAM), provide a source for pluripotent stem cells. The (pro)cambium is part of the vascular tissue and deliver cells to maintain radial growth. The root of *Arabidopsis* represents an ideal model to study plant cell fate determination, due to its stereotypical development, amenability to imaging, and ease of handling. Transverse sections of the root reveal the stable composition of the cell architecture (Dolan et al., 1993). Longitudinally, the primary root is subdivided into four main zones: the meristematic zone (1), characterized by small, actively dividing cells, adjacent the transition zone (2) with slow cell growth and cells still able to divide. Meristematic cells are displaced into the elongation zone (3), in which cells quickly elongate and, once they reach their final size, enter the differentiation zone (4) with fully differentiated cells (Figure 4) (Verbelen et al., 2006).

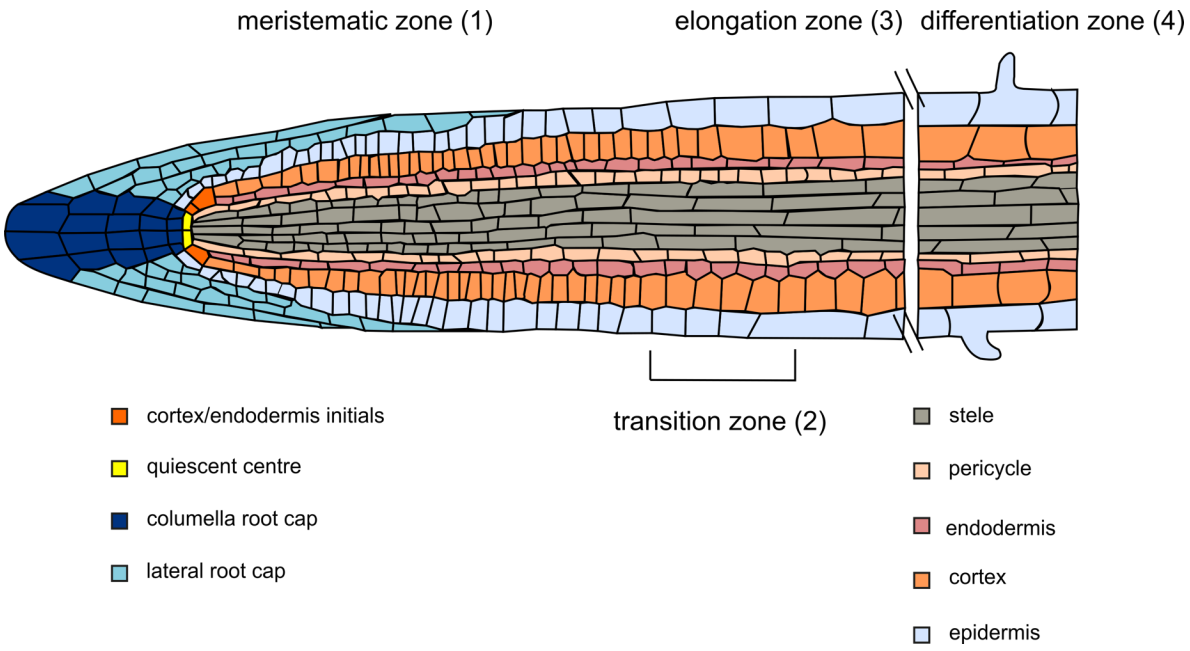


**Figure 4. Model of the *Arabidopsis* root zones**. Apapted from De Smet et al., 2015

Cells progress through each of the four well-defined zones accompanied by distinct alterations of the cell wall (Verbelen et al., 2006). Multiple studies indicate root cell fate to be dependent on positional information and not on lineage, as it has been described for animals (Kidner et al., 2000). Already more than 20 years ago, laser ablation experiments have shown that cells can switch their fate as a reaction to changing positional information

(Van den Berg et al., 1995). Furthermore, clonal analysis of the *Arabidopsis* root revealed that the offspring of one single cell can result in up to five different cell fates (Kidner et al., 2000). In addition, a trans-differentiation protocol has been established in *Zinnia elegans* cell cultures, exhibiting the de-differentiation of single mesophyll cells by loss of their photosynthetic capacity and subsequent differentiation into tracheary elements (Fukuda 1997). This trans-differentiation approach facilitated studies to elucidate the roles of auxin and cytokinin in controlling vascular morphogenesis (please see 1.5 for more details). In conclusion, plant cell fate is mainly determined by the relative position within a tissue and hormonal signals perceived from the surrounding cells. Trans-differentiation strikingly demonstrates how plastic cell fate is, thus we must postulate a mechanism that continuously senses exogenous positional signals and integrates them to control proliferation, growth and differentiation.

## Aims of this study

The integration of extracellular signals with intracellular growth regulation is crucial for the development of multicellular organisms. Communication from the outside to the inside of a plant cell is pivotal for the whole organism to adapt to the environment. This implies that the plant has to assess all the external information, convey an appropriate answer, and continuously adapt post-embryonic growth. In line with this, a high number and diversity of PM-localized receptors has been identified. Recently, we characterized the receptor-like protein 44 (RLP44) as a suppressor of a cell wall modified mutant and assume it has a role in signal transduction.

The aim of this work is to understand the function of RLP44 in cell wall signal transduction. Thus, our objectives are:

- Deciphering the role of RLP44 in sensing cell wall changes and downstream signalling activation.
- Investigating the physiological role of this signalling module.

# 2 Results

## 2.1 RLP44 can interact directly with BRI1

The plant cell wall is a highly complex structure, composed of polysaccharides, proteins, and other polymers like lignin, suberin or cutin (Cosgrove 2005). In the *Arabidopsis PECTIN METHYLESTERASE INHIBITOR 5 OVEREXPRESSING* (PMEIox) mutant, pectin manipulation leads to the loss of cell wall integrity and to a compensatory response by brassinosteroid (BR) signalling (Wolf et al., 2012). PMEIox seedlings show a severe root waving phenotype, whereas adult plants display curled leaves, convoluted shoots, misshapen siliques, and organ fusions (Wolf et al., 2014). To better understand how the changes in the cell wall could influence the development, an ethyl methanesulfonate (EMS) mutagenesis screen had been performed previously. In this forward genetic screen, we identified a mutant of RECEPTOR-LIKE PROTEIN44 (RLP44) as a suppressor of the PMEIox phenotype. It has been demonstrated, that RLP44 forms a complex with BRI1 and its co-receptor BAK1 and additionally split ubiquitin data supported the direct interaction with BAK1 (Wolf et al., 2014). Overexpression of RLP44 activates BR-signalling (Wolf et al., 2014). The observation that overexpression of RLP44 in a BR hypomorphic mutant does not rescue the BR insensitivity of the mutant (Wolf et al., 2014), suggested that RLP44 acts either upstream or together with BRI1. Therefore, we wanted to further analyse the interaction of RLP44 and BRI1. The presence of BRI1 in immunoprecipitates of RLP44-GFP in transiently expressing *N. benthamiana* leaves indicates complex formation (Figure 5A). Similar results were also obtained in the pRLP44:RLP44-GFP (*rlp44*$^{cnu2}$) line, where the presence of BAK1 and BRI1 in immunoprecipitates of RLP44-GFP was detected (Garnelo Gómez 2017).

In cooperation with Friederike Ladwig and Klaus Harter, we were able to show the direct interaction of BRI1 and RLP44 in a mating-based split ubiquitin assay in yeast (data not shown, part of Holzwart et al., in revision). The results are consistent with those already published for the interaction between RLP44-BAK1 and BAK1-RLP44 (Wolf et al., 2014). In addition, Foerster resonance energy transfer and fluorescence lifetime imaging microscopy (FRET-FLIM) analysis after transient expression of 35S:BRI1-GFP and

35S:RLP44-RFP constructs in *N. benthamiana* leaves confirmed interaction of BRI1 and RLP44 (Figure 5B). Moreover, a bimolecular fluorescence complementation analysis independently confirmed the direct interaction of RLP44 and BRI1 (Garnelo Gómez 2017). Thus, several different approaches confirmed the direct interaction of RLP44 with BRI1.

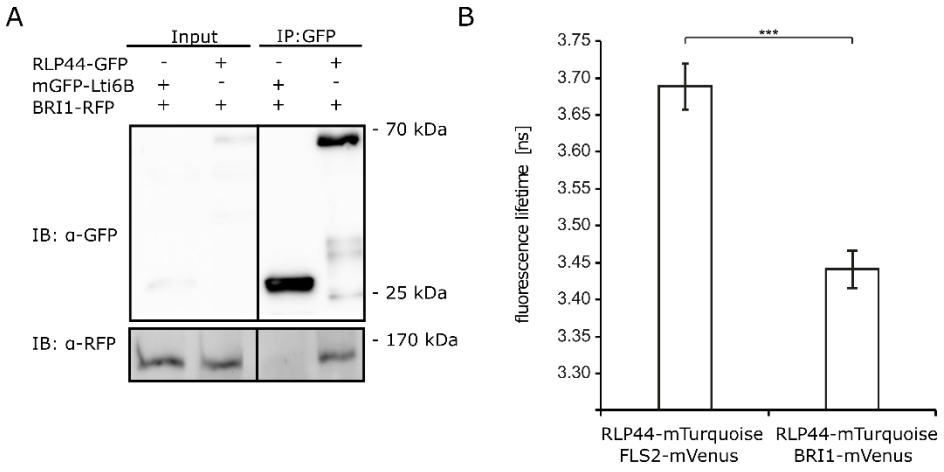


**Figure 5. RLP44 is directly interacting with BRI1.**
(A) Co-immunoprecipitates reveal complex formation of BRI1 with RLP44-GFP. BRI1-RFP is detected in immunoprecipitates of RLP44-GFP but not in the immunoprecipitates of mGFP-Lti6B.
(B) FRET-FLIM analysis in *N. benthamiana* leaves of RLP44-mTurquoise and BRI1-mVenus. FLS2 is used as a negative control. Bars stand for an average of five measurements ±SD (n=11). Asterisks indicate statistically significant differences in mean fluorescence lifetime t-test (***p < 0.001). FRET-FLIM constructs were cloned by Eleonore Holzwart, the measurements were performed by Nina Glöckner. This graph is part of Holzwart et al., in revision.

## 2.2 RLP44 cytoplasmic domain is able to co-immunoprecipitate BRI1

The leucine-riche repeat region is a motif apparent in the extracellular domain of RLK. It is described that the domain is an important platform for interaction with ligands and/or co-receptors (Zhang et al., 2016). Based on previous publications, we hypothesized that RLP44ECD is responsible for protein-protein interactions (Jaillais et al., 2011; Santiago et al., 2013; Smakowska-luzan et al., 2018). According to results using isothermal titration calorimetry perfomed by Ulrich Hohmann (data not shown) the RLP44ECD peptide expressed in insect cells showed no binding to the preformed BRI1-BL-BAK1 complex. Furthermore, another method to study interactions, the analytical gel filtrations was used to test, if RLP44ECD interacts directly with a BRI1-BL-BAK1 complex, only BRI1±BL, and BAK1. Here, we should also consider that it may not have been possible to detect interactions with these *in vitro* techniques, as co-factors present *in planta* may be required.

However, no interaction with any of the tested proteins was shown with the RLP44ECD domain with neither these techniques, nor in co-immunoprecipitation approaches in transiently overexpressed *N. benthamiana* leaves. We decided to dissect the RLP44 protein and analyse also its other domains, and were able to identify that the cytosolic domain of RLP44 (from hereon named RLP44CD) was sufficient to form a complex with BRI1 (Figure 6). The cytosolic domain is highly conserved in RLP44 orthologous across the plant kingdom and can be phosphorylated, which suggesting it interacts with a kinase (Garnelo Gómez 2017). A first approach to complement the *cnu2* mutant with the RLP44CD construct showed no reconstitution of the PMEIox phenotype (data not shown).

To sum up, the truncated RLP44CD is a short, very conserved domain, which is able to form a complex with BRI1 when transiently overexpressed in *N. benthamiana* leaves.

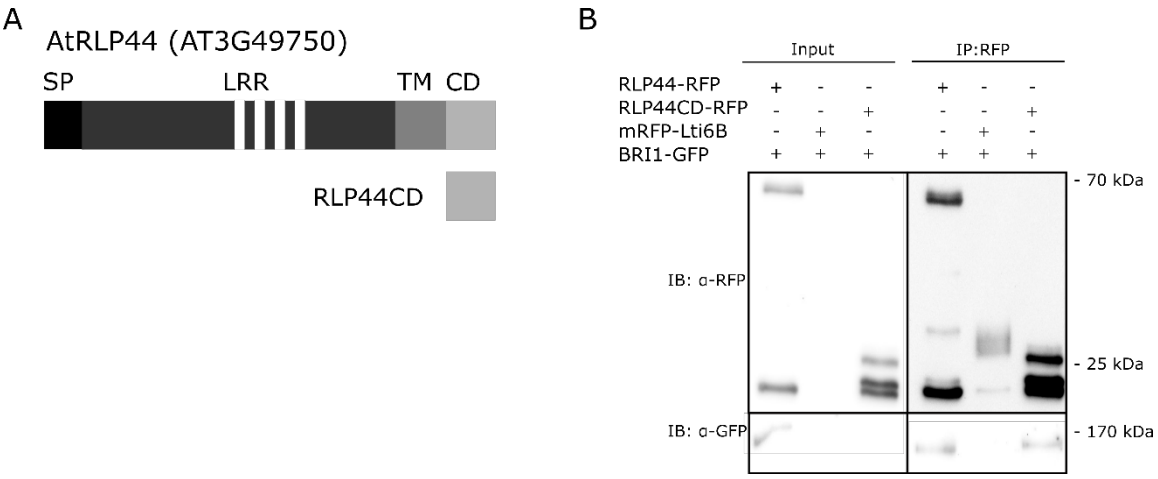


**Figure 6. RLP44 cytoplasmic domain is sufficient to form a complex with BRI1.**
(A) Structural features of RLP44 protein.
(B) Co-immunoprecipitation shows that RLP44CD and BRI1 are in a complex when transiently co-expressed in *N. benthamiana* leaves. BRI1-GFP protein is detected in the immunoprecipitates of RLP44-RFP and RLP44CD-RFP.

## 2.3 RLP44 extracellular domain can associate with the cell wall

RLP44 was characterized as a plasma membrane-localized protein, composed of an extracellular domain (ECD) with an N-terminal signalling peptide, four leucine rich repeat regions (LRRs), a single transmembrane domain (TMD) and a short cytosolic domain (CD) (Figure 7A). Based on the discovery of RLP44 in a cell wall mutant, we decided to study the behaviour of the protein under hypertonic conditions. Transient overexpression of the

RLP44-GFP protein driven by the 35S promoter in *Nicotiana benthamiana* (*N. benthamiana*) leaves suggested plasma membrane (PM) localization (Figure 7B) as previously observed in stable *Arabidopsis* plants. In hypertonic solution (0.6 M sorbitol), the cells were plasmolysed, i.e., the PM was detached from the cell wall to adjust to the surrounding hypertonic solution (Lang et al., 2014). Hechtian strands were visible as thread-like structures in the periplastic zone between the cell wall and the PM. These structures are thought to play a significant role in cell-cell communication events via connection of the plasmodesmata (Lang et al., 2014). We observed that fluorescence distribution after plasmolysis of a PM marker, here Low temperature induced protein 6B (Lti6B), was more regular than the RLP44 signal distribution (Figure 7B). In the plasmolysed cells with RLP44, these thread-like structures occurred more often than in PM localized protein Lti6B (data not shown) and in addition, the detachment was more disorderly compared to the PM marker control (Figure 7C). Lti6B is a small PM protein, which does not bind to the CW (Martinière et al., 2011). The patchy RLP44 pattern was only detected when the PM appeared to be still attached to the cell wall, which suggested a possible interaction of RLP44 with the cell wall matrix. During plasmolysis, the full-length RLP44 protein remains anchored in the PM through the TMD, which is expected to compete with a putative cell wall association. To test whether the RLP44ECD indeed associates with the CW, we studied the localization of the 35S:RLP44ECD-mCherry protein excluding both TMD and CD. To facilitate the visualisation of the PM, mGFP-Lti6B was co-infiltrated. The N-terminal signal sequence of RLP44ECD was still guiding the truncated protein to the extracellular space as we were able to detect an apoplastic accumulation of the signal (Figure 7C), this signal was diffuse and more scattered than RLP44 full-length protein localization. In plasmolysed cells, the signal of RLP44ECD was detected in the apoplastic space between cell wall and PM, as well as, more strongly, in the cell wall. Taken the results together, RLP44 is a PM localized RLP and the RLP44ECD is able to bind a cell wall component.

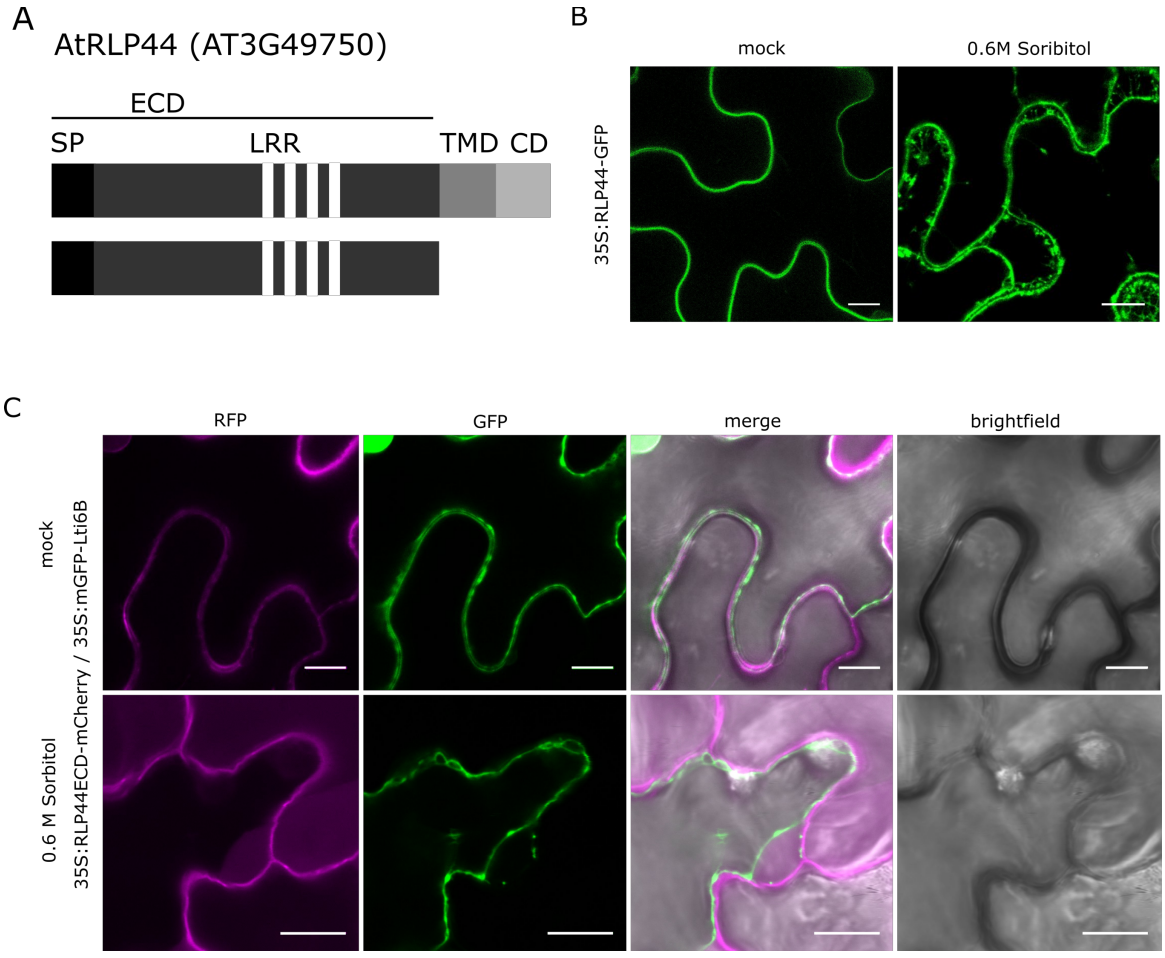


**Figure 7. RLP44 is a plasma membrane localized protein.**
(A) Structural features of the RLP44 protein
(B) Transient overexpression of RLP44 full length protein in *N. benthamiana* under mock conditions and incubated with 0.6 M sorbitol to induce plasmolysis.
(C) 35S:RLP44ECD-mCherry co-infiltrated with the PM marker mGFP-Lti6B, transiently overexpressed in *N. benthamiana* leaves. Under plasmolysed conditions, induced by 0.6 M sorbitol, RLP44ECD-mCherry accumulates in the cell wall and the apoplastic space. Scale bars = 10 µm.

To confirm the cell wall binding ability of RLP44ECD in *Arabidopsis*, we crossed a line expressing RLP44ECD-mCherry to mGFP-Lti6B as a PM marker. Leaf disks of F1 plants resulting from the cross were used to visualise the protein localization during plasmolysis in epidermal cells (Figure 8). The PM detached from the cell wall and was labelled by mGFP-Lti6B, while RLP44ECD seemed to continue to be attached to the cell wall and dispersed in the apoplastic space between cell wall and PM (Figure 8 first row). Verification of the localization was performed by using a secreted red-fluorescent protein (secRFP) in plasmolysed epidermis cells, it accumulated in the newly formed space between the PM

and the cell wall and seems to be excluded from the cell wall (Zheng 2005) (Figure 8 second row). As a positive control, we used a line expressing part of the cell wall binding ECD of FORMIN HOMOLOG 1. When a truncated version without the transmembrane domain part was used (FH107), the protein remained mostly in the cell wall as well as in the apoplastic space (Figure 8 third row), in agreement with published results (Martinière et al., 2011).

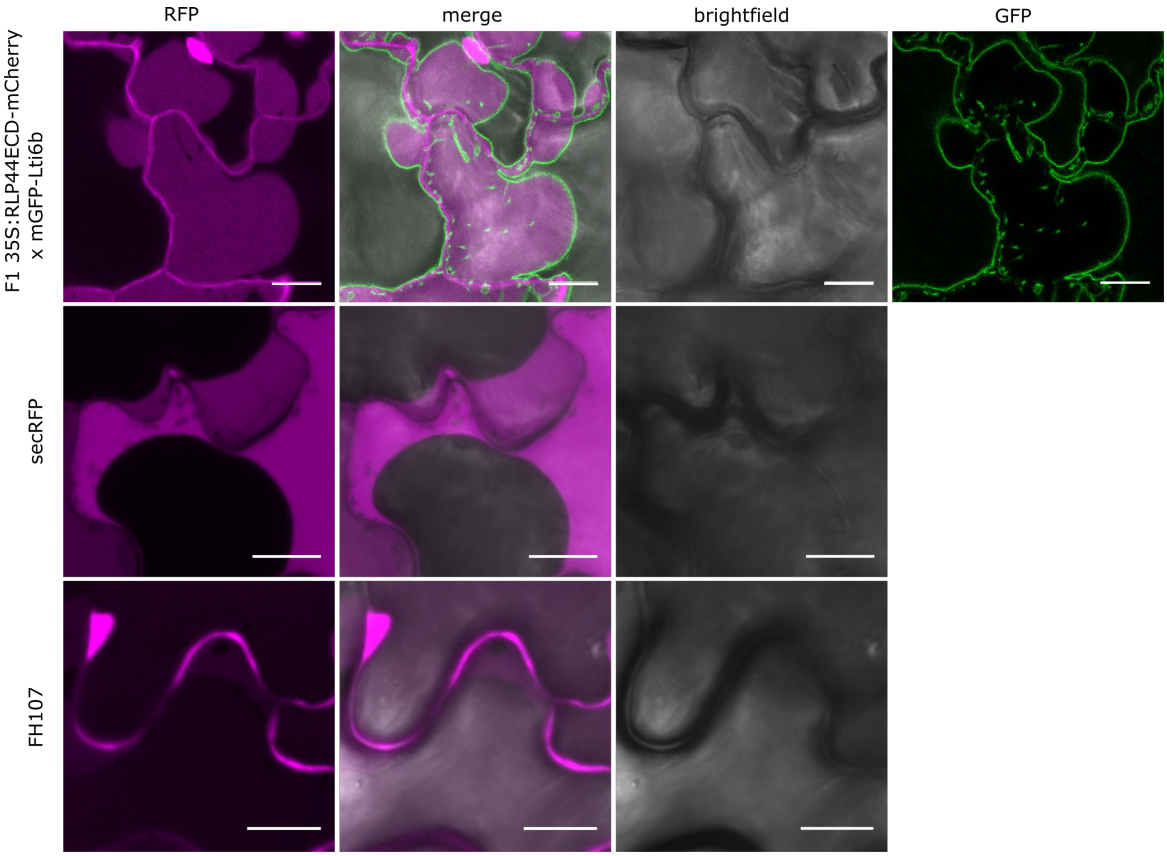


**Figure 8. RLP44ECD-mCherry interaction with the cell wall in in plasmolysis experiments.**
All panels show epidermal cells in *Arabidopsis* leaves incubated with 0.6 M sorbitol to induce plasmolysis.
First row: F1 35S:RLP44ECD-mCherry (Col-0) x mGFP-Lti6. Lti6B is used as a PM marker and RLP44ECD-mCherry distributes in the periplastic space and accumulates in the cell wall region.
Second row: Plasmolysis of secRFP is not showing any interaction with the cell wall.
Third row: Formin 1 deletion construct FH107, lacking the transmembrane domain, remains mostly in the cell wall as well as in the apoplastic space between the PM and cell wall. Scale bars = 10 µm.

## *2.4* Recombinant RLP44ECD binds to pectate *in vitro*

The recently identified plasma-membrane-bound receptor-like kinase THESEUS1 (THE1) was shown to monitor the pectin state. Furthermore, wall-associated kinases (WAKs) have already been linked to the cell wall more than 20 years ago (He et al., 1996). Data from our lab suggested that RLP44 could be a sensor of the cell wall pectate state and further transmit this state to the cell interior of (Kolbeck 2015). Recent literature provides data for the direct binding of the ECDs of FER1 and WAK1 to PGA. (Decreux and Messiaen 2005, Feng et al., 2018; Lin et al., 2018; Cheung and Wu 2011). Detailed studies revealed that the "egg-box" structure which is formed by demethylesterified pectin in the presence of calcium, enables the binding of WAK1 (Decreux and Messiaen 2005).

In order to further characterize how RLP44ECD might monitor cell wall integrity, the DNA sequence encoding amino acids (AA) 25-226 of the extracellular domain of RLP44 were cloned and used to express a soluble recombinant protein in insect cells. The recombinant protein was produced by Ulrich Hohmann. To reveal with which CW component RLP44 might associate, we performed a binding assay with a glycan array provided by William Willats. This array is spotted with a library of in total 84 different oligosaccharides (see appendix for the detailed list of spotted oligosaccharides; Figure 40; Figure 41). The recombinant, StrepII-tagged RLP44ECD was used to probe the glycan array. We could not detect any binding to cellulose and the hemicellulose xyloglucan (Figure 9A). In contrast, RLP44ECD was detected specifically bound to pectin and the signal intensity generally seemed to be negatively correlated with the degree of demethylesterification (DM) (Figure 9A). However, we could still observe differences in binding affinity between pectin spaces, e.g. base random deesterified blocks DM96 the interaction appeared as intensive as low degree DE pectins from lime, suggesting that the pattern of demethylesterification might play a role in the interaction with RLP44. To further confirm these results, we spotted nitrocellulose membranes with commercially available pectins with different degrees of methyesterification (Figure 9B). In order to rule out any false positive interactions, we used the ECD of BAK1 as a negative control (data not shown, no quantification possible, no signal detected).

We identified pectate or high methylesterified pectin as the ligands of RLP44 *in vitro* and were able to confirm this result with self-dissolved oligosaccharide solutions spotted on a nitrocellulose membrane.

A

| | |
|---|---|
| Xylan (beechwood) | 0 |
| Xylan (Aspen) | 0 |
| Arabinoxylan (wheat) | 0 |
| Xyloglucan Tamarind seed | 0 |
| Carboxymethyl Cellulose | 0 |
| Ethyl cellulose | 0 |
| 2-hydroxyethyl cellulose | 0 |
| Methyl cellulose | 0 |
| Carboxymethyl Cellulose 4M | 0 |
| Karaya gum | 14 |
| Lime pectin DE: 15% (B15 | 58 |
| Lime pectin DE: 15% (B34) | 41 |
| Lime pectin DE: 43% (B43) | 40 |
| Lime pectin DE: 64% (B64) | 0 |
| Lime pectin DE: 71% (B71) | 0 |
| Lime pectin DE: 11% (F11) | 43 |
| Lime pectin DE: 31% (F43) | 19 |
| Lime pectin DE: 76% (F76) | 0 |
| Lime pectin DE: 16% (P16) | 46 |
| Lime pectin DE: 46% (P53) | 24 |
| Lime pectin DE: 76% (P76) | 0 |
| Pectin with DE 1% & DA 0%, basic hydrolysis of SBP6230 | 41 |
| Pectin with DE 9% & DA 15%, basic hydrolysis of SBP6230 | 25 |
| RGI (soy bean) | 0 |
| Polygalacturonic acid from citrus pectin (Danisco) | 41 |
| Pectin (CP Kelco) | 41 |
| Polygalacturonic acid from citrus pectin (Megazymes) | 63 |
| Pectin, Base, random deesterified blocks, DM 96 | 55 |
| Pectin, Plant PME, big deesterified blocks, DM 14 | 100 |
| Pectin, Plant PME, big deesterified blocks, DM 36 | 79 |
| Pectin, Plant PME, big deesterified blocks, DM 75 | 37 |

B

| | |
|---|---|
| megazyme PGA | 100 |
| Pectin mix of differend estification grades | 14 |
| pectin 70 DE | 13 |
| pectin 40 DE | 23 |
| pectin 10 DE | 48 |
| control | 0 |

**Figure 9. Glycan arrays show direct interaction of RLP44ECD protein with pectate.**
RLP44ECD was cloned from amino acids 25-226 and expressed in insect cells to produce the StrepII-tagged RLP44ECD recombinant protein. (A) This protein was probed with a glycan array spotted with 84 different oligosaccharides (see appendix for detailed list).
(B) RLP44ECD protein was probed with a self-prepared nitrocellulose pectin array. The mean point signals are represented as a heat map in which the colour intensity is correlated to the signal. The most intense signal was set to 100, and all other values were normalized accordingly. Values below 10 were considered as background. Only measureable signals are depicted in this heat-map.

## 2.5 Tyrosin146 & arginine170 may be required for the cell wall binding of RLP44

Interestingly, in Zucchini, it has been shown that an isoperoxidase, an enzyme active in the apoplast, can bind specifically to polygalacturonic acid through a cluster of arginines (Carpin et al., 2001). Furthermore, lysine, another positively charged AA, has been implicated in interactions of proteins with cell wall components, while tyrosine has been shown to form stacking interactions with galacturonic acid (Scavetta et al., 1999; Spadoni et al., 2006). Importantly, cell wall binding through basic amino acids of another LRR protein, PGIP from pea, has been previously described (Spadoni et al., 2006). To assess the role of cell wall association for RLP44 function, we sought to test how cell wall properties influence downstream signalling. To study this, a first step was to identify the AAs responsible for RLP44 cell wall binding. As a second step, a mutation in the respective AAs may lead to the release of RLP44 of the cell wall. RLP44 is a LRR protein, and although the crystal structure of this specific protein is not available, it is possible to estimate the structure of the ECD based on homology modelling using other LRR proteins, at least for the ECD domain. Several structures have already been studied in detail and literature agrees on a helical shape of the LRR ECD domains (Bella et al., 2008, Hothorn et al., 2011; Han et al., 2014). To identify the AAs responsible for the cell wall binding, Michael Hothorn provided us with an RLP44ECD structure model by homology modelling on SOMATIC EMBRYOGENESIS RECEPTOR-LIKE KINASE 1 (SERK1). Based on this modelling, four consisting each of two predicted AAs clusters were identified by Michael Hothorn that could be involved in pectate binding (Table 1).

**Table 1. Predicted clusters for cell wall binding**

| cluster | amino acids |
|---|---|
| I | Arg47/Lys77 |
| II | Tyr146/Arg170 |
| III | Arg192/Arg198 |
| IV | Lys180/Lys208 |

We used site-directed mutagenesis to change both AAs of each cluster. Based on the TMD of the RLP44, the full-length protein retained partially in the PM during plasmolysis (Figure 7B), presumable the anchor though the TMD is stronger than the interaction with the cell wall. With the RLP44ECD protein, we were able to highlight the interaction with the CW during plasmolysis (Figure 7C). Consequently, to simplify the analysis, the mutated RLP44ECD was transiently expressed in *N. benthamiana* to check for expression of the protein and behaviour during plasmolysis. For better visualization, the mutated ECD of RLP44 was transiently co-expressed with the wildtype RLP44ECD. The wildtype control (RLP44ECD) displayed the already described CW association and distribution in the apoplastic space (Figure 7C and Figure 10 first raw). Plasmolysis in *N. benthamiana* identified clusterII (Tyr146 and Arg170) to be responsible for cell wall interaction, as mutations to alanine caused a release from the cell wall (Figure 10 middle row). However, mutations in cluster I and IV had no effect on the cell wall binding ability (Figure 10 bottom row, clusterIV not shown). Unfortunately, clusterIII mutant construct was not expressed in *N. benthamiana.* The difference in RLP44ECD-clusterII behaviour compared to the wildtype RLP44ECD-RFP was considerable, as RLP44ECD-clusterII was comparable to the distribution of secRFP during plasmolysis (Figure 8).

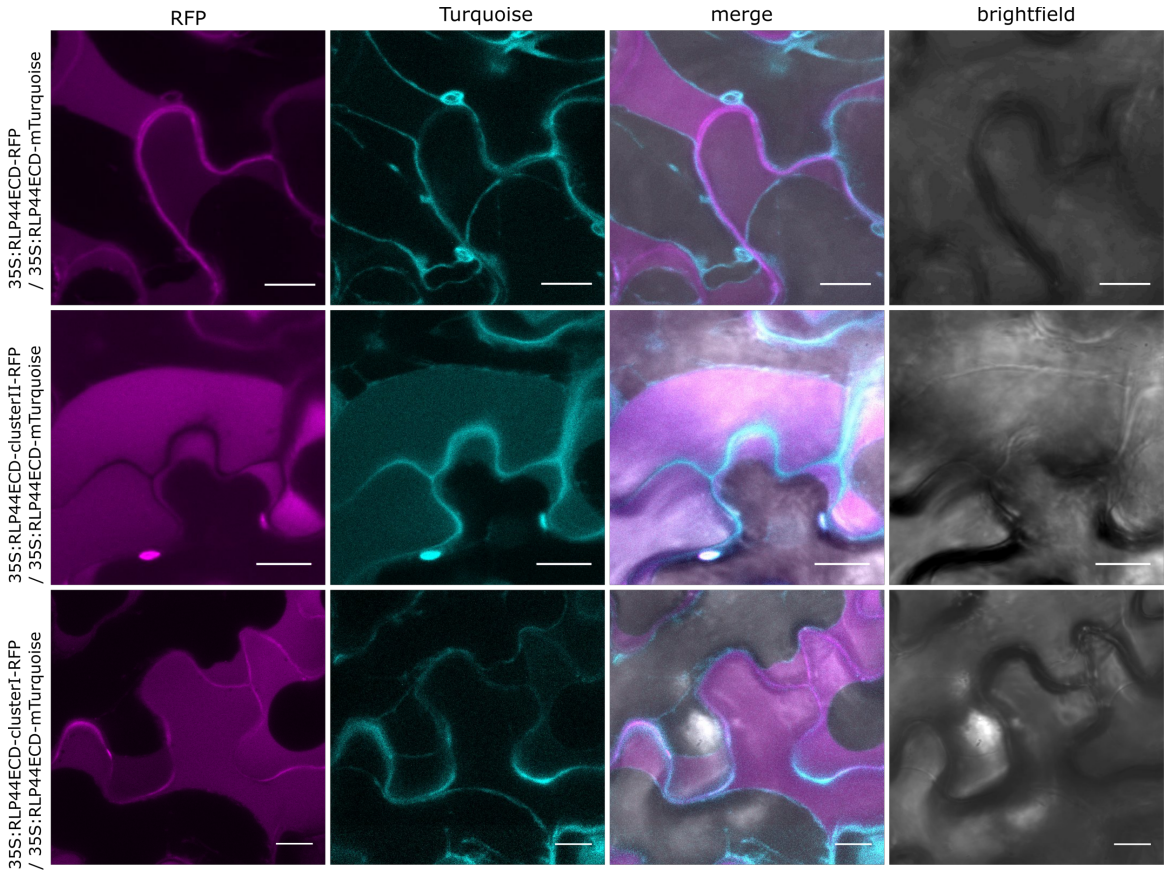


**Figure 10. Transient expression reveals that RLP44ECD-clusterII does not bind the cell wall in *N. benthamiana* epidermal cells during plasmolysis.**
All panels show plasmolysed epidermal cells in *N. benthamiana* leaves treated with 0.6 M sorbitol.
First row: co-expression of 35S:RLP44ECD-RFP and 35S:RLP44ECD-mTurquoise. Both RLP44 wildtype ECDs are dispersed in the apoplastic space and accumulate in the cell wall region as well.
Second row: co-expression of 35S:RLP44ECD-clusterII-RFP and 35S:RLP44ECD-mTurquoise. RLP44ECD-clusterII signal is completely removed from the cell wall region and only found in the apoplastic space between the cell wall and the PM, in contrast to the wildtype RLP44ECD, which is still bound to the cell wall as well as dispersed in the apoplastic space.
Third row: co-expression of 35S:RLP44ECD-cluster I-RFP and 35S:RLP44ECD-mTurquoise. RLP44ECD-clusterI behaves similarly to wildtype RLP44ECD and remains associated with the PM and simultaneously dispersed in the apoplastic space. Scale bars = 10 µm.

To reveal the role of CW interaction, the functionality of the mutated RLP44-clusterII version was investigated. Foremost, we checked the ability of the mutated version of RLP44-clusterII and wildtype RLPP, both fused to GFP and driven by the native RLP44 promoter, to rescue the *cnu2* phenotype. This complementation assay can be ambiguous, as the degree of complementation was highly variable. Therefore, a sub-division into three classes of complementation of the T1 plants was introduced (Figure 11). Class I T1 plants showed *cnu2* characteristics, class II T1 plants exhibited only misshaped siliques, and class

III T1 plants had in addition organ fusions of the shoots (Figure 11). As expected, expression of wildtype pRLP44:RLP44-GAGA-GFP was able to complement the PMEIox phenotype in the *cnu2* background (Figure 11) (Wolf et al., 2014). T1 plant expressing the pRLP44:RLP44-GAGA-GFP construct (Table 2) could be assigned to all three classes based on the characteristics. However, taking into account that RLP44 did not bind the cell wall in the presence of PMEIox (see below) and that RLP44-clusterII protein was unable to bind the cell wall (Figure 10) we expected to find predominantly T1 plants expressing the pRLP44:RLP44-clusterII-GAGA-GFP construct similar to the PMEIox phenotype. Surprisingly, only class I or class II plants were observed, while no T1 plants displayed organ fusion and misshaped siliques (Table 2). Unfortunately, in the T2 generation, most introduced constructs, wildtype and cluster II, were silenced. Amongst the T2 plants expressing the RLP44 wildtype construct, there were five lines showing root waving in seedlings, whereas only one RLP44-clusterII mutant expressing line was obtained, which also showed root waving in seedlings (data not shown).

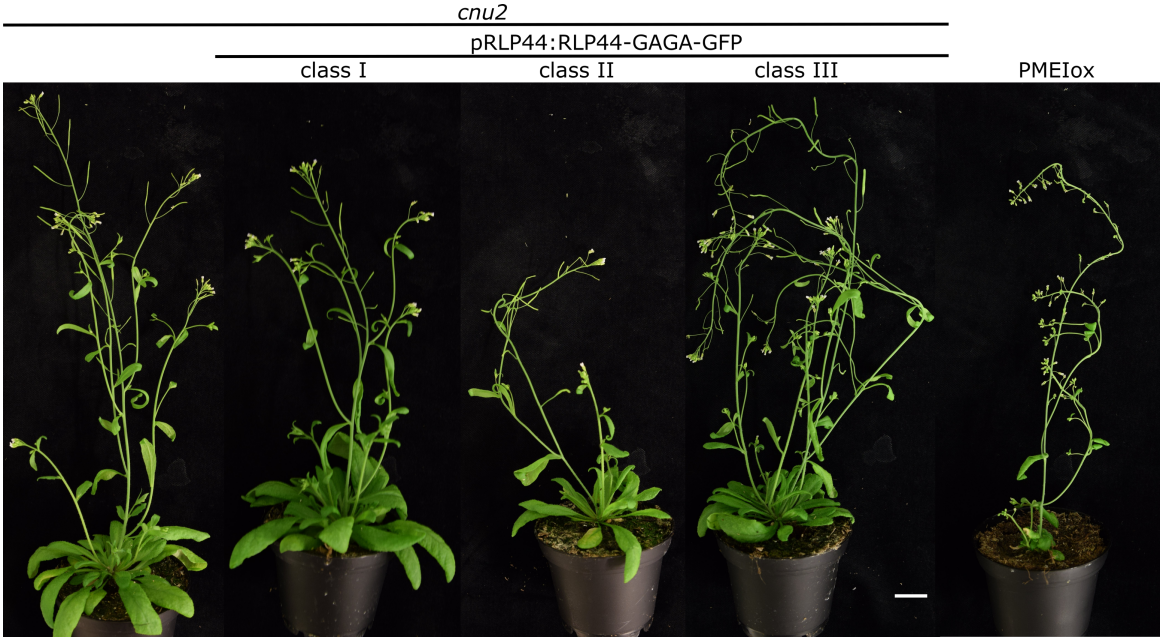


**Figure 11. Overexpression of pRLP44:RLP44-GAGA-GFP in *cnu2* is able to complement the PMEIox phenotype.** 5-weeks-old plants illustrate the different classes of complementation grade. Class I T1 plants show wildtype characteristics. Class II plants have misshapen siliques and class III plants show additionally organ fusions. Scale bar = 1 cm

**Table 2. Evaluation of T1 plant selection for *cnu2* complementation**.
Selection was performed with *cnu2,* therefore T0 plants were transformed with either pRLP44:RLP44-GAGA-GFP or pRLP44:RLP44-clusterII-GAGA-GFP to reconstitute the PMEIox phenotype.

| construct | Class I | Class II | Class III |
|---|---|---|---|
| pRLP44:RLP44-GAGA-GFP (*cnu2*) | 12 plants | 19 plants | 5 plants |
| pRLP44:RLP44-clusterII-GAGA-GFP (*cnu2*) | 20 plants | 20 plants | 0 plants |

We repeated the complementation assay with RLP44 and RLP44-clusterII driven by the 35S promoter instead of the native 5' region, to achieve a more pronounced complementation. Unfortunately, we were only able to obtain one T1 transformant each. Based on this, the analysis of the results was challenging, however they were in agreement with the obtained observations with the native 5' promoter region. The T1 plants derived from the wildtype RLP44 construct under the 35S promoter was categorized to class III as an adult plant, however RLP44-clusterII construct also driven by the 35S promoter only showed misshaped siliques as adult, but the seedling plant also showed root waving.
In Summary, AAs tyrosine 146 and arginine 170 were identified to be responsible for the cell wall binding of RLP44ECD, since upon mutation to alanine the 35S:RLP44ECD-clusterII is not able to stay associated with the cell wall during plasmolysis in *N. benthamiana*. However, pRLP44:RLP44-clusterII-GAGA-GFP it is not as efficient in complementing *cnu2* plants as the wildtype pRLP44:RLP44-GAGA-GFP construct. In addition, wildtype RLP44 driven by the 35S promoter show complete complementation of the *cnu2* phenotype, but the RLP44-clusterII construct only partially.

## 2.6 RLP44 is a putative sensor for pectate

RLP44ECD was shown to directly bind to pectate *in vitro* (Figure 9), supporting our hypothesis that RLP44 might be a sensor for pectate in the plant cell wall. Based on this, we next assessed if the presence or absence of PMEIox has an influence on the association of RLP44ECD with the cell wall. Upon inhibition of the demethylesterification of cell wall pectin by PMEI, RLP44 activates the BR signalling as a compensatory response (Wolf et al., 2014). PMEIox inhibits the formation of the "egg-box" structure of demethylesterified pectins, considering this, a similar mechanism to WAK1 for RLP44ECD could be expected. It was previously shown that the WAK1 ECD binds to demethylesterified "egg-box" structured pectate (Decreux and Messiaen 2005).

During plasmolysis, RLP44ECD was not able to associate with the cell wall in PMEIox and *cnu2* background mutants (Figure 12A). The CW modification was not suppressed in *cnu2* as PMEIox were still present, only RLP44 is lacking thus the BR-signalling cannot be over-activated. Contrarily, RLP44ECD associated with the CW in Col-0 and in the *rlp44*$^{cnu2}$ background (Figure 12A). We concluded that the change of the pectin/pectate state of the cell wall in the presence of PMEIox may cause the release of RLP44ECD from the cell wall association.

Furthermore, we tested whether overexpression of the ECD affects BR-signalling. The depletion of the endogenous BR levels with propiconazole (PPZ) (Hartwig et al., 2012) enabled the visualisation of the BR sensitivity. Until 0.5 nM BL there was a growth inducing effect in all lines and with increasing BL concentrations the growth inhibiting effect of BL was induced. However, root growth of RLP44ECD overexpression lines in both backgrounds were indistinguishable from wildtype response for both growth-promoting and growth-inhibiting doses of BL (Figure 12B).

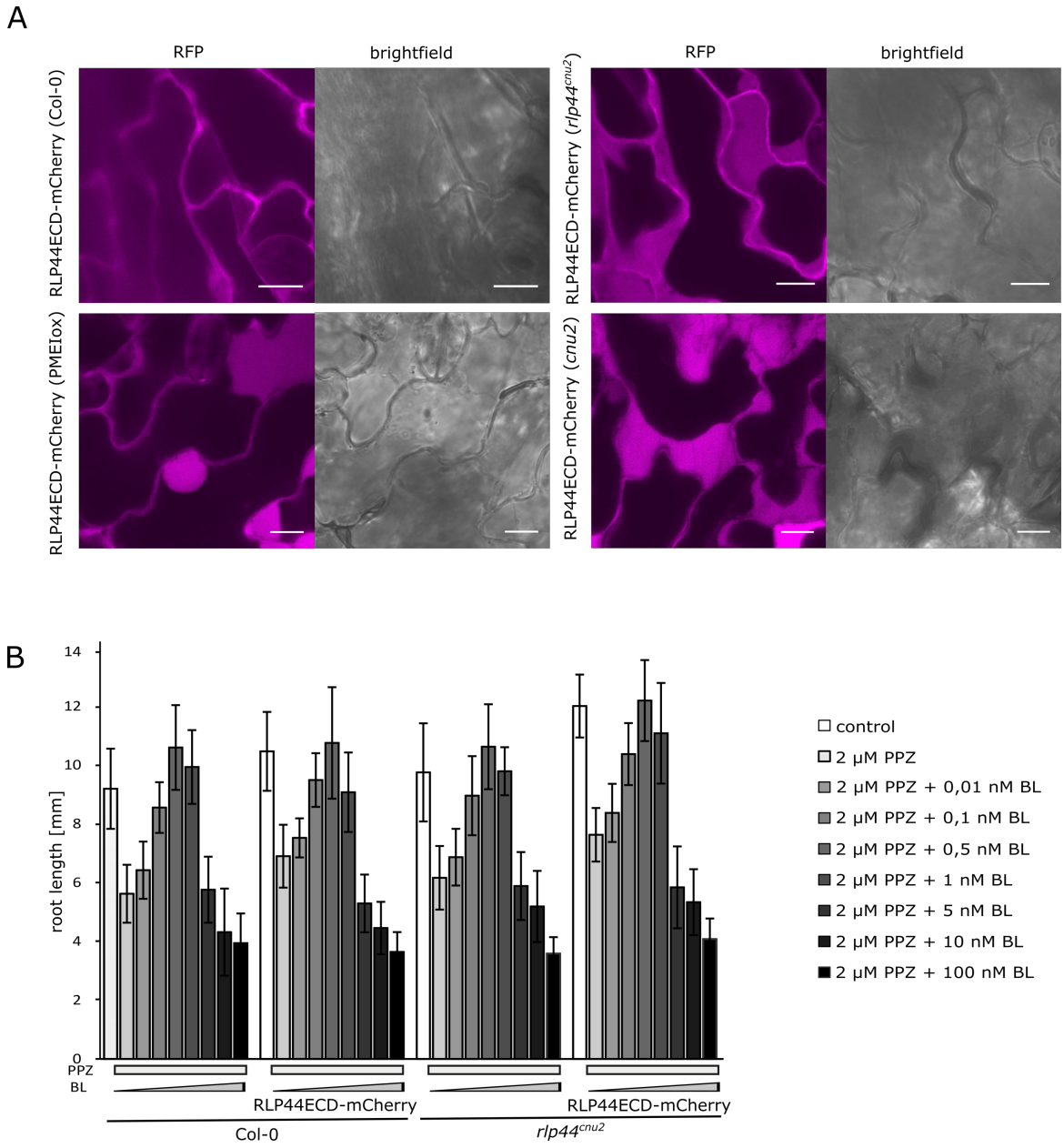


**Figure 12. Characterization of RLP44ECD-mCherry in four different backgrounds.**
(A) Plasmolysis of leaf disks of RLP44ECD-mCherry overexpressed in wildtype, *rlp44*$^{cnu2}$, *cnu2* and PMEIox in 4-weeks-old *Arabidopsis* plant leaves. In presence of the PMEIox transgene (PMEIox and *cnu2*) RLP44ECD-mCherry does not appear to bind to the cell wall as it is visible in Col-0 and *rlp44*$^{cnu2}$. In Col-0 and *rlp44*$^{cnu2}$, RLP44ECD seems to locate to the apoplastic space between the detached PM and the cell wall, but signal accumulation is visible at the predicted cell wall location. Scale bars = 10 µm.
(B) Overexpression of RLP44ECD-mCherry does not affect BR sensitivity. Bars indicate mean root length of 5-d-old seedlings ±SD (n= 23-33) in response to PPZ and increasing levels of BL.

To study the interaction between RLP44ECD and the cell wall, we expressed the truncated RLP44 to test for complementation of the *cnu2* mutant. Accordingly, we generated crosses of the RLP44ECD-mCherry (*cnu2*) line with *Arabidopsis* Columbioa-0 (Col-0) wildtype plants to obtain the same transgene in four different backgrounds: PMEIox, *cnu2*, *rlp44*$^{cnu2}$ and Col-0. However, the extracellular domain alone was not able to fulfil the function of the full-length RLP44 protein, as overexpression of RLP44ECD in *cnu2* did not complement (Figure 13A). Nevertheless, the truncated protein appears to be partially functional, since the earlier described growth-affected phenotype of *rlp44*$^{cnu2}$ (Wolf et al., 2014) seemed to be recovered in the adult plant rosette phenotype (Figure 13A) and in terms of root length (Figure 13B). It was published before that overexpression of the RLP44 full length protein caused a phenotype reminiscent of the BRI1 overexpression phenotype with elongated petioles, and long, narrow and turned leaves (Figure 13) (Friedrichsen et al., 2000; Wolf et al., 2014). However, the plant phenotype in the RLP44ECD overexpression in the Col-0 background did not show any evidence of BR overexpression characteristics (Figure 13A).

In summary, the overexpression of PMEI, prevented RLP44ECD interaction with the cell wall (Figure 12A). Nevertheless, there is no effect the BL perception between the lines (Figure 12B). The RLP44ECD-mCherry construct partially rescued the *rlp44*$^{cnu2}$ phenotype, since before the plant growth was shown to be growth affected (Wolf et al., 2014).

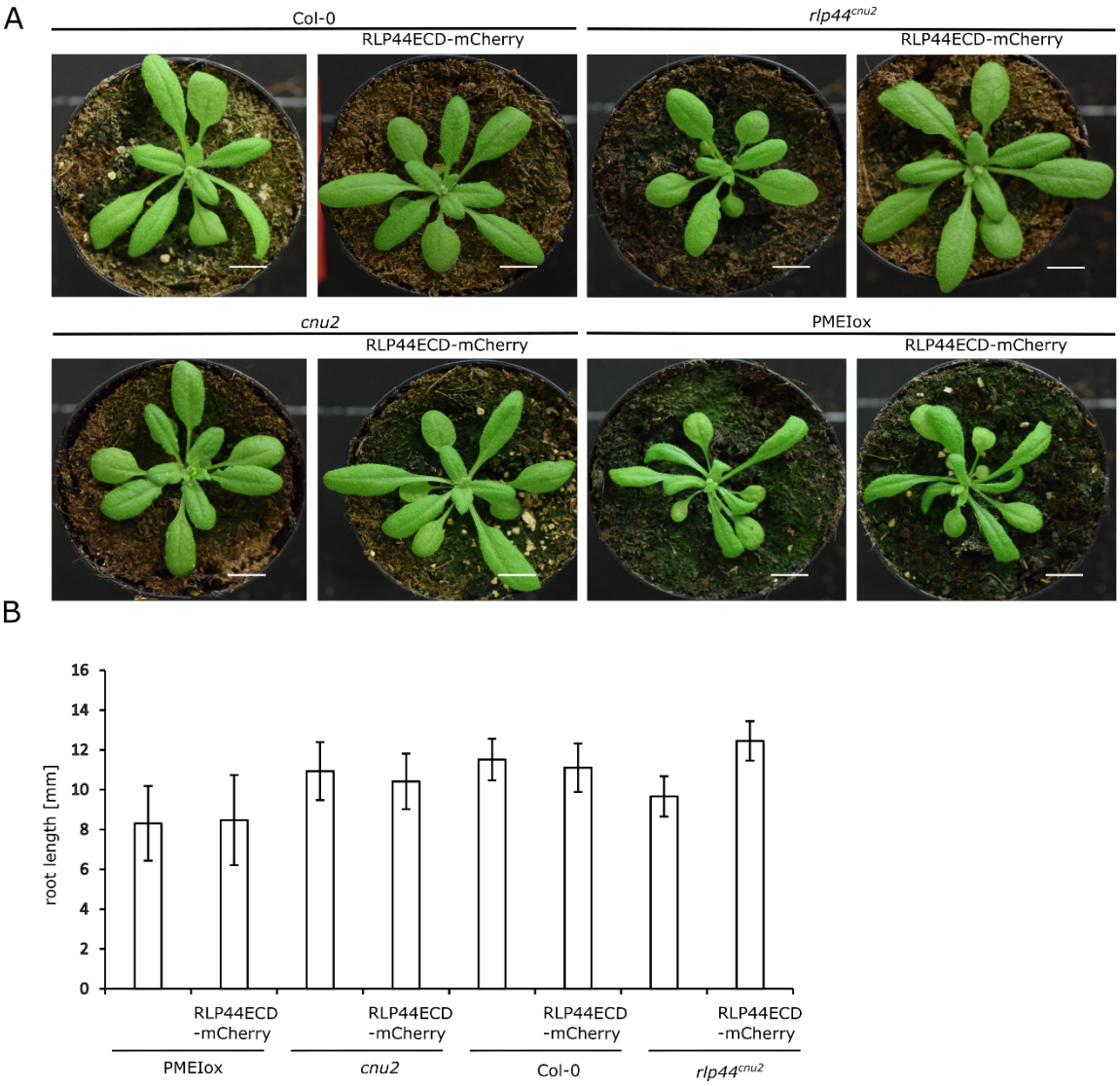


**Figure 13. Phenotype of RLP44ECD overexpression in wildtype, *rlp44*$^{cnu2}$, *cnu2* and PMEIox background.**
(A) RLP44ECD-mCherry overexpression in wildtype, *rlp44*$^{cnu2}$, *cnu2* and PMEIox background. RLP44ECD cannot complement the *cnu2* phenotype but is able to rescue the *rlp44*$^{cnu2}$ phenotype. Pictures are showing 4-weeks-old plants Scale bars = 1 cm
(B) The overexpression of the RLP44ECD-mCherry only rescues the *rlp44*$^{cnu2}$ root length. Bars indicate mean root length of 5-d-old seedlings ±SD (n = 23-32).

## 2.7 *cnu3* and *cnu4* are two new *bri1* alleles

To further study the biochemical processes by which cell wall signalling is integrated into the plant cell, we searched for more key players using the same EMS screen, that identified RLP44.

Indeed, we were able to detect two new suppressor mutants named *cnu3* and *cnu4*, which almost completely suppress the PMEIox phenotype (Figure 11-13). Using a map-based cloning approach, the *cnu3* mutation, an arginine to tryptophan change at position 769 (R769W), was located in an unassigned, membrane-proximal region of BRI1. Further, the *cnu4* mutation is located in the last LRR of BRI1, the glycine at position 746 is substituted by serine (G746S).

To elucidate the genetic connection between the *cnu* mutations, we analysed F1 hybrid seedlings from various crosses, assaying the root waving phenotype caused by PMEIox (Figure 14A). The allelism test revealed that *cnu3* and *cnu4* fail to complement each other and confirmed the previously obtained results, suggesting mutations reside in the same gene. However, the F1 hybrid seedling derived from the cross of *cnu2* and *cnu4*, as well the F1 offspring from *cnu2* and *cnu3* showed complementation, i.e. restored the PMEIox root waving phenotype, indicating that the mutations are not interchangeable (Figure 14A). In line with this, silique shape (Figure 14B) and overall adult plant phenotype (Figure 14C) were only complemented by crosses of *cnu3* and *cnu4* with cnu2, respectively.

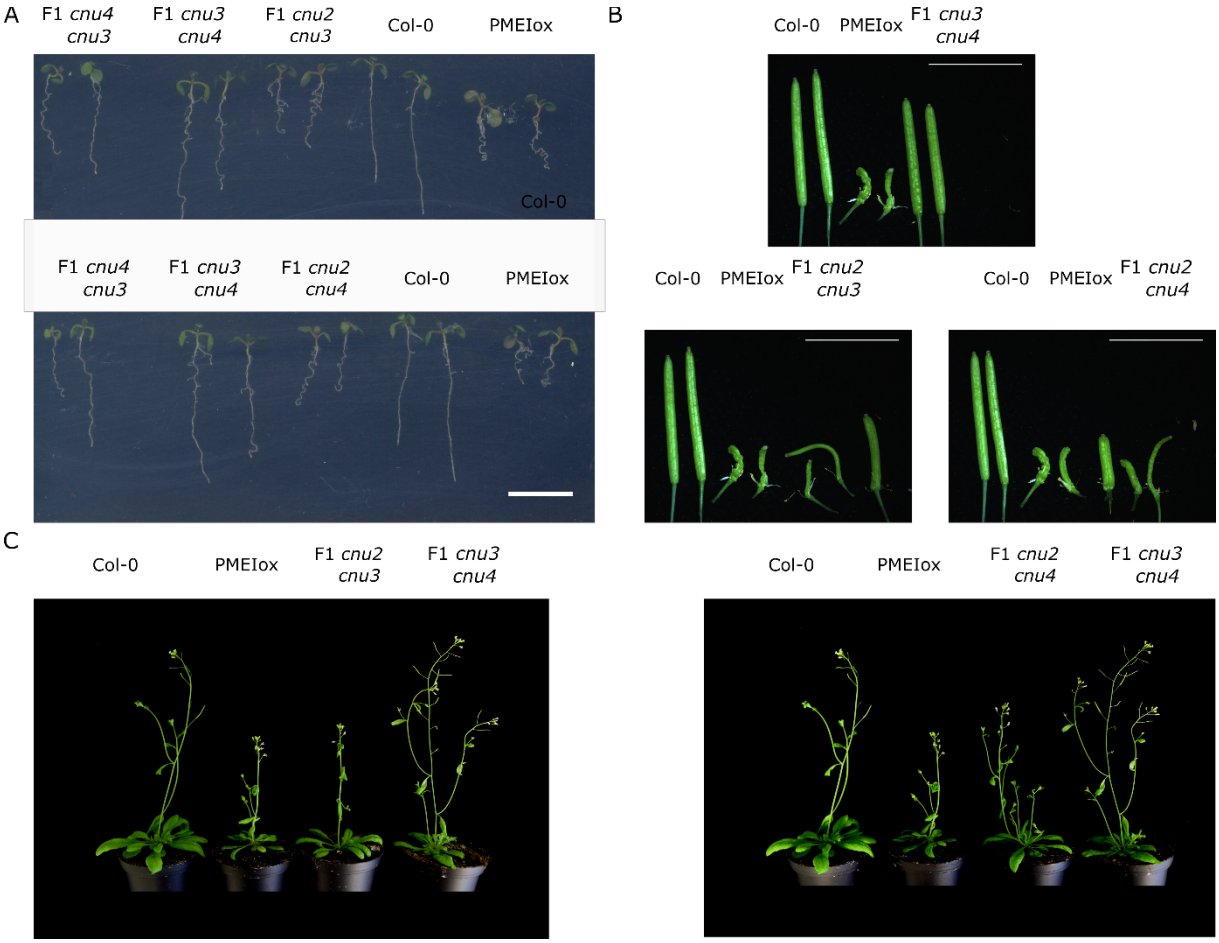


**Figure 14. Genetic characterization of PMEIox suppressor mutants.**
(A) 5-d-old seedlings of different F1 hybrid seedlings *cnu2* x *cnu3* complement the PMEIox phenotype, *cnu4*x*cnu3* F1 hybrid seedlings are not complemented. Scale bar = 1 cm.
(B) Developed siliques of F1 hybrid plants show complementation of *cnu2* crosses with *cnu3* and *cnu4*, respectively.
(C) 5-weeks-old plants show the complementation of *cnu2* crosses with *cnu3* and *cnu4*, respectively.

Furthermore, plants heterozygous for the *cnu4* mutation were not able to suppress the PMEIox phenotype. The same was observed with the *rlp44*$^{cnu2}$ mutation, which is not able to suppress the PMEIox phenotype as a heterozygous F1 hybrid seedling, deriving from a *cnu2* x PMEIox cross (Figure 15). The results suggest that the mutants are recessive.

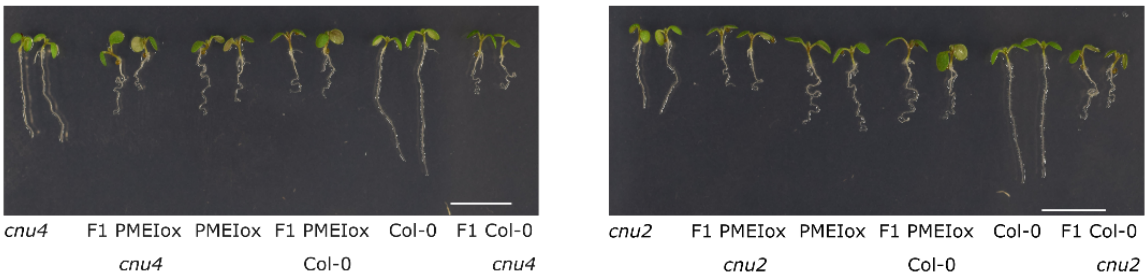


**Figure 15. Genetic characterization of suppressor mutants.**
Figure shows 5-d-old seedlings of different F1 hybrid seedlings. Heterozygous plants for *cnu4* and *cnu2* are not able to suppress the PMEIox phenotype. Scale bars = 1 cm.

The two new suppressor mutants named *cnu3* and *cnu4* suppressed the PMEIox phenotype in seedling and adult plant phenotypes (Figure 16A,C). The vertical growth index, the ratio of root tip ordinate and root length, was reduced in PMEIox plants but was rescued completely in the *cnu* mutant plants (Figure 16B) (Grabov et al., 2005). The same suppression trend was apparent for the rescued silique length in the respective mutants. (Figure 16E). It is known that BR detection of BRI1 activates downstream transcription factors, which in turn regulate numerous genes involved in cell wall biosynthesis and remodelling (Belkhadir and Jaillais 2015). The BZR1 protein is one of the downstream targets (Wang et al., 2002) and is itself inhibiting the transcription of BR biosynthesis genes such as *DWF4* (Asami et al., 2001). Based on these observations, the BR-signalling module constitutes a negative feedback loop (Belkhadir and Jaillais 2015). Consequently, as PMEIox plants exhibit an over-activation of the BR-signalling pathway, we expected lower DWF4 mRNA levels, whereas, in the suppressor mutants *cnu1-4*, the DWF4 mRNA levels were also rescued back to the wildtype levels (Figure 16D). Interestingly, PMEIox was not influenced by the depletion of endogenous BR, since no growth inhibiting effect upon PPZ treatment can be observed (Figure 16F), and furthermore was insensitive to different BL concentrations. Although the suppressor mutants had a wildtype appearance, they were impaired in their BL sensitivity, since the growth promoting effect was diminished (Figure 16F).

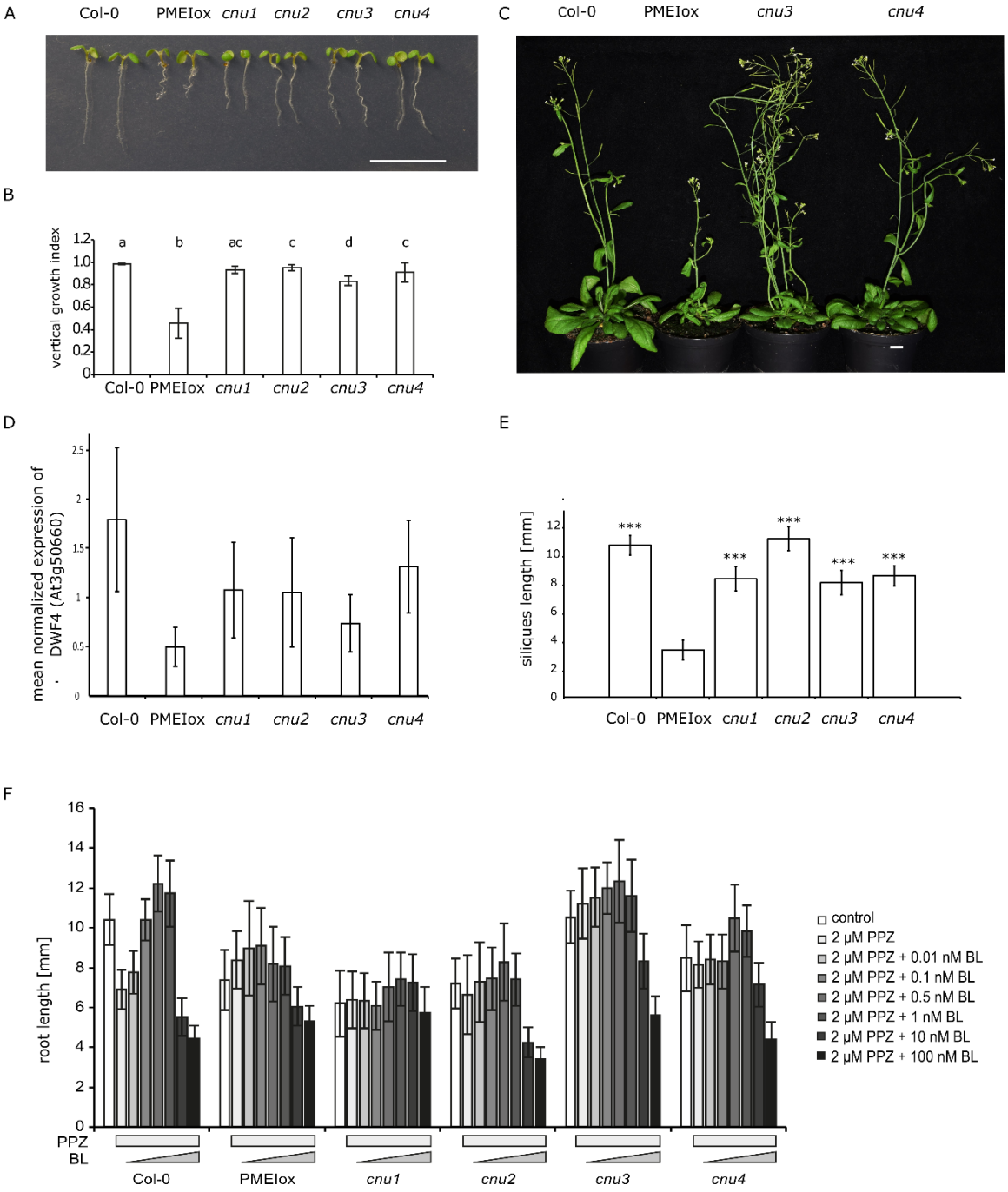


**Figure 16. Identification of two novel *bri1* alleles, both are able to suppress the PMEIox phenotype.**
(A) Overexpression of *PMEI5* leads to pectin modification and results in compensatory upregulation of BR-signalling (Wolf et al., 2012). Mutations in BRI1 - *cnu1* (Wolf et al., 2012), *cnu3* (this study), *cnu4* (this study), and in RLP44 (*cnu2*) (Wolf et al., 2014) can suppress the PMEIox phenotype.
(B) Two new alleles with mutations in the extracellular domain suppress the PMEIox directional growth phenotype, as visualized by root vertical growth index (Grabov et al., 2005). Letters indicate statistically significant difference according to one-way ANOVA with $p < 0.05$ ($n = 13$).
(C) PMEIox adult morphological phenotype is suppressed in *cnu3* and *cnu4*.
(D) *DWF4* expression levels in PMEIox are rescued in *cnu1-4* back to Col-0 levels. Bars indicate expression level normalized to Col-0 ± SD (n=3).

(E) Misshapen siliques of PMEIox are rescued by *cnu1-4*. Bars indicate relative silique length ± SD (n=30-49). (F) Response of Col-0, PMEIox, *cnu1*, *cnu2*, *cnu3*, and *cnu4* to depletion (PPZ) and exogenous supply of brassinosteroids. Bars indicate average relative root length ± SD (n = 19 - 53).

We further assessed causality of the mutation in BRI1 *via* a complementation assay. It can be assumed that restoring the function of BRI1 reconstitutes the PMEIox phenotype. For this approach, *cnu3* and *cnu4* plants were transformed with BRI1 driven by its native promoter. Selected T1 plants showed a distinctly more severe PMEIox phenotype with strong organ fusions and curled leaves in the rosettes. In case of pBRI:BRI1-GFP (*cnu4*), the T1 plants were not able to develop a shoot (Figure 17). This indicated that the Bri1cnu4 protein might have a more severe effect on the signalling cascade when compared to the BRI1cnu3 protein. Unfortunately, all T1 plants were infertile and we were not successful in generating stable lines. This was in line with PMEIox crossed with BRI1-GFP expressing line, the offspring were infertile plants, suggesting an over-activation of the BR-signalling lead to a more severe PMEIox phenotype (Wolf et al., 2012).

Two new *bri1* alleles were identified in a forward EMS screen to suppress the PMEIox phenotype (Figure 16). Both mutated BRI proteins were shown to be still functional (Figure 17).

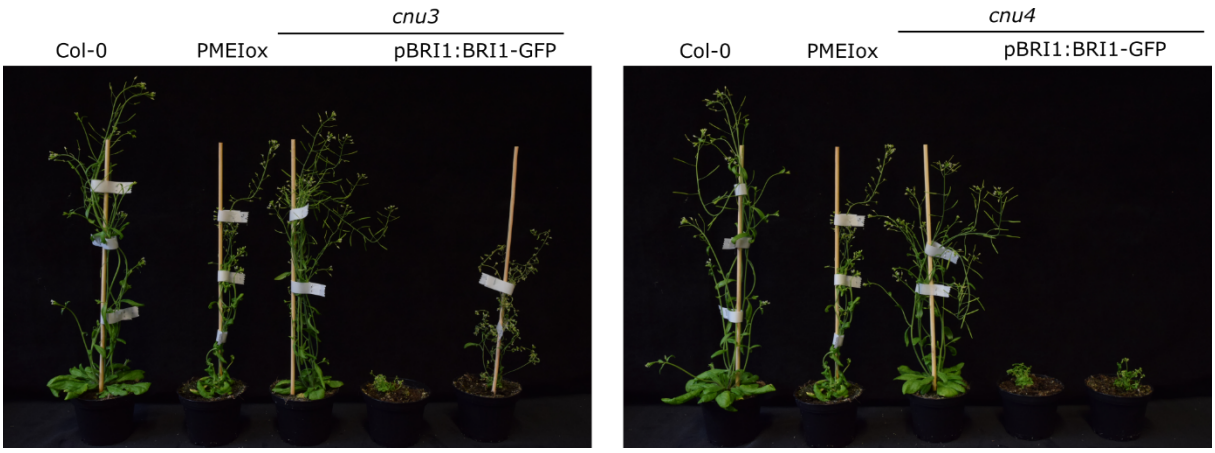


**Figure 17. BRI1cnu3 and BRI1cnu4 proteins are still functional.**
Complementation of *cnu3* and *cnu4* by introducing a pBRI1:BRI1-GFP under control of the native *BRI1* 5' regulatory sequence, resulted in recapitulation of PMEIox phenotype.

## 2.8 *bri1$^{cnu3}$* and *bri1$^{cnu4}$* show only a mild BR insensitivity

Considering the presence of the PMEIox transgene in the *cnu3* and *cnu4* mutants, we next backcrossed the mutants to the Col-0 wildtype to remove the transgene. Moreover, as BRI1 is an important developmental regulator, it was especially interesting to characterize the newly identified *bri1* alleles. We named the mutants devoid of the PMEIox transgene *bri1$^{cnu3}$* and *bri1$^{cnu4}$*, respectively. Mutants in BR-signalling are affected in BL sensitivity (Li et al., 2002). However, *bri1$^{cnu3}$* and *bri1$^{cnu4}$* did not show strong BR-signalling deficiency growth effects such as reduced fertility, smaller plants, and darker green (Figure 18A) (Friedrichsen et al., 2000). In contrast to the previously described *bri1$^{cnu1}$* an intermediate allele with a mutation in the kinase domain (G944D) resulted in restricted BRI1 activity (Wolf et al., 2012) and exhibiting a BR-deficient phenotype, the two new alleles exhibit wildtype characteristics. This wildtype-like phenotype can be visualized in siliques length, as those of *rlp44$^{cnu2}$*, *bri1$^{cnu3}$* and *bri1$^{cnu4}$* show no indication of developmental defects, in contrast to the siliques of *bri1$^{cnu1}$*, which are significantly smaller compared to wildtype siliques (Figure 18B). However, the overall morphological phenotype of *bri1$^{cnu4}$* is distinguishable from Col-0 wildtype due to more roundish and flat leaves, which is visible in the rosette stage (Figure 24A).

*DWF4* is involved in BR biosynthesis and part of a feedback loop where its transcription is inhibited by BZR1 upon BR-signalling activation (Sun et al., 2010). In contrast, *SAUR15* is induced upon activation of the BR-signalling cascade (Sun et al., 2010). To scrutinize the transcriptional regulation, we next used quantitative Real-Time PCR to analyse the relative *DWF4* expression. Congruent with former results, in *bri1$^{cnu1}$* the expression of *DWF4* appeared to be induced, whereas its expression in the other mutants did not seem to be severely altered (Figure 18C). Moreover, *SAUR15* expression levels correlated with *DWF4* expression levels, as the expression was only affected in *bri1$^{cnu1}$*, leading to a reduction of the expression levels, but not in the other mutants (Figure 18D).

Hence, we investigated the BL sensitivity of the newly identified *bri1* mutants. Upon depletion of endogenous BRs by addition of the biosynthesis inhibitor PPZ, root growth of *bri1$^{cnu1}$* appeared insensitive to BL up to concentrations of 100 nM BL, whereas *bri1$^{cnu3}$* and *bri1$^{cnu4}$* demonstrated BL-sensitivity and behaved similar to the wildtype in response to both growth-promoting and growth-inhibiting doses of BL. The *bri1$^{cnu3}$* and *bri1$^{cnu4}$* mutant showed only mild insensitivity in the presence of growth modulating doses of the

potent BR brassinolide (BL) (Figure 18E). Consistent with this mild growth phenotype, BRI1 protein accumulation was not affected either in *rlp44* or in *bri1* mutants (Figure 18F). Taking all the data into consideration, *bri1*$^{cnu3}$ and *bri1*$^{cnu4}$, which carry a mutation in the extracellular domain of BRI1 and were only mildly affected in BR sensitivity.

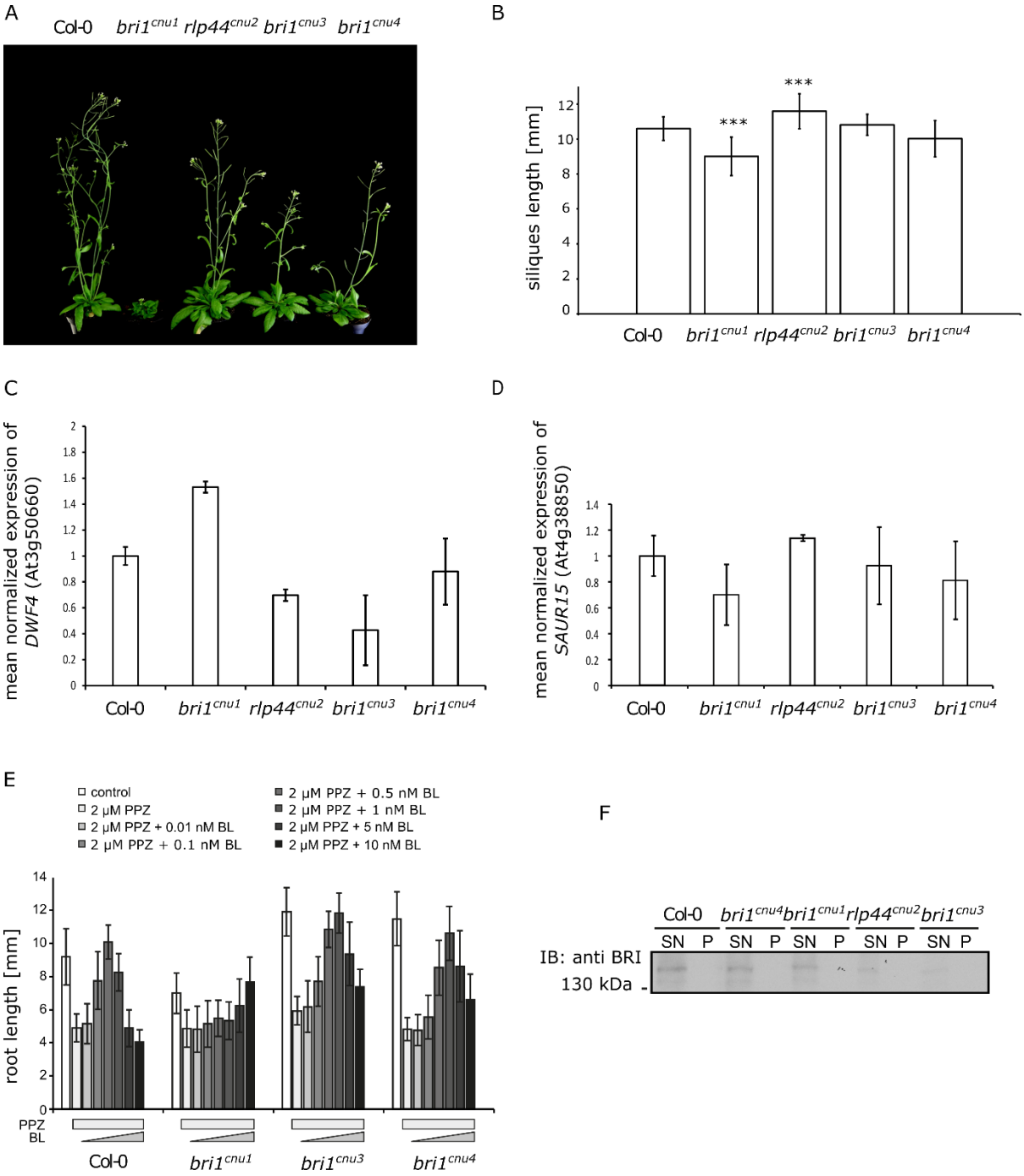


**Figure 18. *bri1*$^{cnu3}$ and *bri1*$^{cnu4}$ show only mild BR-signalling defects.**

(A) Mutants with the adult morphological phenotype of *cnu3* and *cnu4* were crossed to the Col-0 wildtype. Segregating homozygous mutant plants that do not carry the PMEIox transgene and are named *bri1*$^{cnu3}$ and *bri1*$^{cnu4}$.
(B) The siliques of *bri1*$^{cnu1}$ are smaller compared to wildtype siliques. Bars indicate average root length ±SD (n = 30-49). Asterisks indicate statistically significant differences from BRI1-GFP after pairwise t-test (***p < 0.001).
(C) Mean normalized *DWF4* expression levels in Col-0, *bri1*$^{cnu1}$, *rlp44*$^{cnu2}$, *bri1*$^{cnu3}$ and *bri1*$^{cnu4}$. Bars indicate expression level normalized to Col-0 ± SD (n=3). Bars denote mean of qRT-PCR experiments ±SD, n = 3.
(D) Mean normalized *SAUR15* expression levels in Col-0, *bri1*$^{cnu1}$, *rlp44*$^{cnu2}$, *bri1*$^{cnu3}$ and *bri1*$^{cnu4}$. Bars indicate expression level normalized to Col-0 ± SD (n=3). Bars denote mean of qRT-PCR experiments ±SD, n = 3.
(E) Response of Col-0, *bri1*$^{cnu1}$, *bri1*$^{cnu3}$ and *bri1*$^{cnu4}$ to depletion (PPZ) and exogenous supply of brassinosteroids. Bars indicate average relative root length ± SD (n = 34 - 70).
(F). Similar levels of BRI1 proteins in immunoblotting of total protein extracts of Col-0, *bri1*$^{cnu4}$, *bri1*$^{cnu1}$, *rlp44*$^{cnu2}$ and *bri1*$^{cnu3}$ using antiserium against BRI1 (Bojar et al., 2014). (supernatant =SN, pellet =P).

## 2.9 BR receptor function is only mildly affected in BRI1cnu3 and BRI1cnu4

BL sensitivity seemed only to be mildly affected in the *bri1*$^{cnu3}$ and *bri1*$^{cnu4}$ mutants, which indicated a functionally active receptor. However, to confirm that the mutated proteins BRI1cnu3 and BRI1cnu4 were still functional, we introduced the constructs encoding BRI1cnu3, BRI1cnu4 and a version of the protein that carries both mutations (BRI1cnu3,4) into published *bri1* mutants. The expression of the mutated genes was able to complement the weak *bri1-301* (Li and Nam 2002) allele and a T-DNA insertion line (GK-134E10) that constitutes a transcriptional null allele, from hereon named *bri1-null* (Jaillais et al., 2011) (Figure 19A,C). The *bri1-301* is still fertile, this made it possible to directly transform homozygous mutant plants with the respective constructs and we found that plants expressing the constructs were able to rescue the dwarf *bri1* phenotype (Figure 19A).

To assess whether the mutations have an effect on subcellular localization, we analysed the complemented *bri1-null* plants with the pBRI1:BRI1cnu4-GFP and pBRI1:BRI1-GFP constructs with CLSM (Figure 19C). The PM was stained with the endocytic tracer dye FM4-64. The GFP signal derived from the BRI1 mutant and wildtype proteins was associated prominently with the PM, as indicated by the co-localization with FM4-64. No differences in subcellular localization of the pBRI1:BRI1cnu4-GFP could be observed (Figure 19B).

To sum up this part, the proteins BRI1cnu3, BRI1cnu4 and BRI1cnu3,4 were able to display function similar to wildtype BRI1 protein. The three mutated versions complemented the hypomorphic *bri1-301* and the *bri1-null* mutants. Furthermore, subcellular localization was indistinguishable between BRI1cnu4 and BRI1.

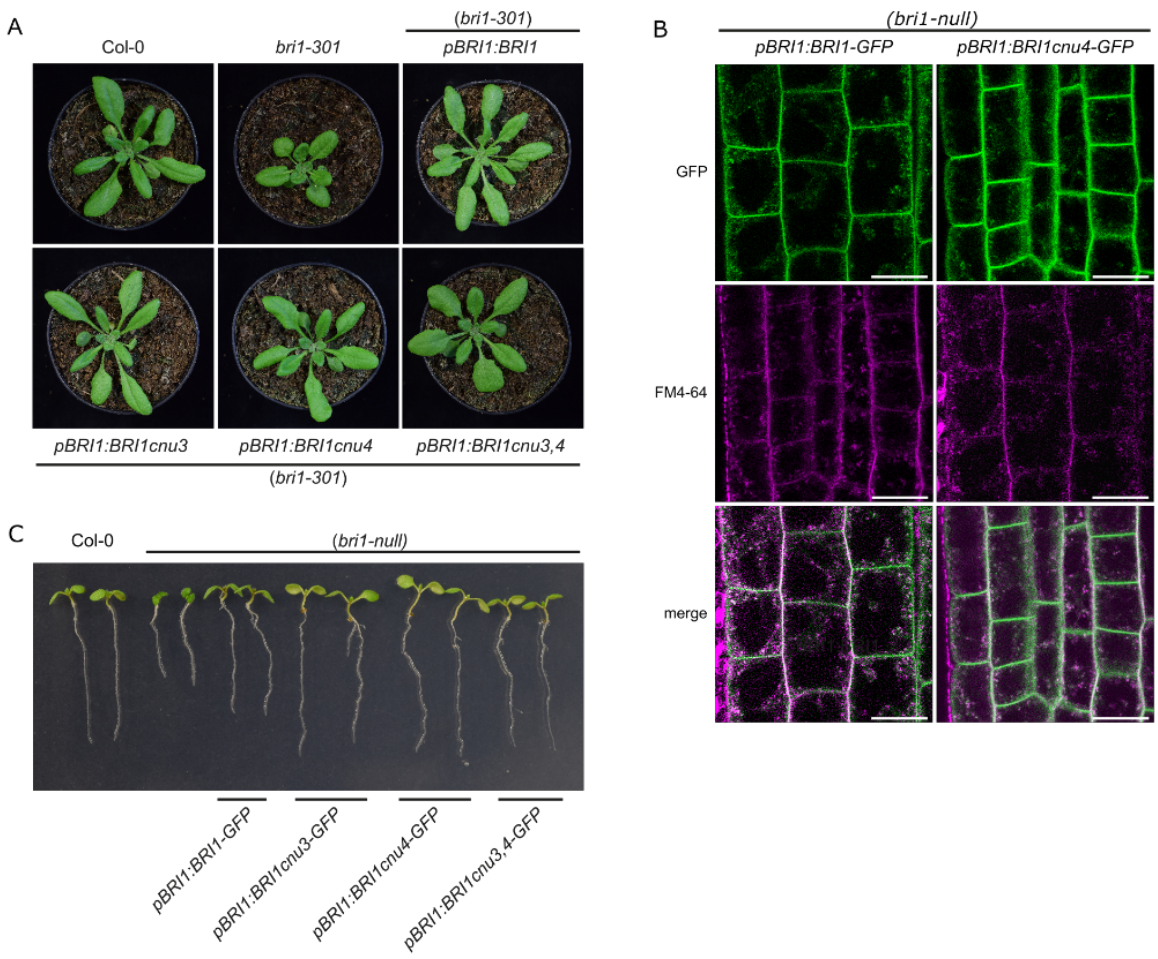


**Figure 19. BRI1 mutant proteins are still functional.**
(A) Mutant BRI1 constructs complement the hypomorphic *bri1-301* mutant.
(B) GFP fluorescence in root meristems of *bri1 null* mutants complemented with GFP fusion proteins from either the construct pBRI1:BRI1-GFP and for the BRI1cnu4 mutant pBRI1:BRI1cnu4-GFP, show no differences in subcellular localization. FM4-64 was used as an endocytic membrane tracer dye. Scale bars = 10 µm.
(C) Mutant BRI1 constructs complement the *bri1-null* mutant.

## 2.10 RLP44 is expressed in the vasculature

To understand the role of RLP44 in plant development, it was important to visualize the expression driven by the endogenous promoter. The transgenic line pRLP44:RLP44-GFP, expressing RLP44 fused to a C-terminal GFP under the control of the RLP44 promoter, enabled us to visualize the expression of RLP44 under *in vivo* conditions. The transgenic plants showed elongated, narrow leafs and elongated petioles, reminiscent of the BRI1 overexpression phenotype (Figure 20A,B) (Friedrichsen et al., 2000). This is consistent with the previously observed BR-signalling activation caused by RLP44 overexpression

(Wolf et al., 2014). Confirmation of the functionality of the transgene was achieved by rescuing the phenotype by crossing it into the *rlp44*$^{cnu2}$ mutant background (Figure 20C). This suggests that the pRLP44:RLP44-GFP construct behaves like the endogenous RLP44. Expression was observed in all tested tissues, however, more prevalent in the root epidermis and root vasculature (Figure 20 D-F). The vasculature of the primary root has a very regular structure and consists of two phloem poles embedded in procambial domains, which are separated by a central xylem axis consisting of two outer protoxylem cells and three inner metaxylem cells. Intriguingly, RLP44-GFP fluorescence in the differentiating part of the root was relatively weak in the phloem, intermediate in xylem, and highest in the undifferentiated procambial cells (Figure 20 G-I).

Briefly summarized, RLP44 driven from the native promoter region enabled us to track RLP44 expression *in planta.* The expression of RLP44 was predominantly present in the stele of the primary root, especially in the procambial cells.

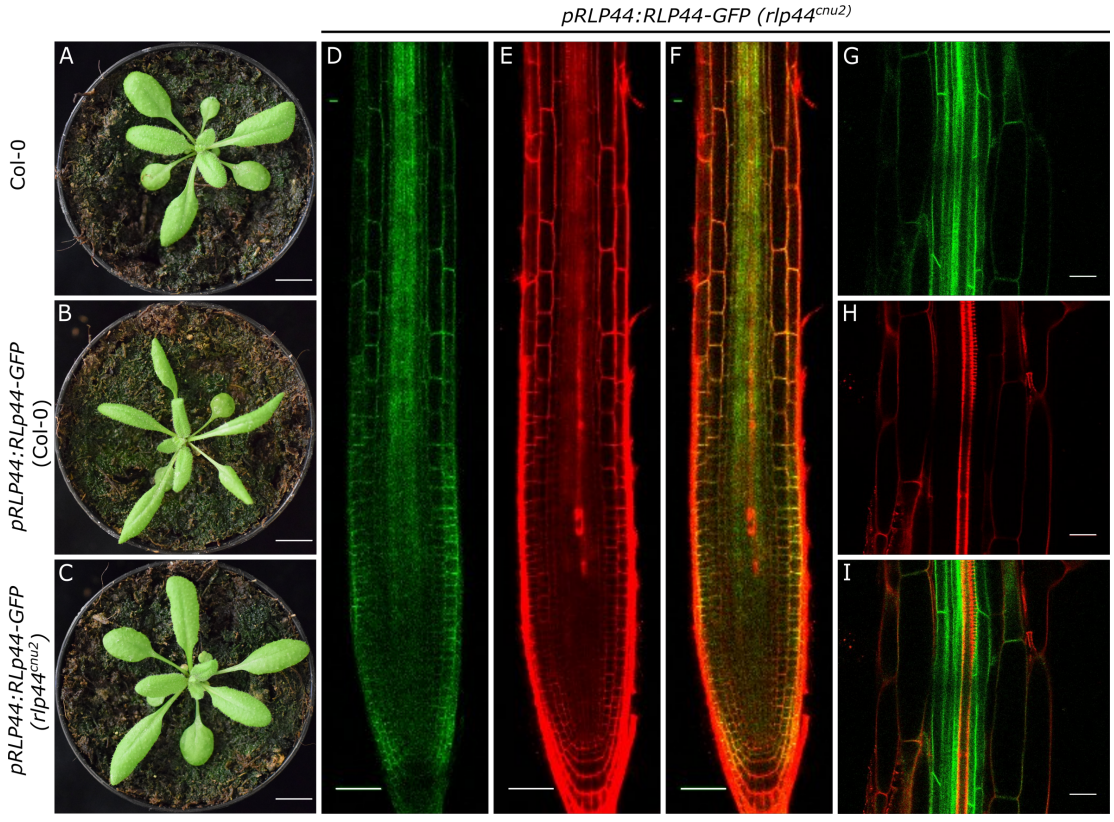


**Figure 20. RLP44 is expressed in the root vascular tissue**
(A-C) pRLP44:RLP44-GFP expression in different backgrounds. Scale bars = 1 cm. (A) adult wildtype plant, Col-0. (B) pRLP44:RLP44-GFP in wildtype background shows a BRI1 overexpression phenotype. (C) pRLP44:RLP44-GFP in *rlp44*$^{cnu2}$ background shows a wildtype-like phenotype.

(D-F) pRLP44:RLP44-GFP expression in *rlp44*$^{cnu2}$ background (D) Root meristem counterstained with (E) propidium iodide and (F) merged. Scale bars = 50 µm.
(G-I) Expression of pRLP44:RLP44-GFP (*rlp44*$^{cnu2}$) (G) in differentiating xylem cells (H) counterstained with propidium iodide and (I) merged. Scale bars = 10 µm.

## 2.11 *rlp44*$^{cnu2}$ and *bri1*$^{cnu4}$ mutants have an increased number of xylem cells

Within this work, we showed that RLP44 is expressed in the vascular tissue (Figure 20). Based on the RLP44 expression, we decided to analyse the vascular development of the primary root in our mutants. The vasculature of the plant is a distinct structure and each tissue type has very specific tasks. During the development of the cell wall of the xylem cells which make up the middle axis of the vasculature – the secondary cell walls get lignified. Lignin can be stained by basic fuchsin, thus we were able to follow the differentiation of tracheary elements by fluorescence microscopy. In wildtype roots, mainly three metaxylem cells in one plane axis are present (Figure 21 A left panel). However, we found an increased number of metaxylem cells in the *rlp44* mutant, primarily in the primary xylem axis. In addition, we frequently observed cells with a metaxylem-like secondary cell wall pattern outside this axis at the position of the procambium (Figure 21 A middle panel). These data suggest a role of RLP44 in determining cell fate of the xylem. Since we already knew that RLP44 can interact with BRI1 and BAK1 to activate the BR-signalling, we wanted to investigate the mechanism in more detail. Further analysis of various *bri1* mutants were mainly performed by Apolonio Ignacio Huerta within his master thesis (Huerta 2016). Hypomorphic *bri1* alleles like the previously described *bri1*$^{cnu1}$ (Wolf et al., 2012), *bri1-301* and *bri1-5* (Noguchi et al., 1999) and as well the BR biosynthetic mutant *constitutive photomorphogenic dwarf (cpd)* (Szekeres et al., 1996) did show a xylem cell number comparable to wildtype (Huerta 2016). On the other hand, *bri1-null* (Jaillais et al., 2011) and a *bri1 brl1 brl3* triple mutant (Vragović et al., 2015), were described to show a strong increase in metaxylem cells (Huerta 2016, Holzwart et al., in revision). Based on these observations, the presence of BRI1 appears to be crucial for the proper development of the vasculature (Caño-Delgado et al., 2004). Next, we analysed the xylem of the *bri1*$^{cnu4}$ mutant. Interestingly, despite its subtle BR-signalling-related defects, *bri1*$^{cnu4}$ displayed a strongly increased number of differentiated xylem cells, in marked contrast to *bri1*$^{cnu1}$, but similar to *rlp44* mutants (Figure 21 A right panel). This clearly distinguished *bri1*$^{cnu4}$ from other BR-related mutants, since they either showed no

abnormalities or showed a xylem phenotype aberrant from the wildtype distribution (*bri1-null* mutants) (Holzwart et al., in revision). This suggested that the mutation in the *BRI1cnu4* gene could have a negative effect on RLP44 protein function.

Metaxylem cells arise within the middle axis and outside this axis, as depicted in Figure 21 B. Next, we analysed if the increase in lignified xylem cells only was the result of an over-proliferation of the vasculature cells in total. For xylem cell quantification, we stained cellulose with calcofluor white and imaged transverse cross-sections in the early elongation zone to count the cells (Figure 21D). Intriguingly, the number of vascular cells did not differ between *rlp44*$^{cnu2}$ and Col-0. However, on average, *bri1*$^{cnu4}$ had more vascular cells (Figure 21D). More vascular cells were also counted in *bri1-null* mutants, consistent with a recent publication (Kang et al., 2017). Thus, we concluded that these phenomena, the disrupted xylem phenotype and increased total stele cell numbers, were based on two independent events. Moreover, in seedlings treated with PPZ, the total vascular cell number was increased, but the metaxylem cell number was not significantly affected in the different genotypes (data not shown, Huerta 2016, Holzwart et al., in revision).

In summary, we assumed that the increase in metaxylem cells phenotype is uncoupled of the outputs of BR-signalling, but depends on the presence of the BRI1 protein.

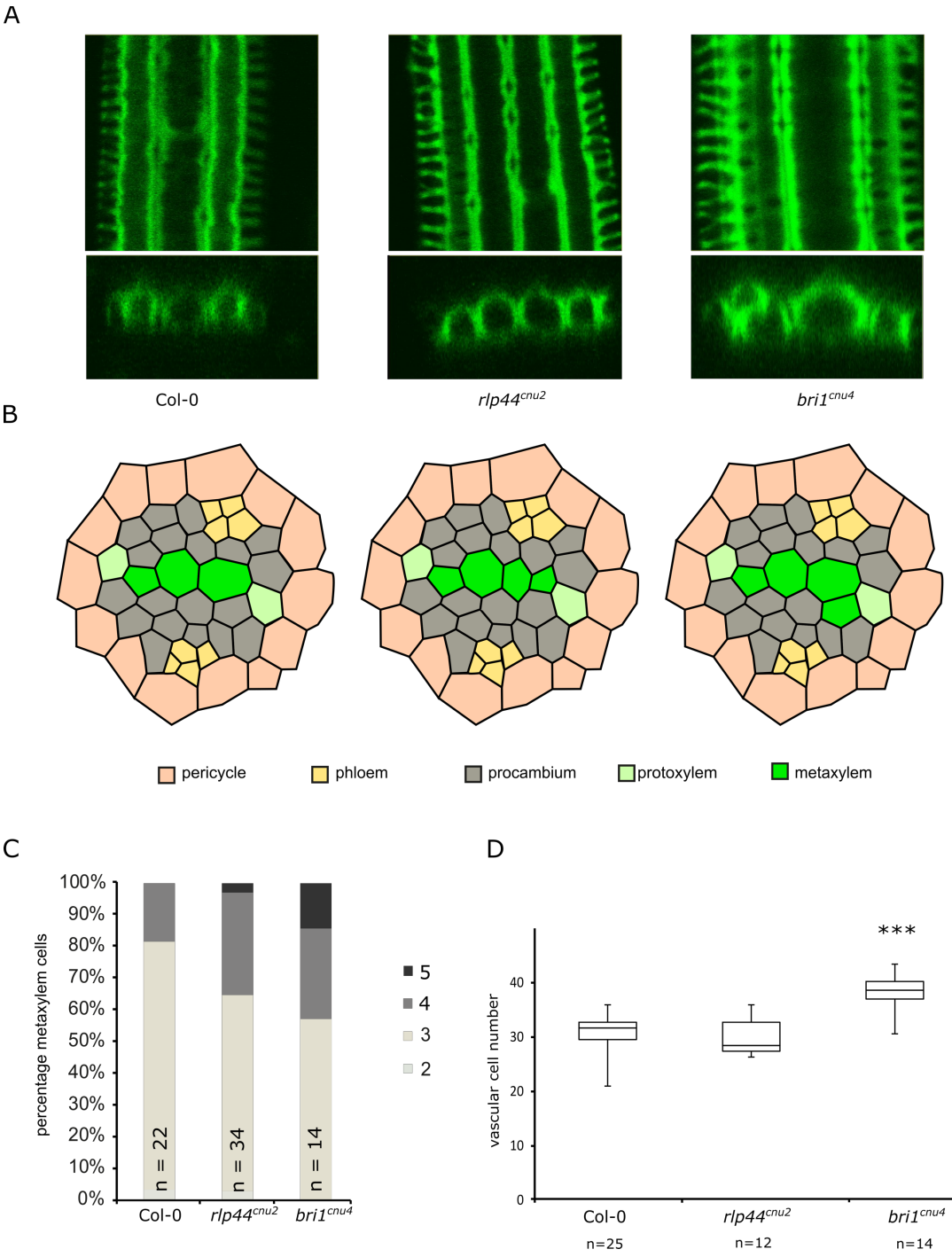


**Figure 21. Description of the xylem phenotype.**
(A) Lignified secondary cell walls of Col-0, *rlp44*$^{cnu2}$ and *bri1*$^{cnu4}$ are stained with basic fuchsin. Confocal stacks allow the quantification of the metaxylem and protoxylem cells numbers.
(B) Schematic overview of the *Arabidopsis* stele.
(C) Quantification of the metaxylem cells of Col-0, *rlp44*$^{cnu2}$ and *bri1*$^{cnu4}$.
(D)Total vascular cell number composed of phloem, procambium, protoxylem and metaxylem. Asterisks indicate statistically significant differences from Col-0 after pairwise t-test with ***$p < 0.001$.

To test the hypothesis that the xylem phenotype is independent from the BR-signalling output, we analysed another BR-deficient mutant, *dwf4-102.* In both *cpd* and *dwf4-102* (Nakamoto 2006), an enzyme of the BR biosynthetic pathway is dysfunctional. We first analysed if both mutants are still responsive to BL. For this, we measured the growth recovery after transferring the seedlings after three days on standard ½ MS plates to plates with supplemented BL. Both BR-deficient mutants showed a rescued growth on the BL-supplemented plate, in contrast to Col-0, which showed a BL-induced growth inhibition (Figure 22A). As a negative control, we used *bri1-null*, which was not responsive (Figure 22A). The lignified cell walls of the vasculature of seedlings were stained with fuchsin and metaxylem cells were quantified on dag 6 without any BL supplemental. Interestingly, besides a weak increase in metaxylem cell number in *dwf4-102* (Figure 22B), the protoxylem showed noticeable gaps or was lacking completely (data not shown). The same protoxylem defect was also reported in previous results of metaxylem quantification after PPZ treatment (data not shown part of Holzwart et al., in revision). PPZ also inhibits the BR biosynthesis though blocking the biosynthetic enzyme DWF4. The effect on the protoxylem may be independent of the previously described effect on the metaxylem cells, because the gaps appeared only in the *dwf4-102* and in the *bri1 brl1 brl3* triple mutant, suggesting a role of BR signalling in protoxylem maintenance (data not shown).

Taken together, these results showed both, *cpd* and *dwf4-102* phenotypes were rescued with BL supplementation. However, while *cpd* exhibited a wildtype-like xylem, *dwf4-102* had a slight increase of seedlings with four metaxylem cells.

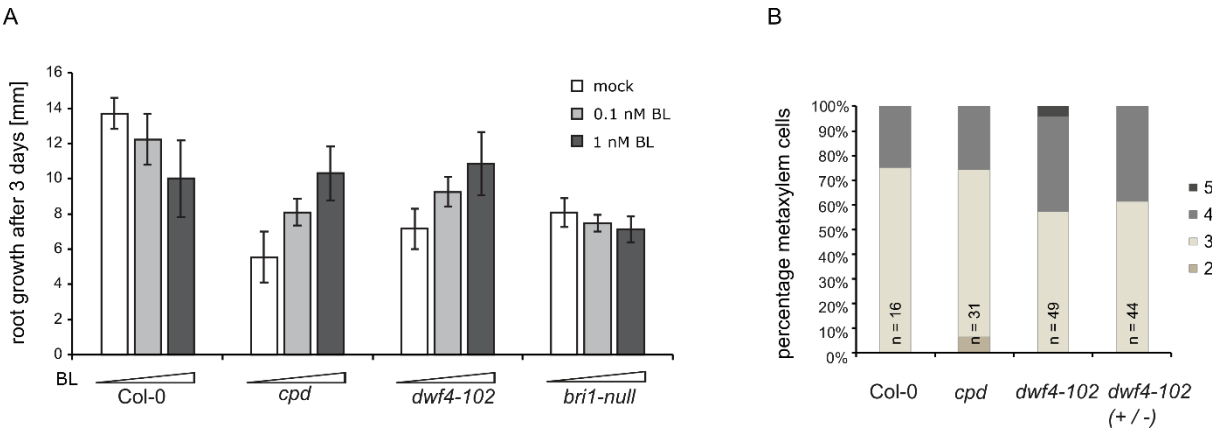


**Figure 22. BR-deficient mutants are rescued with exogenous BL supplementation.**

(A) Root length after 3 days on BL-supplemented plates with indicated concentrations. BR-biosynthesis mutants responds to BL supplementation in a growth-promoting manner. The *bri1-null* mutants is not responsive to BL. Bars denote average root length in mm ±SD after transfer from standard ½ MS plates to BL or DMSO mock treated plated from 4dag to 7 dag.
(B) Quantification of metaxylem cell numbers of Col-0, *cpd*, *dwf4-102, dwf4-102 (+/-).*
This graph is part of Holzwart et al., in revision.

## 2.12 RLP44 levels are decreased in *bri1* mutants

To gain better insight into how BRI1 and RLP44 are linked in the control of xylem cell fate determination, we analysed RLP44 expression levels in BR signalling mutants, as well as in seedlings treated with substances affecting BR signalling. Only the *bri1-null* mutant showed a strong reduction in *RLP44* expression, which might be causative for the xylem phenotype in this mutant (Figure 23A). Overexpression of RLP44-GFP driven by the 35S promoter in the *bri1-null* background was able to rescue the disrupted xylem phenotype (data not shown, Figure is part of Holzwart et al., in revision, experiment performed by Dr. Garnelo Gómez), indicating that RLP44 acts downstream of BRI1 in determining xylem cell fate. However, no effect on *RLP44* expression was detected in either *bri1* hypomorphs like $bri1^{cnu1}$ and *bri1-301* or in the *cpd* mutant (Figure 23C). In addition, neither PPZ, which inhibits BL biosynthesis nor activation of BR-signalling by adding more BL did strongly affect *RLP44* expression (Figure 23D). Furthermore, BR-signalling activation *via* the constitutively active BR-responsive transcription factor BRASSINAZOLE RESISTENT (BZR1-1D) (Wang et al., 2002) or BRI1 EMS SUPPRESSOR dominant mutant (*bes-1D)* (Yin et al., 2002) had an influence on *RLP44* mRNA levels (Figure 23D). Finally, a mutant in the brassinosteroid-insensitive BRASSINOSTREOID-INSENSITIVE2-1 mutant (*bin2-1)* (Li et al., 2001), which did not exhibit an *rlp44* mutant xylem phenotype (data not shown, Huerta 2016), also displayed *RLP44* expression levels comparable to wild type (Figure 23B). Bikinin is an inhibitor of the glycogen synthase kinase 3 (GSK3), like BIN2, thus is BR-signalling promoting but did not effect *RLP44* expression (Figure 23A).

These results suggested that *RLP44* expression requires presence of the BRI1 protein; however, it is independent of BR-signalling outputs. Furthermore, we conclude that BRI1 and RLP44 are part of the same pathway and claim that *RLP44* expression depends on BRI1.Thus RLP44 is acting downstream of BRI1 as part of a pathway distinct from BR-signalling.

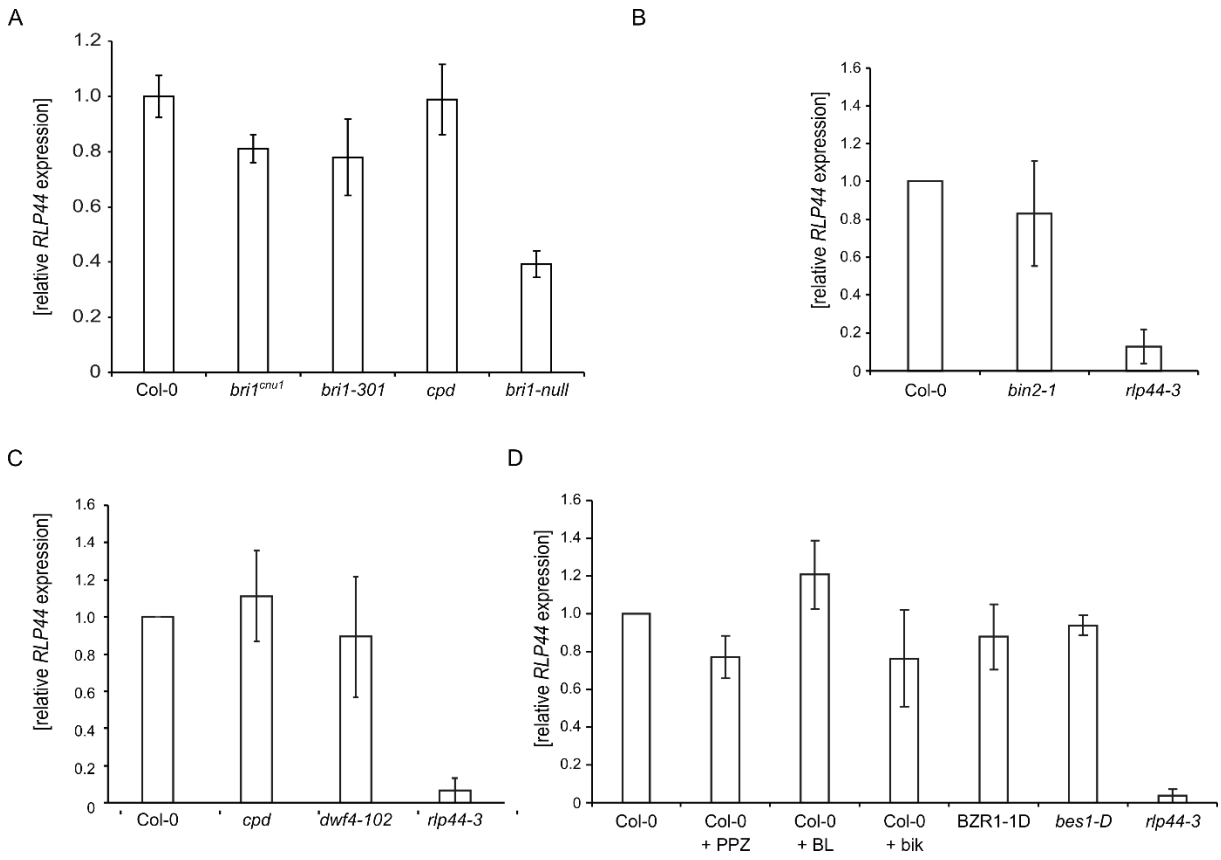


**Figure 23. *RLP44* expression is controlled by BRI1**
(A) qRT-PCR shows reduced RLP44 expression levels *of bri1-null*, but not in the biosynthetic mutant *cpd*. A representative experiment is shown, two independent replicates showed similar results.
(B) qRT-PCR of RLP44 expression levels in the *bin2-1* mutant. Bars indicate expression level normalized to Col-0 ± SD (n=3).
(C) qRT-PCR of RLP44 transcripts in the *cpd* and *dwf4-102* mutants. Bars indicate expression level normalized to Col-0 ± SD (n=3).
(D) Relative RLP44 transcript levels upon the indicated treatments and genotypes. RLP44 expression level is not affected by BR-signalling related cues. Bars indicate expression levels normalized to Col-0 ± SD (n=3). These graphs are part of Holzwart et al., in revision.

## 2.13 RLP44 and BRI1 act in the same pathway

Previously, we showed that RLP44 and BRI1 interact directly (Figure 5). Further, BRI1cnu4 was a still functional BRI1 protein (Figure 19), which was able to suppress the PMEIox phenotype (Figure 16).

To analyse the biochemical influence of the mutation in BRI1cnu4 on the interaction with RLP44, we generated an RLP44-RFP overexpressing line in the *bri1*$^{cnu4}$ background and

analysed the homozygote offspring (Figure 24). Surprisingly, the phenotype of the plants resembled the RLP44-RFP phenotype, which is comparable to the BRI1 overexpression phenotype (Wang et al., 2001) (Figure 24A). This finding was in contrast to the plant phenotype of *bri1*$^{cnu1}$ crossed with RLP44-RFP, which still showed a BR-deficient phenotype (Wolf et al., 2014). Thus, RLP44 could rescue the phenotype of *bri1*$^{cnu3}$ (data not shown) and *bri1*$^{cnu4}$ (Figure 24A), but not the BR-deficient phenotype of *bri1*$^{cnu1}$ (Wolf et al., 2014). Immunological detection of co-purified BRI1 protein with antiserum against the BRI1 kinase domain (Bojar et al., 2014) indicated an enrichment of BRI1cnu4 in complex with RLP44 (Figure 24B). This observation led to the idea, that BRI1cnu4 could have an increased number of metaxylem cells initiated by sequestering RLP44 and preventing its activity in another signalling pathway. This could mean as well that the RLP44-induced BR-activation was not blocked by the *bri1*$^{cnu4}$ mutation and indicates further the participation of both proteins in the same pathway.

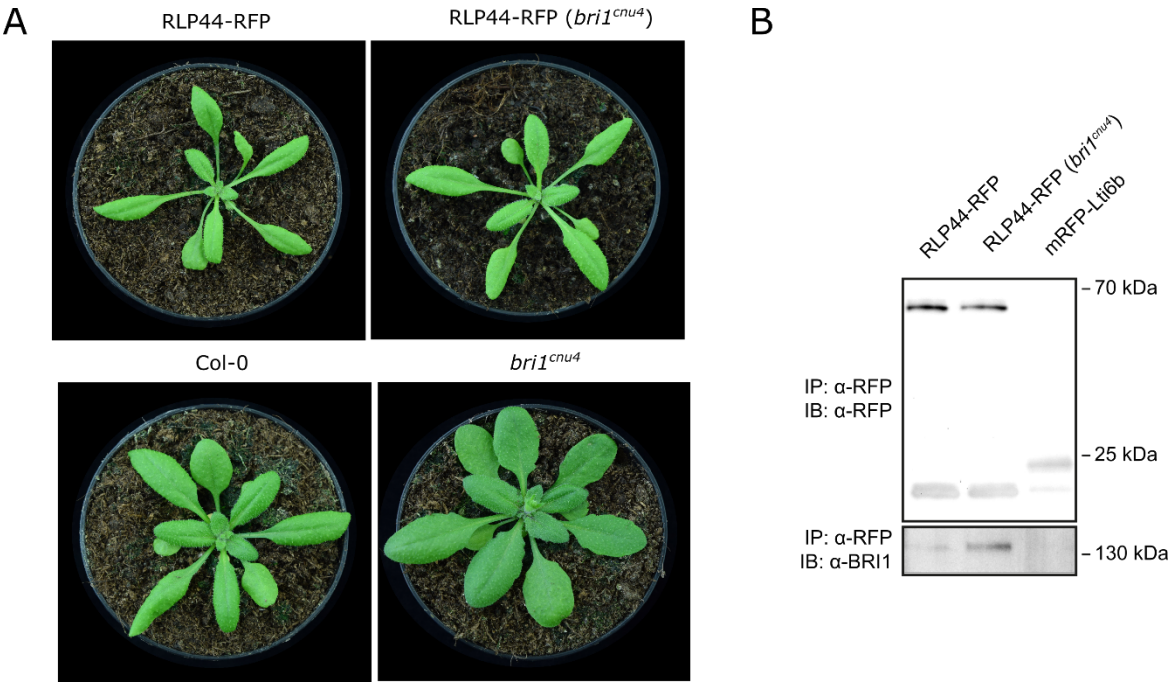


**Figure 24. RLP44 is sequestrated by BRI1cnu4.**
(A) RLP44 overexpression can partially rescue the morphological phenotype of *bri1*$^{cnu4}$.
(B) Co-immunoprecipitation reveals increased complex formation of BRI1cnu4 in 35S:RLP44-RFP containing complexes compared to BRI1. mRFP-Lti6B was used as a negative control and shows no complex formation with BRI1.

As both RLP44 and BRI1 seemed to play a role in determining xylem cell identity, we generated plants harbouring both mutations, *rlp44*$^{cnu2}$ and *bri1*$^{cnu4}$. The morphological phenotype of 3-weeks-old plants showed a similar mutant phenotype in the rosette stage (Figure 25). The leaves of *bri1*$^{cnu4}$ had rounder shape, and this characteristic appeared to be dominant in the double mutants, which displayed a phenotype reminiscent of *bri1*$^{cnu4}$ (Figure 25).

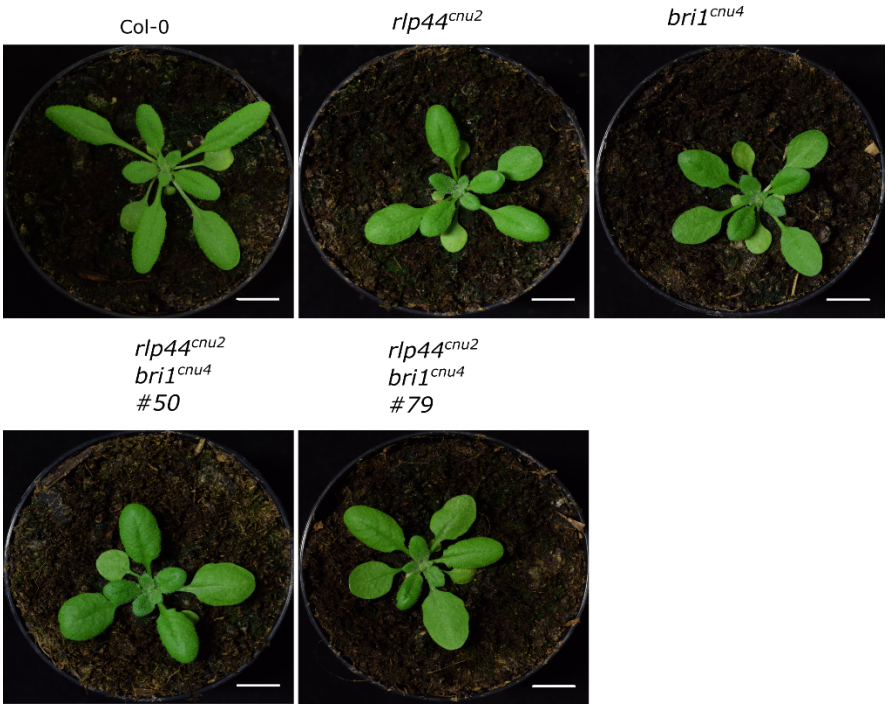


**Figure 25. Morphological phenotype of Col-0, *rlp44*$^{cnu2}$, *bri1*$^{cnu4}$ and *rlp44*$^{cnu2}$/*bri1*$^{cnu4}$.**
Pictures show 3-weeks-old plants. Scale bars = 1 cm

Furthermore, the vasculature of six-day-old mutant seedlings was analysed by staining the lignified secondary cell walls with fuchsin. Interestingly, both independent lines with *bri1*$^{cnu4}$ and *rlp44*$^{cnu2}$ mutations showed the same disordered xylem phenotype, with an increase in metaxylem cells, as the single mutants, respectively (Figure 26).

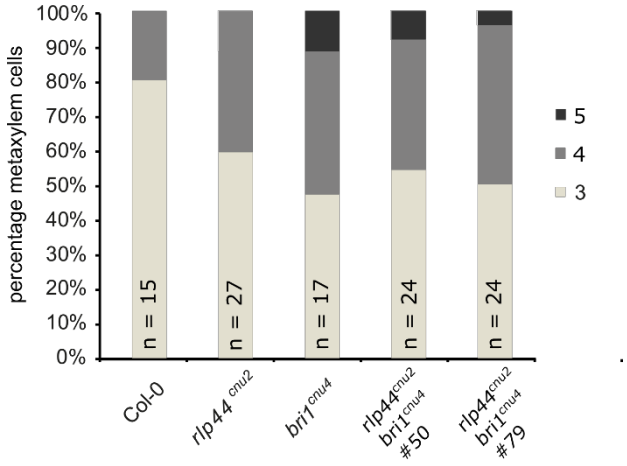


**Figure 26. RLP44 and BRI1cnu4 are active in the same signalling pathway.**
Quantification of metaxylem cells reveals no additional increase in metaxylem cells numbers in two independent double *rlp44*$^{cnu4}$ *bri1*$^{cnu4}$ mutants.

## 2.14 *bri1*$^{cnu4}$ mutation appears to be dominant

In order to assess if the BRI1cnu4 protein has a negative effect on RLP44's function, it was important to test whether the mutation had a dominant effect. Thus, the F1 hybrid seedlings of a *bri1*$^{cnu4}$ and Col-0 crosses were examined for BL-sensitivity, xylem phenotype and morphological phenotype. The BL-sensitivity phenotype seemed to be recessively inherited, since the F1 hybrids did not show the mild BL-insensitivity of the *bri1*$^{cnu4}$ mutant (Figure 27A). Here, mild BL-insensitivity refers to the shift of the response in BL-response for one BL concentration (Figure 27A). Contrary to this trait, the disordered xylem phenotype was dominant in the F1 seedlings (Figure 27B,C).

These results supports our hypothesis that the mutation in BRI1cnu4 is dominant and sequesters RLP44 from being active in another signalling pathway.

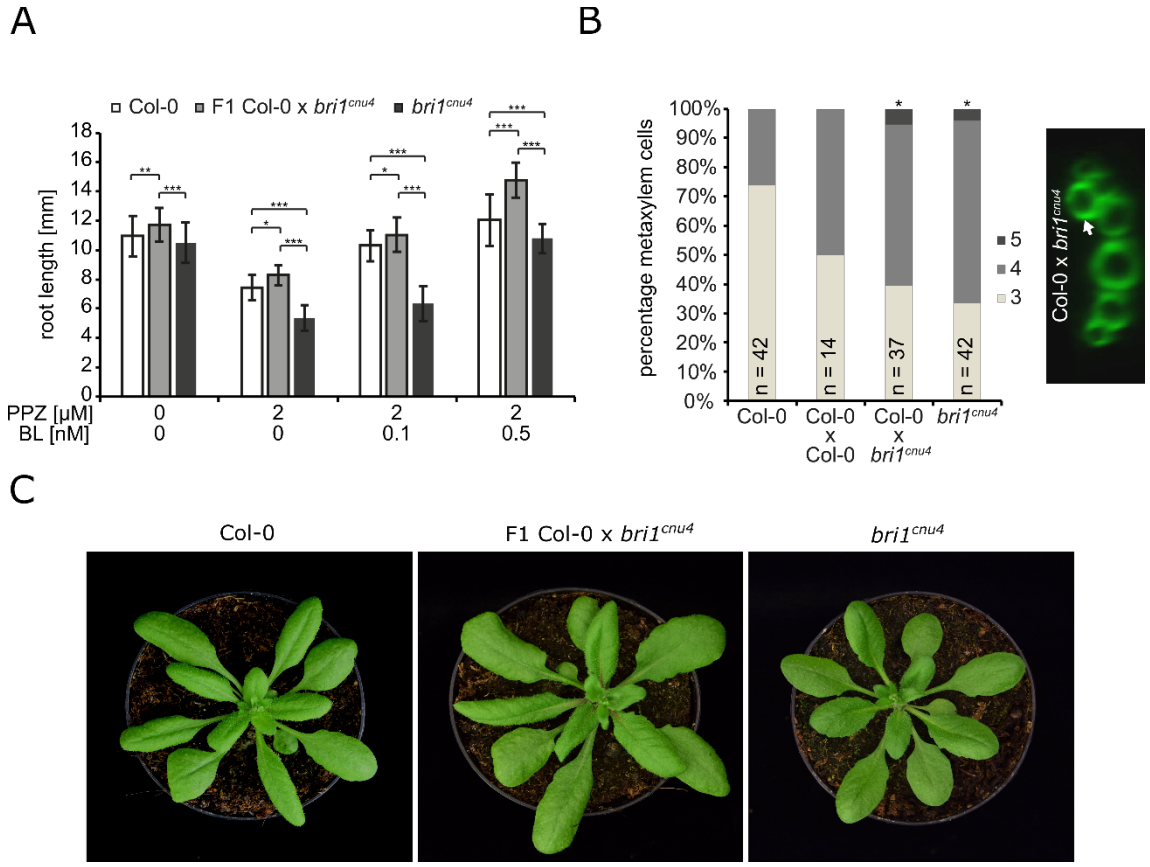


**Figure 27. *bri1*$^{cnu4}$ mutant allele seems to be dominant**.
(A) F1 hybrid seedlings of a cross between *bri1*$^{cnu4}$ and Col-0 show wildtype-like response to depletion (PPZ treatment) and exogenous supply of BL, indicating that mild BL insensitivity conferred by *bri1*$^{cnu4}$ is a recessive trait. Bars indicate mean root length of 5-d-old seedlings ± SD (n = 22-49). Asterisks indicate significance with *p < 0.05, **p < 0.01, and ***p < 0.001 as determined by Tukey's test after two-way ANOVA. Note that significance is only indicated for comparisons within each treatment.
(B) The ectopic xylem phenotype caused by the *bri1*$^{cnu4}$ allele is dominant, as indicated by metaxylem cell number quantification in F1 plants from a cross between *bri1*$^{cnu4}$ and Col-0. Asterisks indicate statistically significant difference from Col-0 based on Dunn's post-hoc test with Benjamini-Hochberg correction after Kruskal-Wallis modified U-test (*p < 0.05)
(C) Morphological phenotype of Col-0, *bri1*$^{cnu4}$, and F1 plants resulting from crossing the both genotypes.

## 2.15 RLP44 directly interacts with PSKR1

The fact that the *rlp44* mutant and the *bri1*$^{cnu4}$ mutant displayed the same disorganized vascular pattern suggests a mechanism in which RLP44 is not functionally active in *bri1*$^{cnu4}$, but cannot activate downstream signalling. As we exclude that RLP44 controls xylem cell fate *via* the BR- signalling pathway, we concluded there could be another pathway of which RLP44 is part of. The structurally most similar based on homology receptor-like kinase to BRI1 is, besides its paralogs BRI LIKE 1-3 (BRL1-3), the receptor

for the phytosulfokine (PSK) peptide, PHYTOSUFOKINE RECEPTOR1 PSKR1 (Shiu and Bleecker 2001). In *Zinnia elegans,* the PSK-signalling pathway was described to induce the trans-differentiation of mesophyll cells into tracheary elements (Yoshikatsu Matsubayashi et al., 1999, Motose et al., 2009). Interestingly, PSK has already been reported to be dependent on functional BR-signalling (Hartmann et al., 2013). Subsequently, in a co-immunoprecipitation experiment performed in infiltrated *N. benthamiana* leaves, we showed that RLP44 was present in immunoprecipitates of PSKR-GFP (Figure 28A). This complex formation appeared to be independent of the availability of the peptide PSK (Figure 28A). Furthermore, direct interaction of PSKR1 and RLP44 was indicated by FRET-FLIM analysis, which showed a clear fluorescence lifetime reduction, indicating a strong interaction (in cooperation with Friederike Wanke and Nina Glöckner) (Figure 28B).

Taken together, we propose that RLP44 interacts with PSKR1.

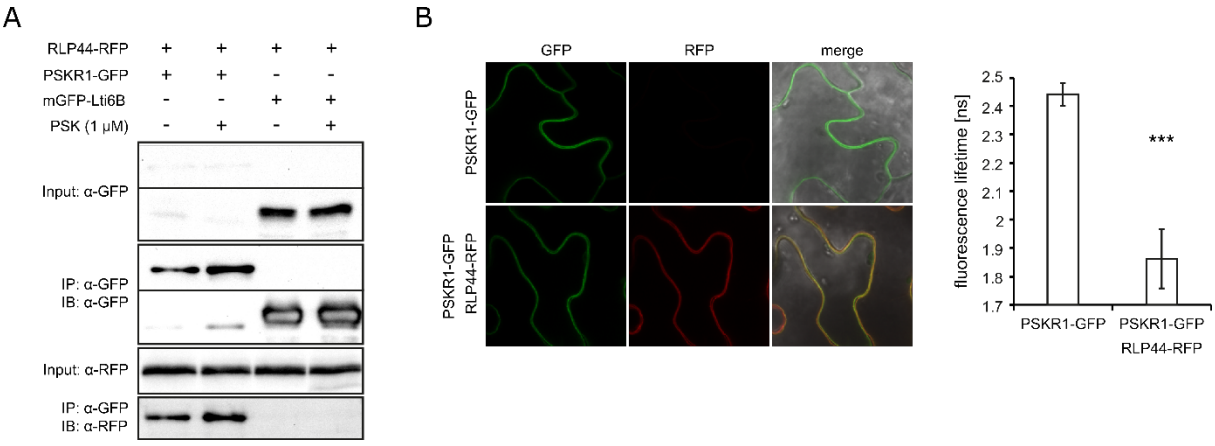


**Figure 28. RLP44 directly interacts with PSKR1**

(A) Co-immunoprecipitation analysis after transient protein co-expression in *N. benthamiana* leaves demonstrates presence of RLP44-RFP in PSKR1-GFP immunoprecipitates, in contrast to immunoprecipitates of mGFP-Lti6B control.

(B) FRET-FLIM analysis of PSKR1-GFP/RLP44-RFP interaction in *N. benthamiana* leaves. Bars denote average of n=9 ± SD. Asterisks indicate statistically significant difference from PSKR1-GFP according to pairwise t-test (***$p < 0.001$).

Nina Glöckner and Friederike Wanke performed FRET-FLIM measurements. This graph is part of Holzwart et al., in revision.

## 2.16 PSK-signalling disturbs the xylem formation

In *Arabidopsis,* two genes encode PSK receptors, *PSKR1* and *PSKR2*. Expression of *PSKR1* is described in roots, hypocotyl (only low levels), leaves, stem and flowers, and *PSKR2* was shown to be mainly expressed in the hypocotyl (Kutschmar et al., 2009, Stührwohldt et al., 2011). Another plant receptor PSYR1, a LRR receptor-like kinase closely related to PSKR1 and PSKR2 (Amano et al., 2007). PSK is sulphated by TPST. To further investigate if PSK-signalling had an impact on xylem cell fate determination, we examined a number of PSK-signalling affected mutants. Amongst them, the *pskr1-3 pskr2-1* double mutant (Kutschmar et al., 2009) showed an increased number of xylem cells, similar to the *rlp44* mutant (Figure 29A). The same was observed for the double mutant of *pskr1-3 psy1r* and the *tpst-1* mutant (Komori et al., 2009; Matsuzaki et al., 2010). In addition, overexpression of PSKR1 (Ladwig et al., 2015) led to an increase to four metaxylem cells (Figure 29A). Furthermore, we generated *rlp44*$^{cnu2}$ *pskr1-3* double mutant and the *rlp44*$^{cnu2}$ *pskr1-3 pskr2-1* triple mutants. These mutants exhibited the same disordered xylem mutant phenotype, indicating that the proteins are likely involved in the same signalling pathway (Figure 29B).

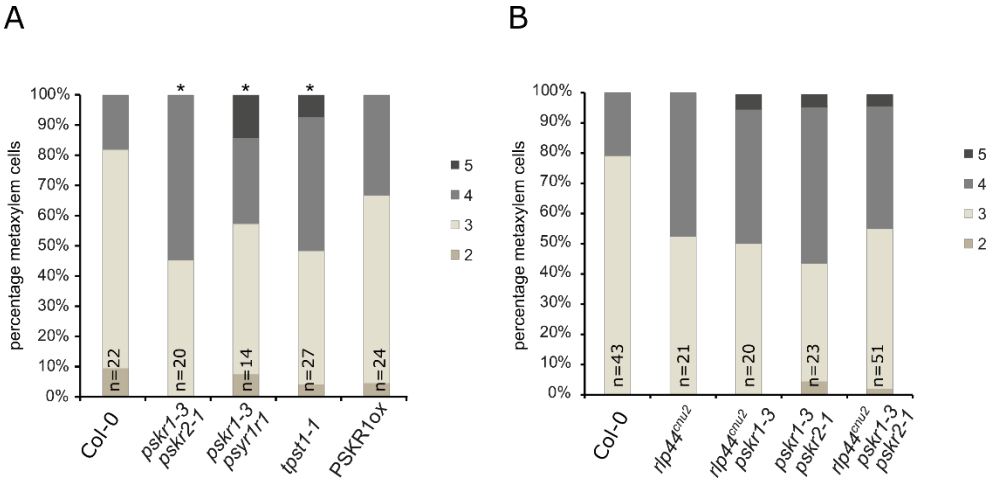


**Figure 29. PSK-signalling related mutants show a disordered xylem phenotype**.
Quantification of metaxylem cell number in Col-0 and PSK-signalling-related mutants. Asterisks indicate statistically significant difference from Col-0 based on Dunn's post-hoc test with Benjamini-Hochberg correction after Kruskal-Wallis modified U-test (*p < 0.05).
This graph is partially in Holzwart et al., in revision.

## 2.17 PSK but not BL has an effect on the xylem phenotype

Our results indicated that the xylem phenotype was caused by the absence of RLP44, the interaction partner of PSKR1. If this was the case, we could try to compensate for the absence of RLP44 by activating PSKR1 *via* exogenous PSK supplementation. Consequently, we exogenous supply with the 1 µM PSK for six days in liquid media was able to rescue the phenotype and restore the wildtype composition of xylem in *rlp44* mutants. Interestingly, it was not possible to rescue the xylem phenotype of *bri1*$^{cnu4}$ (Figure 30). In addition, Split-ubiquitin data from yeast provided by Nina Glöckner hint to a sequestration of BAK1 by BRI1cnu4.

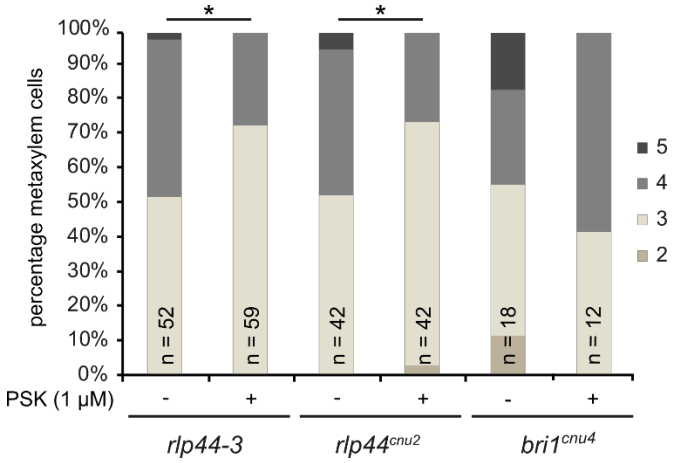


**Figure 30**. **PSK rescues the disrupted *rlp44* xylem mutant phenotype.**
Application of PSK peptide rescues the ectopic xylem phenotype of *rlp44*$^{cnu2}$ but not the one of *bri1*$^{cnu4}$. Asterisks indicate statistically significant difference according to Mann-Whitney U-test (*p < 0.05).
This graph is partially in Holzwart et al., in revision.

With the supplementation of 1 µM PSK we were able to partially rescue the short root phenotype of the *tpst-1* mutant (Figure 31B) (Matsuzaki et al., 2010). In contrast to the Col-0 wildtype control, which did not respond to the PSK treatment with respect to xylem development, *tpst-1* xylem showed an alteration to wildtype metaxylem cell distribution (Figure 31A).

We noted a strong, PSKR1 and 2-dependent root elongation effect upon PSK treatment in Col-0, which occurred after we used a freshly dissolved peptide (Thermo Fisher). The PSK (PolyPeptide) induced root elongation effect on Col-0 in another approach (Figure 35) was less pronounced, but consistent with the literature (Matsubayashi 2006). Nevertheless, PSK

did not affect the xylem phenotype of Col-0. Furthermore, the PSK effect on root length was not significantly different in the *rlp44*$^{cnu2}$ mutant (Figure 31A).

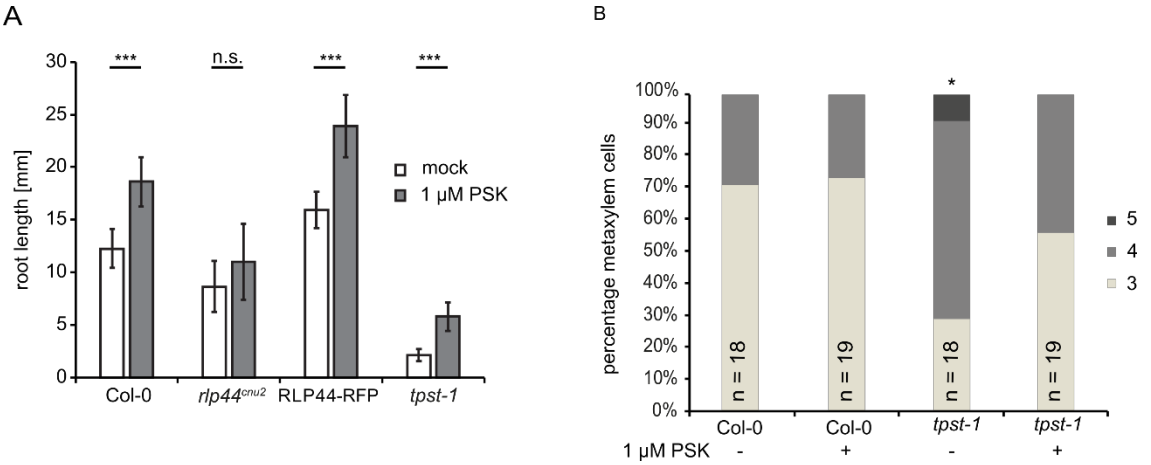


**Figure 31. PSK rescues partially the disrupted xylem phenotype of *tpst-1*.**
(A) Col-0, RLP44-RFP and *tpst-1* respond to 1 µM PSK treatment, however *rlp44*$^{cnu2}$ appears to be insensitive. Bars indicate mean root length of 5-d-old seedlings ± SD (n = 19-21). Asterisks indicate significance with ***p < 0.001 as determined by Tukey's test after two-way ANOVA.
(B) Quantification of metaxylem cell numbers in Col-0 and *tpst-1* mutants. Exogenous application of 1 µM PSK partially rescues the disrupted xylem phenotype to a more wildtype-like xylem. Asterisks indicate statistically significant difference from Col-0 based on Dunn's post-hoc test with Benjamini-Hochberg correction after Kruskal-Wallis modified U-test (*p < 0.05).

According to the previously obtained results, indicating that BR-deficient mutants such as *cpd* did not show altered xylem cell number, we next wanted to confirm the BL-independence of the xylem phenotype. Therefore, we first estimated the appropriate concentration for the BL supplement, without prior depletion using PPZ. We determined that growth inhibiting effects can be observed at 0.1 nM BL (Figure 32A), however, no shift on xylem cell formation in seedlings of neither Col-0 wildtype, nor the *pskr1-3 pskr2-1*, *rlp44*$^{cnu2}$ and *bri1*$^{cnu4}$ mutants was detected (Figure 32B).

In conclusion, the exogenous PSK application was able to rescue the *rlp44* mutant xylem phenotype, but not in *bri1*$^{cnu4}$, and any additional BL did not have any consequence on the xylem cells.

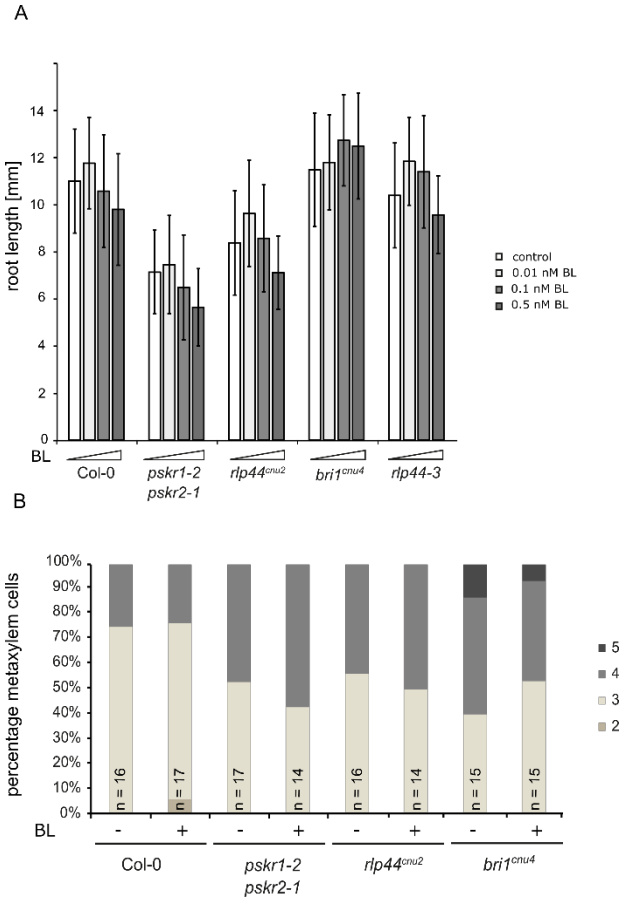


**Figure 32. Effect of BL supplement on root length and xylem formation.**
(A) Response of Col-0, *pskr1-2/pskr2-1, rlp44*$^{cnu2}$, *bri1*$^{cnu4}$ and *rlp44-3* to depletion (PPZ) and exogenous supply of brassinosteroids indicates no differences between the genotypes besides the already described mild BR-insensitivity of *bri1*$^{cnu4}$. Bars indicate average relative root length ± SD (n = 43 - 58).
(B) Quantification of metaxylem cells of 6-d-old seedlings treated continuously with 0.1 nM BL show no influence of BL on metaxylem cell formation.

## 2.18 PSK-signalling impaired genotypes are still brassinosteroid sensitive

A relation between PSK and BR-signalling has already been suggested, and previously, it has been shown that PSK-signalling depends on functional BR-signalling (Hartmann et al., 2013). Therefore, we wanted to investigate if BL-sensitivity depends on PSK-signalling, and analysed if PSK-signalling-defective mutants are still able to sense BL. Hence, we used *pskr1-3 pskr2-1* (Kutschmar et al., 2009), *rlp44*$^{cnu2}$ (Wolf et al., 2014), *rlp44*$^{cnu2}$ *pskr1*-3, PSKR1ox (Ladwig et al., 2015), and *tpst-1* (Komori et al., 2009) plants and monitored BL response after BL-depletion with PPZ. In Figure 33, absolute root lengths are depicted. The mutants related to the receptors for PSK were not affected in their BR-sensitivity, as the growth promoting and inhibiting effect of BL was indistinguishable from the Col-0

wildtype (Figure 34A). However, the overexpression of the PSKR1 lead to an insensitivity to PPZ. Furthermore, *tpst-1* was hypersensitive to PPZ and exhibited a reduced response to BL (Figure 34A). In addition, we analysed the impact of PSKR1 overexpression in the *bri1*$^{cnu4}$ background on the BL sensing. Impaired BL-sensitivity of *bri1*$^{cnu4}$ appeared to be epistatic when overexpressing PSKR1, as it led to the same mild BL- insensitivity mentioned above as a characteristic for *bri1*$^{cnu4}$ (Figure 34B).

These results suggested that PSK-signalling defective genotypes were still able to perceive BL comparable to the wildtype.

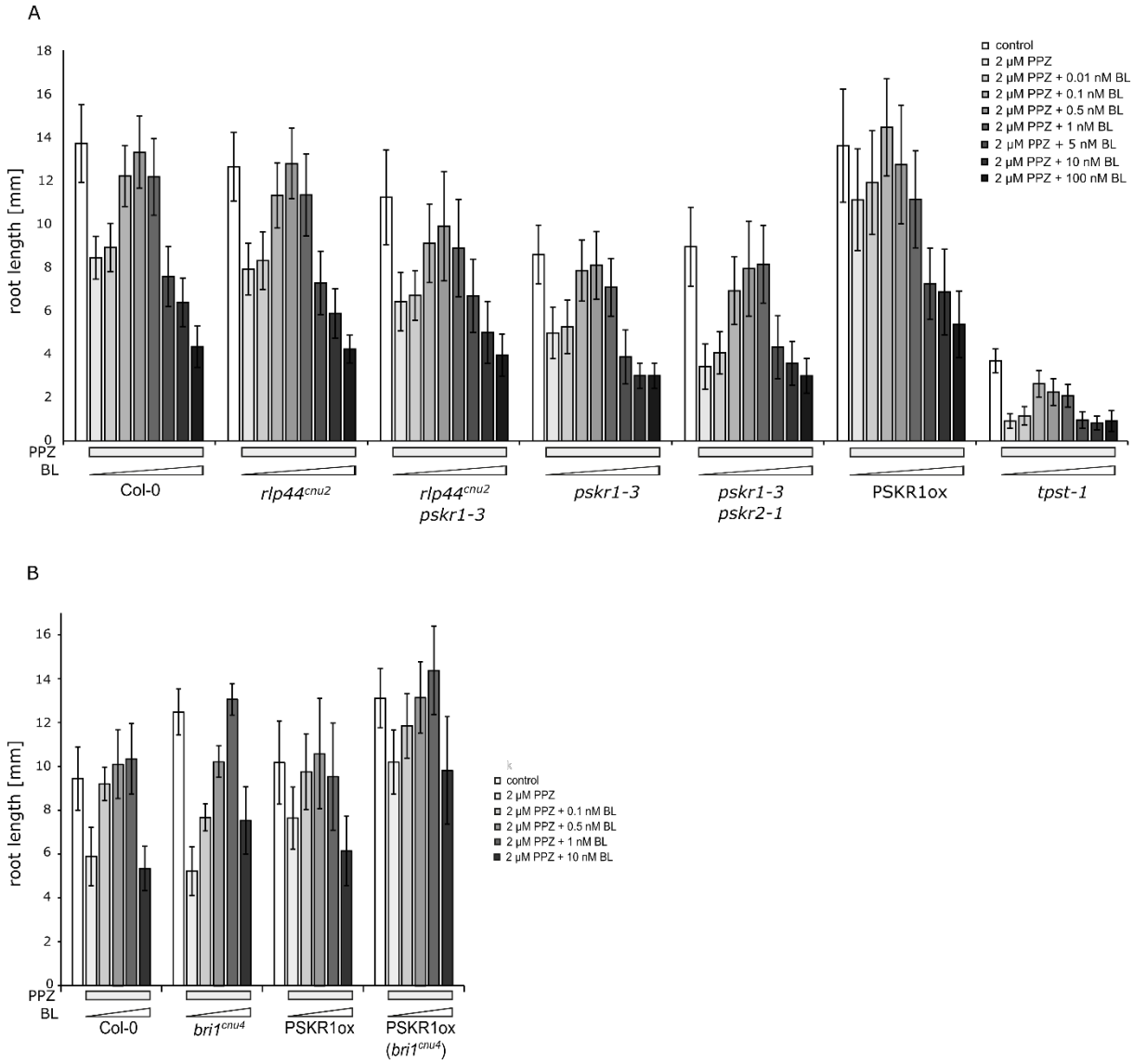


**Figure 33. PSK-signalling impaired mutants are still BL-sensitive.**

(A) Response of Col-0, *rlp44*$^{cnu2}$, *rlp44*$^{cnu2}$ *pskr1-3, pskr1-3*, *pskr1-3 pskr2-1*, PSKR1ox and *tpst-1* to depletion (PPZ) and exogenous supply of brassinosteroids. Bars indicate average relative root length ± SD (n = 36 – 93).
(B) Response of Col-0, *bri1*$^{cnu4,}$ PSKR1ox, PSKR1ox (*bri1*$^{cnu4}$) to depletion (PPZ) and exogenous supply of brassinosteroids. Bars indicate average root length ± SD (n = 16-20).

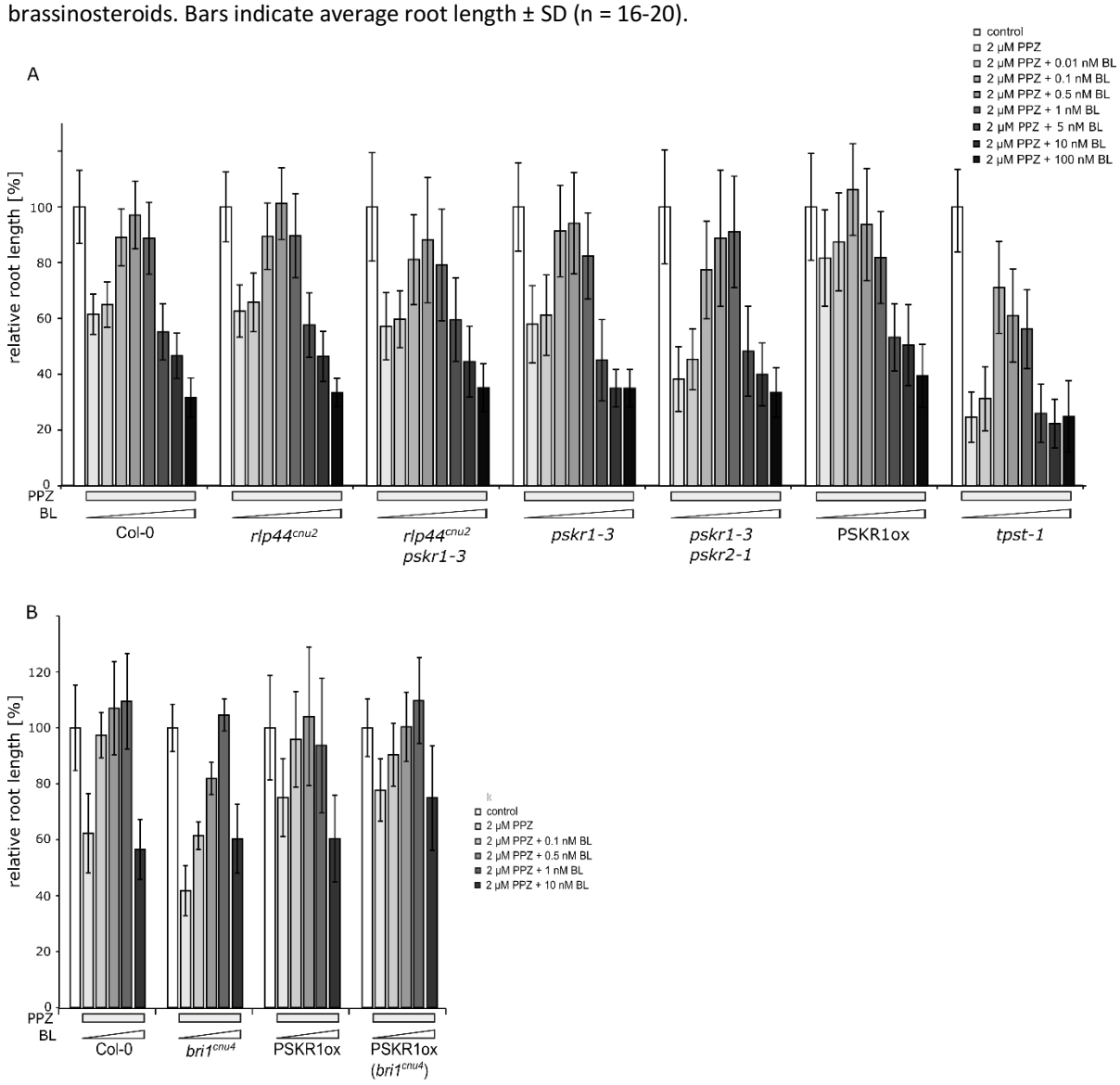


**Figure 34. PSK-signalling impaired mutants are still BL-sensitive (relative representation).**
(A) Response of Col-0, *rlp44*$^{cnu2}$, *rlp44*$^{cnu2}$ *pskr1-3, pskr1-3*, *pskr1-3 pskr2-1*, PSKR1ox and *tpst-1* to depletion (PPZ) and exogenous supply of brassinosteroids. Bars indicate average relative root length ± SD (n = 36 – 93).
(B) Response of Col-0, *bri1*$^{cnu4,}$ PSKR1ox, PSKR1ox (*bri1*$^{cnu4}$) to depletion (PPZ) and exogenous supply of brassinosteroids. Bars indicate average relative root length ± SD (n = 16-20).

## 2.19 BL-sensitivity is independent of PSK

The BL-sensitivity after depletion of endogenous BL with PPZ showed wildtype-like growth-promoting and growth-depletion responses in *pskr* mutants (Figure 34). To assess the effect of PSK, we compared root length of seedlings with additional 1 µM PSK to mock treated plants. Previously, a PSK-induced root elongation effect of 10% on Col-0 roots was described (Matsubayashi 2006). We were able to reproduce this effect on Col-0 and no effect was visible on the *pskr* mutants, and neither on *rlp44*$^{cnu2}$, *bri1*$^{cnu4}$. Contradictory to the literature (Hartmann et al., 2013) longer roots upon exogenous application of PSK were measured in the hypomorphic *bri1*$^{cnu1}$ mutant (Figure 35).

To decipher the connection between PSK and BR-signalling we next examined how the BL-sensitivity was affected in presence of additional PSK in *pskr* mutants, *rlp44*$^{cnu2}$, *bri1*$^{cnu4}$, and *bri1*$^{cnu1}$. However, the results indicated that an excess of PSK did not affect the BL-response (Figure 37). In Figure 36, absolute root lengths are depicted.

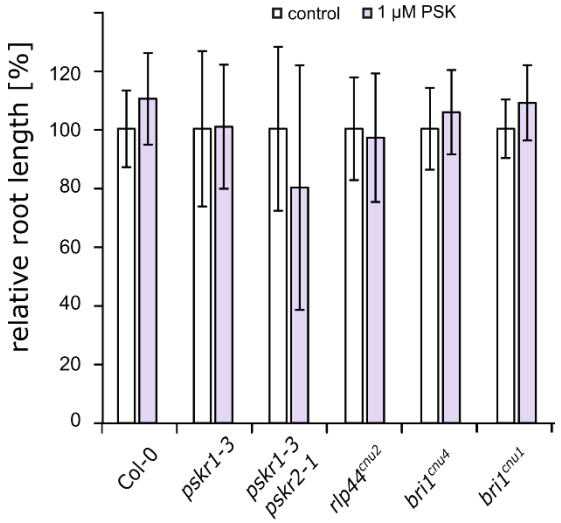


**Figure 35. PSK has an effect on root length root.**
Root elongation effect on root length of Col-0, *pskr1-3*, *pskr1-3 pskr2-1*, *bri1*$^{cnu4}$, *rlp44*$^{cnu2}$, *bri1*$^{cnu4}$ and *bri1*$^{cnu1}$ upon 1 µM PSK treatment. Bars indicate average relative root lengths ± SD (n = 13 – 21).

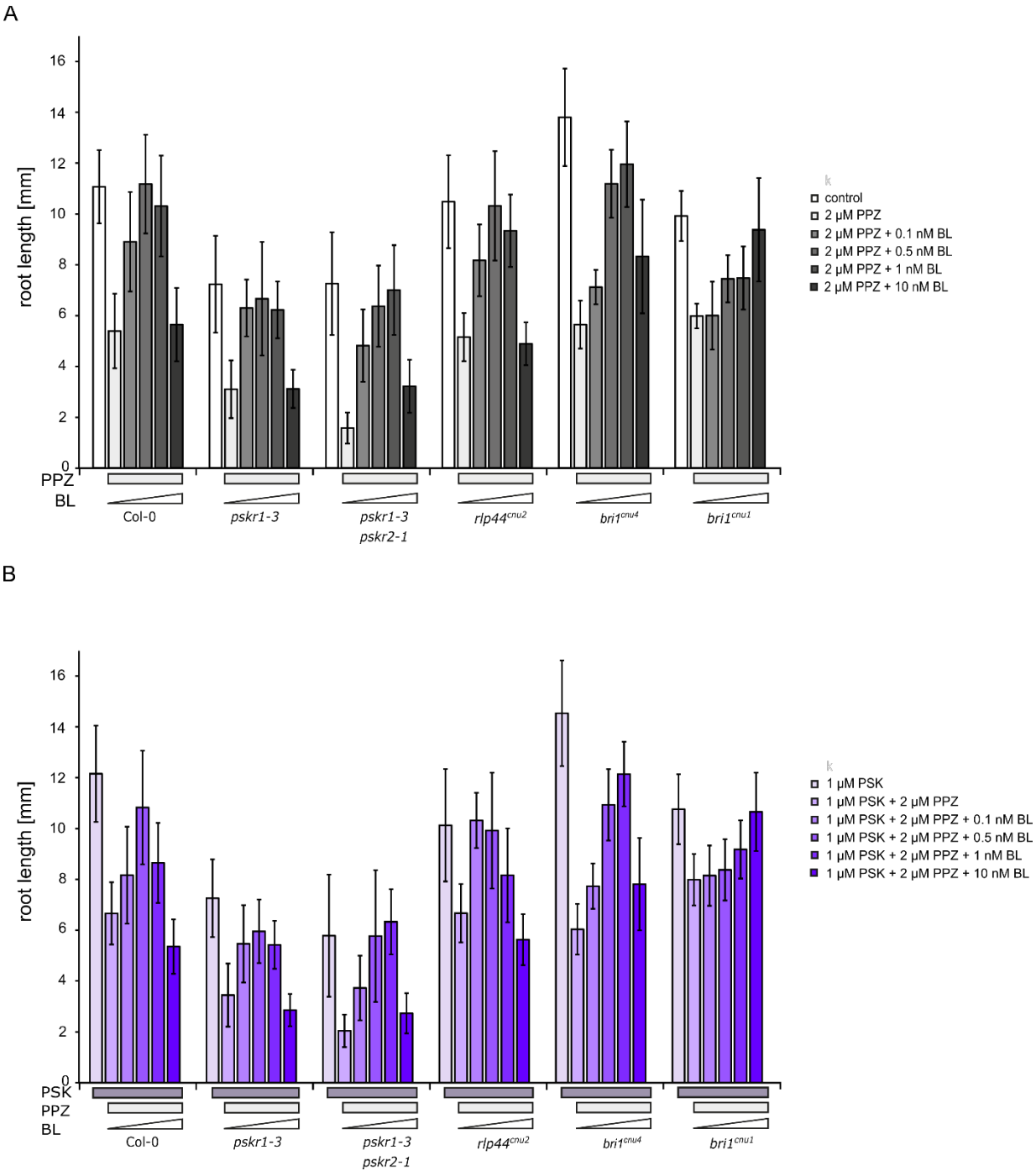


**Figure 36. Additional supply with PSK has no effect on BL sensitivity**
(A) Response of Col-0*, pskr1-3*, *pskr1-3 pskr2-1*, *rlp44*$^{cnu2}$*, bri1*$^{cnu4}$ and *bri1*$^{cnu1}$ to depletion of endogenous BL by PPZ and exogenous supply of brassinosteroids. Bars indicate average root lengths ± SD (n = 13 – 21).
(B) Response of Col-0*, pskr1-3*, *pskr1-3 pskr2-1*, *rlp44*$^{cnu2}$*, bri1*$^{cnu4}$ and *bri1*$^{cnu1}$ to depletion of endogenous BL by PPZ and exogenous supply of brassinosteroids in presence of PSK. Bars indicate average root lengths ± SD (n = 14-21).

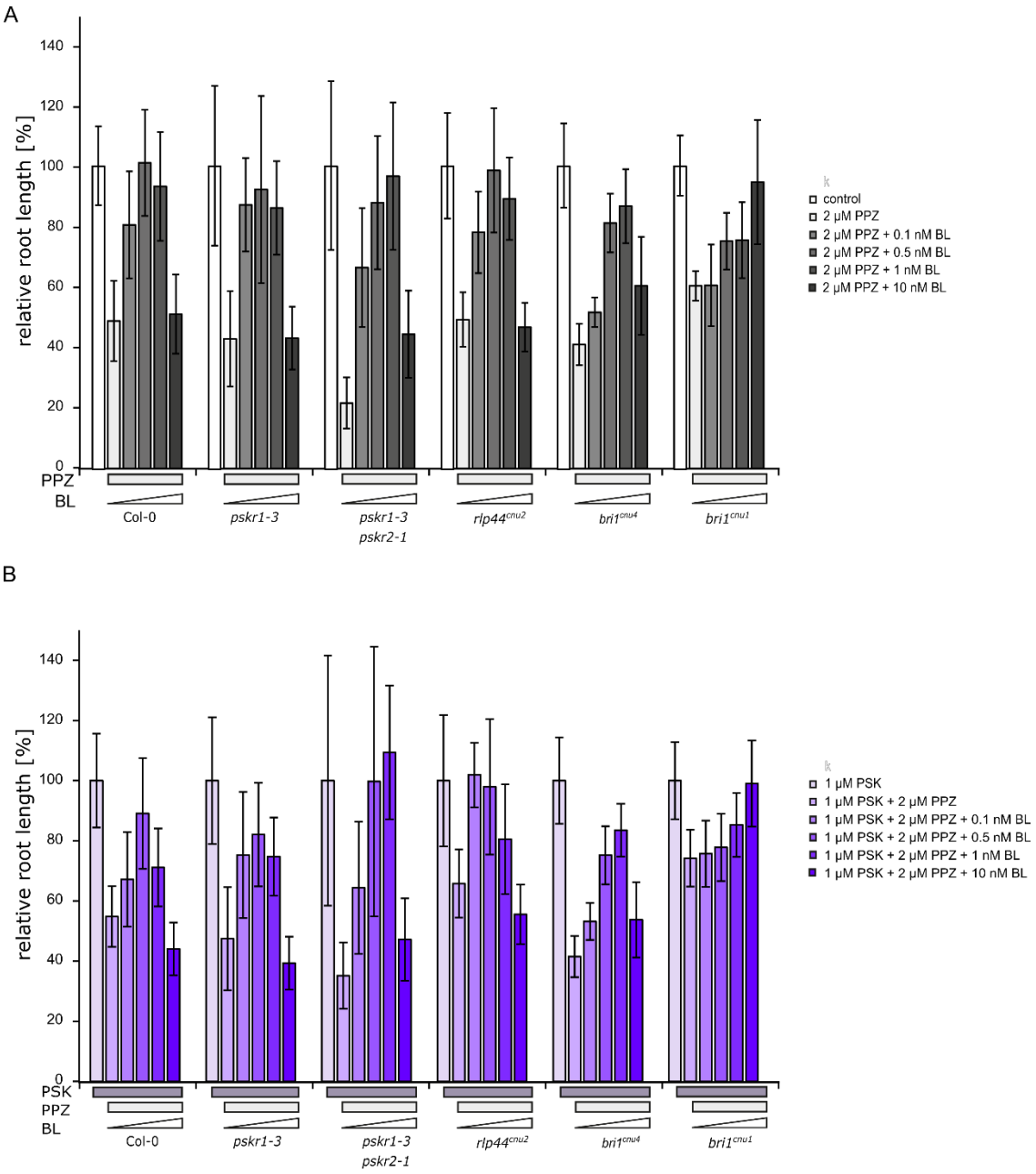


**Figure 37. Additional supply with PSK has no effect on BL sensitivity (relative representation).**
(A) Response of Col-0*, pskr1-3*, *pskr1-3 pskr2-1*, *rlp44*$^{cnu2}$*, bri1*$^{cnu4}$ and *bri1*$^{cnu1}$ to depletion of endogenous BL by PPZ and exogenous supply of brassinosteroids. Bars indicate average relative root lengths ± SD (n = 13 – 21).
(B) Response of Col-0*, pskr1-3*, *pskr1-3 pskr2-1*, *rlp44*$^{cnu2}$*, bri1*$^{cnu4}$ and *bri1*$^{cnu1}$ to depletion of endogenous BL by PPZ and exogenous supply of brassinosteroids in presence of PSK. Bars indicate average relative root lengths ± SD (n = 14-21).

## 2.20 RLP44 promotes BAK1 and PSKR1 interaction

RLP44 is localized in the PM and lacks a kinase domain. Presumable as other RLPs it cannot execute its function without the help of kinases to transfer the signal (Ma et al., 2016). Previously, we were able to demonstrate that RLP44 interacts with BAK1 (Wolf et al., 2014) and with BRI1 (Figure 5). To understand the mechanism of RLP44-mediated promotion of BR signalling we used stable *Arabidopsis* plants overexpressing RLP44-mCherry in a pBRI1:BRi1-mCitrine / pBAK1:BAK1-HA line for co-immunoprecipitation experiments. We detected stronger level for BAK1 in the BRI1-mCitrine GFP-trap co-immunoprecipitates when RLP44 was present (Garnelo Gómez 2017).

This led to the assumption that RLP44 takes on a scaffolding role and promotes the interaction between BAK1 and BRI1. Notably, PSRK1 has also been published to interact with BAK1 (Ladwig et al., 2015), hence we investigated if RLP44 could influence the complex of PSKR1 and BAK1 in a similar manner. Co-immunoprecipitation analysis after transient expression of 35S:PSKR1-GFP, 35S:BAK1-HA and 35S:RLP44-RFP in *N. benthamiana* leaves resulted in an increased signal of BAK1-HA in PSKR1-GFP immunoprecipitates in the presence of RLP44-RFP (Figure 38A). This effect could be enhanced by increasing RLP44-RFP expression via the used amount of Agrobacteria used. With higher levels of RLP44-RFP (indicated via ++ in Figure 38A), more BAK1-HA was detected in PSKR1-GFP co-immunoprecipitates.

Additionally, this result was confirmed in stable *Arabidopsis* line overexpressing 35S:PSKR1-GFP in the *rlp44*$^{cnu2}$ background, where higher levels of BAK1 were immunodetected in presence of RLP44 (wildtype background) (Figure 38B).

Therefore, we proposed that RLP44 acts as a scaffolding protein for BAK1 and PSKR1 and modulates their complex formation, however, independent of additional PSK ligand (Figure 28A).

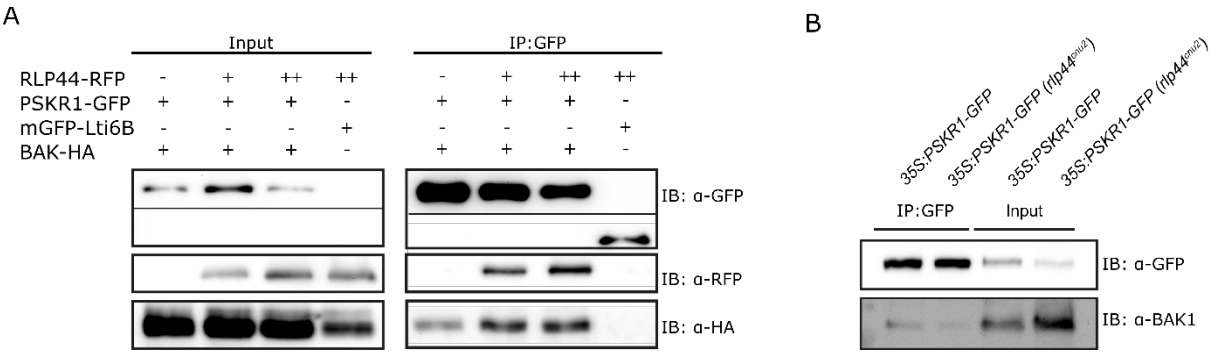


**Figure 38. Presence of RLP44 modulates the PSKR1-BAK1 complex formation.**
(A) Co-immunoprecipitation after transient expression in *N. benthamiana* leaves shows an increased amount of BAK1-HA in PSKR1-GFP immunoprecipitates in presence of RLP44-RFP. RLP44 levels were adjusted through increasing the density of Agrobacteria (denoted by + or ++).
(B) BAK1 is decreased in immunoprecipitates of stable *Arabidopsis* lines overexpressing PSKR1-GFP in the *rlp44*$^{cnu2}$ background. Antiserum was raised against BAK1.
This figure is part of Holzwart et al., in revision.

## 2.21 Do PSKR1 and BRI1 compete for RLP44?

RLP44 was shown to interact through its cytoplasmic domain with both PSKR1 (data not shown) and BRI1 (Figure 6). BRI1 and PSKR1/2 belong to the LRR X subfamily of LRR-RLKs (Shiu and Bleecker 2001) and both are able to interact with SERK co-receptors and form heterodimers to activate downstream signalling cascades (Ladwig et al., 2015; Santiago et al., 2013; Wang et al., 2015). Considering all those similarities, it is not surprising that RLP44 can modulate the interaction of the RLKs with their co-receptor BAK1 through the same mechanism (Figure 38). To assess if there could be a competition between the RLKs PSKR1 and BRI1 for binding to RLP44, we performed a transient co-expression approach in *N. benthamiana* leaves with either both RLKs and RLP44 present or only one RLK in combination with RLP44. While overexpressing PSKR/BRI1 and RLP44, less RLP44 levels were detected in co-immunoprecipitates of BR1-RFP, compared to co-expression of only BRI1-RFP and RLP44 (Figure 39).

In transient co-expression of both RLKs with RLP44, the interaction of RLP44 with one RLKs was decreased (Figure 39), suggesting that the two pathways might compete for

RLP44. Generation of double overexpression lines with tagged proteins in *Arabidopsis* would be necessary to further confirm this hypothesis.

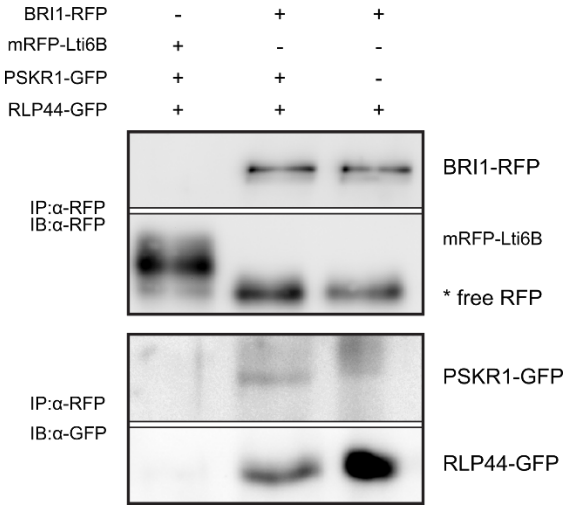


**Figure 39. RLKs compete for complex formation with RLP44.**
Presence of PSKR1-GFP and BRI1-RFP in *N. benthamiana* leaves after agroinfiltration reduces the amount of RLP44-RFP in immunoprecipitates of BRI1-RFP. mRFP-Lti6B is used as PM-localized control and neither RLP44-RFP nor BRI1-RFP are precipitated.

# 3 Discussion

## 3.1 Effects of cell wall binding on RLP44 mediated downstream signalling

### *3.1.1 RLP44 interacts with the cell wall*

Plants face a constantly changing environment, which they have to continuously monitor and adapt. Plant cells must grow in a strictly coordinated manner as they are tightly fixed together by cell walls. This cell wall is a rigid but also ever-changing layer as plants continuously grow and divide. These are processes which require inter- and intracellular communication between cells and their cell walls. The plasma membrane-localized protein receptor-like protein 44 (RLP44) was first identified in a cell wall modified mutant, therefore it is close to link the receptor function to the cell wall. *RLP44* is a suppressor of the severe root waving phenotype caused by the overexpression of the *PECTIN METHYLESTERASE INHIBITOR 5 (PMEI5)* gene. The suppressor mutant in the PMEIox background is called *comfortably numb 2* (*cnu2*). The cell wall surveillance mechanisms have been studied before and it was shown that THESUS 1 (THE1) (Hématy et al., 2007) can presumably sense cellulose and FERONIA (FER) binds to polygalacturonic acid (PGA) (Feng et al., 2018; Lin et al., 2018).

During plasmolysis in transformed tobacco leaves, the plasma membrane detaches from the cell wall. However, we show that the truncated RLP44ECD-mCherry protein remains in the cell wall (Figure 7C). This is neither observed for the plasma membrane-localized control Lit6B, nor for a highly mobile and secreted RFP (Figure 8). We also document the specificity of the RLP44ECD binding to the cell wall *in vivo,* generating stable *Arabidopsis* lines overexpressing the RLP44ECD-mCherry transgene (Figure 12A). In presence of PMEIox however, RLP44ECD does not bind the cell wall anymore, neither in the PMEIox background, nor in the *cnu2* background (Figure 12A). This leads to our hypothesis, that the specific binding of RLP44ECD to pectate depends on the methylesterification status (Figure 9). This suggests that RLP44 indeed is involved in sensing the pectate state, which is manipulated by PMEIox. Previously, we could not rule out that the monitoring of the cell wall components happens indirectly *via* interaction of RLP44 not as a first sensor.

However, in this work we provide data showing the direct interaction with a recombinant peptide assay on a glycan array. Furthermore, with the glycan array, we performed a screening with 84 different spotted oligosaccharides and were able to determine the direct binding of the recombinant RLP44 peptide to highly demethylesterified pectin/pectate (Figure 9).

The association with lime pectins is very specific. Binding occurs below or equal to 46% degree of esterification, but this is diminished by a higher degree of esterification. At first, these results seem contradictory, as in oligosaccharides with large or random deesterification blocks or random deesterification blocks of even 75-96%, a signal still can be detected (Figure 9A). Yet, a possible explanation could be that PME activity can lead to a broad pattern of esterification and even small differences can influence the binding to, in this case, RLP44ECD (Wolf and Greiner 2012). We assume that not only the total level of methylesterification is relevant for the binding of RLP44 to pectate, but also the distribution of methylesterification has an impact on the binding ability.

Previous publications have shown that WAK1 cannot bind to methylesterified PGA, as the methylester groups mask the carboxyl groups of PGA, which are needed to form the inter-chain calcium bridges to allow WAK1 binding (Liners et al., 1992). For the WAK1-PGA interaction, the requirements of methylesterification are quite specific: At least a degree of 34% is necessary to build stable inter-chain calcium bridges and thus allow WAKs binding to it (Decreux and Messiaen 2005). In addition, it as expected that the recombinant RLP44 protein is not binding to different compositions of cellulose and hemicellulose, which are also spotted on the glycan array (Figure 9, Appendix: Figure 40 and Figure 41). Another LRR-protein, that was also already shown to bind to pectin, is the polygalacturonases-inhibiting protein (PGIP). It is important in plant defence and can directly bind to demethylesterified homogalacturonans (Spadoni et al. 2006). It is assumed that PGIP binds the cell wall to prevent degradation by fungal endopolygalacturonanses. However, the feedback mechanism back from the cell wall and regulating the expression of those cell wall binding proteins is still unclear. Maybe RLP44, as it interacts also with BAK1 which is enrolled in many plant defence (Chinchilla et al., 2007) mechanisms could be the sensor for cell wall integrity (Wolf et al., 2014).

Unlike the full-length protein, truncated RLP44ECD is not able to complement the *cnu2* phenotype (Figure 13). This result already hints to the importance of the other domains of RLP44. However, the ECD appears to have a function in addition to cell wall binding, as it partially rescues both the slightly smaller rosette phenotype and shorter roots of *rlp44*$^{cnu2}$ (Figure 13). However, until now, no function has been detected in any other background. Surprisingly, no overexpression phenotype in the Col-0 background was observed (Wolf et al., 2014). Indeed, considering that RLP44ECD binds to the cell wall, it might compete with the endogenous full length RLP44, which could then be "free" to enhance BR signalling. It is possible that the ECD can still partially participate in the complex formation. However, further experiments are necessary to assess the full function of the RLP44 ECD.

### *3.1.2 Downstream effects of cell wall binding and RLP44 as mediator between BR and PSK signalling*

Previously, we demonstrated the direct interaction of RLP44 with BAK1 (Wolf et al., 2014). In this work, we also show the direct interaction of RLP44 with BRI1 (Figure 5). It is conceivable that RLP44 interacts with BRI1 to activate BR signalling in response to cell wall changes. Furthermore, first preliminary results of Nina Glöckner from Tübingen hint at a ternary complex BRI1-BAK1-RLP44 (data not shown). She was able to demonstrate in preliminary triple FRET-FLIM measurements an additional reduction of the fluorescence lifetime in presence of the RLP44-BAK1-BRI1 complex (data not shown).
Beyond that, we identified PSKR1 as a new interaction partner of RLP44. Taken together, RLP44, although a small RLP, can interact with at least three different RLKs regulating the downstream signalling pathways. We determine the cytoplasmic domain as the crucial domain of RLP44 for the interaction with BRI1 (Figure 6) as well as with PSKR1 (data not shown). It is unlikely that a small domain like the cytoplasmic domain, which consists of only 25 AAs, can carry out all those interactions. Hence, we hypothesise that RLP44 can either bind to PSKR1 or to BRI1 at a given time and RLP44 may act as a mediator of the cell wall state and integrates the signals to the internal signalling pathways. We assume a key function for RLP44 in balancing the BR and PSK signalling pathways by forming

ternary complexes with either BRI1-BAK1-RLP44 for cell proliferation control or PSKR1-BAK1-RLP44 for maintaining procambial identity.

Another explanation could be that RLP44 integrates the cell wall state and fine-tunes the signalling strength of both pathways. Cell elongation processes have been shown to be regulated by PSK and BR signalling. Therefore, one hypothesis would include the positioning of RLP44 at the very top of both signalling cascades.

We propose RLP44 as a scaffold protein stabilizing the complex (Figure 38 and for BRI1-BAK1-RLP44 data not shown). These results suggest that cell wall binding of RLP44 exerts a fine-tuning function. If binding to the cell wall is restricted, RLP44 may bind to another RLK to induce the appropriate downstream signalling. As an RLP, RLP44 cannot execute the downstream signal pathway like removing or adding phosphate to other proteins by itself because it is lacking a catalysing domain. Besides the partial rescuing of the *rlp44*$^{cnu2}$ phenotype by overexpressing RLP44ECD, there are no hints on the functionality of this truncated protein. Moreover, the fact that RLP44ECD is unable to rescue the *cnu2* phenotype is supporting the hypothesis that RLP44 needs to interact with a RLK to trigger downstream signalling cascades.

Therefore the questions remains: What functions are regulated by the binding of RLP44 to cell wall?

Although the crystal structure of RLP44 is not available, the structure can be deduced from similar proteins, especially the well-described LRR region (Kobe and Deisenhofer 1994). Michael Hothorn provided us based on homology modelling on SOMATIC EMBRYOGENESIS RECEPTOR KINASE (SERK)1 with a number of clusters (Table 1) consisting of two AAs, which were mutated to alanine, respectively (Santiago et al., 2013). This approach is based on previous studies which indicated specific interactions of AAs with negatively charged carboxylic groups in HG dimers, like e.g. the cell wall isoperoxidase in Zucchini (Penel and Greppin 1994; Carpin et al., 2001).

The creation of a non-cell wall binding mutant version of RLP44 by mutating Tyr146 and Arg170 to alanine, provides a good tool to uncouple the integration of cell wall binding from downstream signalling pathways. This construct was named RLP44-clusterII. To test interaction capacity of the deletion constructs of the RLP44ECD, we expressed them transiently in *N. benthamiana* leaves. The clusterII mutant construct with Tyr146 and

Arg170 replaced with alanine shows a prominent difference in binding behaviour during plasmolysis (Figure 10). This construct behaves similar to the secreted RFP control, and seems to be excluded from the cell wall in all the investigated cases (Figure 8). So far, we are able to show that the RLP44-clusterII version can only partially rescue the *cnu2* phenotype. We would have expected that, when RLP44 is not able to bind the cell wall, it is free to interact with BRI1, in agreement with the reduced ECD cell wall association in PMEIox. However, this hypothesis could not be confirmed. There are several imaginable reasons why this could be. One possible explanation could be that phosphorylation of RLP44 is inhibited and it is kept inactive, presumable if phosphorylation is implied for its activation (Garnelo Gómez 2017). The position of the mutations may of course not only affect the interaction with the cell wall, but also affect the interactions with BAK1 therefore may affect downstream signalling. This should be investigated next by co-immunoprecipitation approaches to get a first hint for the complex formation and then in more detail for affecting the direct interaction maybe with the help of FRET-FLIM. Moreover, also the cellular trafficking of RLP44 could be affected by the mutations and has to be analysed. The subcellular localization and the proper folding of the protein has also to be confirmed. Finally, the initial hypothesis may be wrong, and the cell wall interaction could be crucial for RLP44 for the subsequent complex formation with the RLKs. To further unravel the cell wall binding we also want to include the single mutated AA of the clusters in our investigations.

The RLP44-clusterII protein could also be involved in the activation of the PSK-signalling. Unfortunately, the PSK-signalling pathway is not yet been studied well and no molecular downstream targets of the pathway are known. Thus, we cannot study effects on a molecular level. However, for we have two possibilities to estimate PSK effect with physiological read-outs. So, as soon as we have stable lines expressing the full length RLP44-clusterII mutants, they need to be analysed for the vascular cell fate and the root elongation effect of exogenous applied PSK.

Within this work, we attempt to find differentially regulated genes using a microarray approach including samples from *pskr1-3, rlp44-3, bri1*$^{cnu4}$ and *bri1-null* to find common downstream targets involved in the process. However, the results are not conclusive, as the variation between the same genotype is times higher than between different genotypes. It

is highly recommended to repeat this experiment to further elucidate the signal cascade pathway of PSK.

If there is a competition for RLP44 interaction between the cell wall and PSKR1 or BRI1, we should be able to investigate it and specify the context of this interaction to understand the biochemical mechanism. However, so far we were unsuccessful in generating a stable mutant line expressing PSKR1 and RLP44 with a detectable tag. Additionally, antibody production against RLP44 also has failed, because the in rabbit raised antibody against the ectodomain of RLP44 (performed by Agrisera) was binding unspecifically to different proteins. First results indicate binding competition between RLP44 and its two interaction partners is provided by this work by using co-immunoprecipitation, experiments. When overexpressing both PSKR1-GFP and BRI1-RFP, less RLP44 is co-immunoprecipitated than if only one receptor is available (Figure 39) but this might also be caused by the overexpression and might be an artefact induced by high protein levels.

### *3.1.3 RLP44 –one protein with many functions*

When we examined the individual domains of RLP44, we were able to establish the individual significance for each domain (Figure 7). The RLP44ECD can bind the pectate, while the RLP44CD is able to interact with RLKs (Figure 6). However, it is difficult to imagine how these interactions are spatially arranged. In addition, we know from isothermal titration calorimetry experiments done by Ulrich Hohmann (data not shown) that RLP44ECD is not binding to a BRI1-BL-BAK1 complex. However, the LRR region is prone to build a platform for protein interactions, which led us to the hypothesis of RLP44 homodimerisation (Zhang et al., 2016). This hypothesis is further supported by co-immunoprecipitation experiments, where RLP44-RFP co-immunoprecipitates RLP44-GFP after transient expression in *N. benthamiana* (Mendel 2017). However, we cannot rule out indirect interaction *via* another protein. To confirm homodimerization of RLP44, a FRET-FLIM approach would be suitable. Similarly, if the homodimerization of RLP44 is a requirement for further signalling, maybe an artificially formed dimer of two cytosolic domains can mimic this, although the signal input from the cell wall would get lost in this scenario. Unfortunately, based on the available data, we cannot predict the detailed molecular mechanism at the moment. Interestingly, the main mechanosensors Wsc1 and

Mid2 of *S. cerevisiae* are PM-localized proteins with a cysteine-rich domain in the ECD, which can specifically interact with glucan in the cell wall and thus trigger a conformational change of the nanospring-like serine/threonine region (Jendretzki et al., 2011; Rodicio and Heinisch 2010). This conformational change enables the cytoplasmic tail to interact with downstream proteins (Jendretzki et al., 2011). However, neither for RLK nor for RLP similar conformational changes are described upon ligand binding. Nevertheless, the establishing the role of the cytoplasmic domain opens a new door for further analyses.

## 3.2 RLP44 downstream signalling controls vascular cell fate in a BRI1-dependent manner

As a first step in deciphering the physiological of RLP44 function, we studied its expression pattern. RLP44 is expressed in the plant epidermis and vasculature, predominantly in the procambium (Figure 20). The procambium is a source for xylem cells, and to study the role of the *rlp44* mutant in xylem development, we followed the tracheary elements visualized with basic fuchsin staining. Meticulous analysis revealed a disrupted metaxylem phenotype, where up to 50% of the *rlp44* mutant seedlings develop four metaxylem cells right below the hypocotyl in the primary root within the xylem axis. Additionally, also some metaxylem cells arise anticlinal on a procambial cell position (Figure 21). Based on the interaction of RLP44 with BRI1, we also examined the vasculature of different *bri1* alleles and the results indicate that the xylem phenotype is dependent on the presence of the BRI1 protein, but is independent of the BR-signalling outputs (data not shown, Huerta 2016; Holzwart et al., in revision). The *bri1-null* mutant has a strong reorganized xylem phenotype and qPCR analysis revealed that *RLP44* expression is drastically decreased only this *bri1-null* mutant (Figure 23). Overexpression of RLP44-GFP in *bri1-null* mutant was rescuing the xylem phenotype and we conclude that RLP44 is presumable downstream of BRI1 and can act independently. Our results are in agreement with transcriptome data, which is provided by the plant community. Within these data sets, a reduction of *RLP44* expression in *bri1-116* is apparent (Sun et al., 2010). With the identification of the $bri1^{cnu4}$ allele, a point mutation in the last LRR of BRI1 protein (G746S), we obtained another tool to study the interaction between BRI1 and RLP44. The $bri1^{cnu4}$ mutant does not show mild BR-deficient phenotype (Figure 18). One

explanation for the same disrupted xylem phenotype in *bri1*$^{cnu4}$ and the *rlp44* mutants is based on the fact that the interaction between RLP44 and BRI1cnu4 is stronger (Figure 24). Consequently, BRI1cnu4 sequesters RLP44, thus exhibits a negative effect on RLP44 function, inhibiting its ability to interact with another protein, in this case: PSKR1. Furthermore, we show the dominant effect of BRI1cnu4 on the plant overall and xylem phenotype in the F1 hybrid crossed with Col-0, emphasising its negative effect on RLP44 (Figure 27). Even though the mutation in BRI1cnu4 is in the extracellular domain, it is the cytoplasmic domain of RLP44 that is crucial for the interaction with RLP44, since truncated RLP44 proteins without the CD were not able to form complexes with BRI1 (data not shown). These results could suggest structural changes within the BRI1cnu4 receptor. The strong loss-of-function mutant *bri1-102* has a mutation leading to an AA exchange at position 750 (T750I), which does not influence BL-binding (Friedrichsen et al., 2000; Wang et al., 2001), however, it leads to the weakening of the complex between SERK1 and BRI1, thereby causes a severe BR-deficient phenotype (Santiago et al., 2013). The AA mutation in *bri1-102* is directly adjacent to the *bri1*$^{cnu4}$ mutation. Both mutations are in close proximity to the PM, however, only the phenotype of *bri1-102* is severely affected and implies the importance of the interactions formed close to the transmembrane domain. Co-immunoprecipitation results also suggest that BRI1cnu4 is not impaired in the interaction with BAK1 (data not shown) it will be part of future work to fully understand the changes in the *bri1*$^{cnu4}$ mutant plant. Split-ubiquitin data from yeast provided by Nina Glöckner also hint to a stronger interaction between BAK1 and BRI1cnu4.

In co-immunoprecipitation experiments, external application of PSK- (Figure 28A) or BR-ligands (Wolf et al., 2014) had no influence on the association between the receptors and RLP44. These results are consistent with ligand-independence of already published RLP-RLK interactions (Albert et al., 2015, Gust and Felix 2014).

## 3.3 PSK signalling is involved in the maintenance of procambial identity

In recent years, an increasing number of peptides have been found to play important roles in the development of plants (Matsubayashi 2014, Tavormina et al., 2015). Occasionally, the involvement of a small secreted extracellular sulfated pentapeptide PSK is proposed, which contributes to several processes (Matsubayashi et al., 2014; Sauter et al., 2015). PSK

was identified as a factor to activate proliferation and crucial for the growth of low-density plant cell cultures (Matsubayashi and Sakagami 1996). Further studies led to the discovery that PSK induces tracheary element differentiation in *Zinnia elegans* cells in addition to auxin and cytokinin (Matsubayashi et al., 1999). To study xylem cell differentiation in *Arabidopsis* a trans-differentiation approach was established (Kondo et al., 2015). It was determined that mesenchymal cells before they develop into tracheary element cells go through an intermediate procambial state. The transcriptome data provided by the same study revealed the a stronger expression of *PSK4* and *PSK5* during early phase of the trans-differentiation process (Kondo et al., 2015; Motose et al., 2009). To study the impact of the RLKs PSKR1/BRI1 or RLP44 on the on the trans-differentiation, it would helpful to establish the trans-differentiation protocol to investigate the respective mutants. As the trans-differentiation is subdivided into different stages, maybe we can decipher the mechanism in more detail and how and where the receptors are specifically involved in the regulation.

With respect to this knowledge, we hypothesize that PSK-signalling may be a determinant for the control of xylem cell fate by promoting maintenance of procambial identity and further, that PSK-signalling may be responsible for the disrupted xylem phenotype observed in the different mutant backgrounds. The phenotype with the additional metaxylem cells within the axis, as well as procambial cells with xylem identity outside the xylem axis were also observed in PSK-signalling impaired mutants (Figure 29). It is noteworthy that the triple mutant *rlp44*$^{cnu2}$ *pskr1-3 pskr2-1* does not show an additive phenotype compared to the double *pskr1-3 pskr2-1* mutant (Figure 29), suggesting that both proteins are acting in the same signalling pathway. Furthermore, we show that overexpression of 35S:RLP44-GFP in *pskr1-3 pskr2-1* background does not affect the xylem phenotype. However, the same 35S:RLP44-GFP in the *bri1-null* background does rescue the disrupted xylem phenotype (data not shown, is part of Holzwart et al., in revision, experiments performed by Dr. Garnelo Gómez). Taken together, these results indicate that RLP44 acts downstream of BRI1 and through PSKR with respect to the maintenance of vascular cell fate.

We examined the effect of PSK on the xylem differentiation of the *rlp44* mutants and on *bri1*$^{cnu4}$ and indeed, PSK treatment rescued the ectopic xylem phenotype in the *rlp44*

mutants (Figure 30). This suggests RLP44 is not required for PSK signalling as the disrupted xylem phenotype can be rescued by external PSK supply. Contradictory, PSK could not rescue the xylem phenotype of *bri1*$^{cnu4}$ mutants. For the time being, we can only hypothesize why PSK does not rescue the *bri1*$^{cnu4}$ mutant. One reason could be that RLP44, BR1cnu4 and BAK1 form a stable ternary complex, which sequesters the co-receptor BAK1 away from the PSK-signalling pathway. Split-Ubiquitin results from our collaboration with Nina Glöckner revealed an enhanced interaction between BRI1cnu4 and BAK1 than between BAK1 and BRI1 (data not shown). This could explain why PSK-signalling is not activated despite exogenous supply with PSK. Besides, while there is no distinguishable phenotype compared to the mock treated control upon exogenous application of PSK on Col-0, the xylem of *tpst-1* is partially rescued. However, the PSK effect on root growth is apparent for Col-0 but not for *tpst-1* (Figure 31).

Noteworthy, PSK-signalling increases longevity and facilitates callus growth, which is also associated with cell identity maintenance (Matsubayashi 2006). The PSK signalling pathway plays an important role in maintaining procambial identity by regulating final xylem cell differentiation though interaction with RLP44. RLP44 promotes the interaction between PSKR1 and its co-receptor BAK1 independently of PSK.

## 3.4 BRI plays a role in root vascular development

Brassinosteroids (BRs) are implicated in the overall plant development and their biosynthesis is highly regulated (Yokota 1997). Various brassinosteroid-deficient mutants show defects in vasculature formation in the shoot (Ibañes et al., 2009; Caño-Delgado et al., 2010; Caño-Delgado et al., 2004). Previously, mesophyll cell differentiation has been studied in *Zinnia elegans,* where BR levels have been shown to increase prior to the differentiation to tracheary element cells (Iwasaki and Shibaok 1991; Yamamoto et al., 1997; Yamamoto et al., 2001). Xylem cell differentiation is a tightly regulated process and for that, the quantity and composition of hormones and peptides have to be under stringent control. In addition to a coordinated auxin and cytokinin supply, BRs are critical for correct differentiation. It was shown recently that glycogen synthase kinase 3 (GSK3) proteins are crucial downstream components affecting xylem differentiation by directly suppressing the downstream transcription factors of BR-signalling (Kondo et al., 2014). This inhibition of

the differentiation into xylem cells is important in e.g. procambial cells of leaf and hypocotyls to prevent their differentiation and maintain their meristematic properties (Kondo et al., 2014). Bikinin is an inhibitor of GSK3, and can be used to promote differentiation of xylem cells (Kondo et al., 2015).

In this study, we investigated the effect of BL on the primary root vasculature development and observed that BR does not play a significant role in the control of xylem differentiation as neither BR-signalling nor biosynthetic mutants show the described disrupted xylem phenotype (Huerta 2016; Holzwart et al., in revision). However, BRI1 is crucial for the maintenance of the vascular cell fate. The severe vascular phenotype, described in shoots of BR-impaired mutants (Ibañes et al., 2009), could not be confirmed in roots. Among other mutants, the BR-impaired *bin2-1* mutant shows a normal xylem phenotype in the root, also the xylem of bikinin treated Col-0 has a normal pattern, both points emphasising that BIN2 is likely not relevant for the maintenance of vascular cell fate in roots (data not shown, part of Holzwart et al., in revision). However the *bin2-1* mutant shows a reduced number of vascular bundles compared to Col-0 in the shoot (Ibañes et al., 2009). One possible scenario for this observation could be that the vascular pattern of the root is determined during embryogenesis by asymmetric divisions of the procambial cells (Jürgens et al., 2001). However, the shoot together with the vascular bundles originates post-embryonically from the shoot apical meristem (Jürgens et al., 2001). Total vascular cell number is also behaving opposed in shoot and root in BR signalling mutants, for instance the cell numbers are reduced in the shoot (Ibañes et al., 2009) whereas increased in the roots (Kang et al., 2017). Further, BRs are crucial for the development of new organs but not necessary during embryogenesis, as *bri1-null* mutants develop a healthy embryo although they lack BR1 receptors. The BRL2 and BRL3 are still functional, however, *bri1-null* mutants adult plants, show severe delayed and development defects (Friedrichsen et al., 2000, Jaillais et al., 2011).

We were not able to show any effect of BL-supplementation on primary root xylem formation (Figure 32B). Neither increasing nor completely depleting endogenous BL levels has a significant influence on the metaxylem cell formation (PPZ data not shown, Holzwart et al., in revision). Furthermore, activation of the BL signalling pathway downstream of BRI1 by bikinin treatment has no effect on Col-0 (data not shown, is part of Holzwart et

al., in revision, experiments performed by Dr. Garnelo Gómez). Moreover, *dwf4-102* and *cpd* are two *Arabidopsis* mutants defective in BL biosynthesis and exhibit the same BR deficient growth phenotype. However, exogenous BL supplement can rescue the impaired growth phenotype, although the xylem phenotype remains unaffected (Figure 22). The effect is in line with the results of the PPZ treatment as PPZ is inhibiting the enzyme DWF4 (data not shown, is part of Holzwart et al., in revision, experiments performed by Dr. Garnelo Gómez). Besides, it is worth mentioning that in *dwf4-102* homozygous mutants and PPZ-treated Col-0 plants have gaps in protoxylem cell development. As a consequence, it is possible that BL signalling is critical for normal protoxylem development independent from metaxylem cell fate.

Our data demonstrates that the PSK-signalling-impaired lines are still able to sense BR (Figure 33) and additionally supplied PSK does not affect BL-sensitivity. However, the results concerning the PSK-signalling are difficult to interpret, as there are no molecular downstream targets known and the root length and xylem phenotype are the only read-outs so far. In summary, our results indicate BRI1 acts as a key regulator, independent of the BR signalling pathway, through RLP44, which interacts with PSKR1 to promote PSK signalling.

## Conclusion

The goal of our work is to decipher how plants gather information about the cell wall and integrate them with intracellular signalling networks to control development. Within this work, we were able to identify the recently described receptor-like protein 44 (RLP44) as a potential sensor for cell wall pectate. Furthermore, we showed that RLP44 balances PHYTOSULFOKINE (PSK) and BRASSINOSTEROID (BR) signalling pathways though direct interaction with receptor-like kinases (RLKs) BR INSENSITIVE1 (BRI1) and PSK RECEPTOR1 (PSKR1). We assume RLP44 to be a scaffold protein, which fine-tunes the interaction of the RLKs with the respective co-receptors. BR1 determines xylem cell fate though the regulation of RLP44 and the PSK-signalling pathway, independently of the classical BR signalling. The balance of both signalling pathways is crucial for the xylem fate determination, an imbalance of the signalling integration, caused by the lacking of one of the receptors leads to a reorganization xylem. In the future, a transcriptome analysis is fundamental to identify downstream signalling members of the PSK pathway and could be helpful to find new readouts for the PSK signalling pathway. Moreover, an earlier readout for cell identity transitions, beside the disrupted xylem phenotype, would be useful to decipher the patio-temporal regulation of this process.

As plants are sessile, they are forced to cope with the environmental conditions and adapt. The amount and diversity of the RLKs and RLPs suggests that signal integration in plants is exceptionally well developed. Our results introduce a new mechanistic model how signals are integrated by the RLKs in plants and how RLPs enable interplay of signalling pathways.

# 4 Materials and methods

## 4.1 Plant material and growth conditions

### *4.1.1 Sterilisation*

Seeds were sterilised in freshly prepared sterilisation solution (1:10 dilution of 1.3% (V/V) sodium hypochlorite with 70% ethanol), for not longer than 2 minutes to avoid damage of the seeds. Subsequently, seeds were washed twice with absolute ethanol and dried in the sterile bench.

### *4.1.2 Standard growth conditions*

Standard experiment plates were prepared with ½ Murashige & Skoog (MS) medium (Duchefa), 1% D-sucrose (Carl Roth) and 0.9% phytoagar (Duchefa) with pH = 5.8 adjusted with KOH. Sterilised seeds were plated and stratified for 2-4 days at 4 °C in the dark and subsequently plates were placed vertically in growth chambers with long day conditions (16 hours light, 8 hours dark), with the number of days indicated for each experiment. For subsequent growth of adult plants, CLT-SM substrate (Einheitserde Classic) was used in growth rooms with long day conditions (16 hours light, 8 hours dark). Pictures of plants were taken at indicated time points.

### *4.1.3 Crossings*

Mature siliques, open flowers, buds with already fertilized tip, and the meristem including too small buds, were removed of the mother plants' inflorescence. By gently removing the petals, sepals, and all the immature anthers, we isolated the stigmas of 3-5 flower buds. One day later the anthers from the father plant were taken and tapped on the already developed stigmata of the mother plant. Developed siliques were harvested and either used for experiments or propagation.

### *4.1.4 Root length measurement*

To assess response of the genotypes to different growth conditions, one possibility is to measure the root length of seedlings. For this, plants were grown on ½ MS medium

supplied with 1% sucrose and 0.9% phytoagar and in addition the substance of interest. For the BL sensitivity assay, plates were supplied with 2 µM PPZ (Sigma-Aldrich) with different concentrations of Brassinolide (BL, Santa Cruz Biotech). For PSK response, plates were supplied with 1 µM α-PSK (PolyPeptide). After stratification, plates were placed in growth chambers and scanned after 5-6 days of growth in long day conditions at 22 °C. Roots were analysed with the image-processing program ImageJ (https://imagej.nih.gov/ij/), by measuring the length from the root tip to the hypocotyl. Root length averages together with the standard deviations were plotted for each experiment.
Used chemicals for the root measurements: PPZ (Sigma-Aldrich) 100 mM stock in 90% Dimethylsulfoxid (DMSO); BL (Santa Cruz Biotech) 10 mM stock in 80% Ethanol; α-PSK (PolyPeptide): 1 mM stock in water.

## 4.2 Generation of plasmid constructs

The Gateway system is a commercial cloning system. It was used following the manufacturer's recommendations (Gateway™ BP Clonase™ II Clonase Enzyme Mix and Gateway™ LR Clonase™ II Clonase Enzyme, ThermoFisher). GreenGate is a variable system for generating a modular construct with a high variability (Lampropoulos et al., 2013). For selection of transformed bacteria, antibiotics according the plasmid backbone was necessary. The concentrations of used antibiotics are listed in Table 3.

**Table 3. Antibiotics used in this study to isolate positive bacterial clones.**

| antibiotics | final concentration |
|---|---|
| Carbenicllin | 50 µg/mL |
| Rifampicin | 25 µg/mL |
| Spectinomoycin | 50 µg/mL |
| Kanamycin | 50 µg/mL |
| Ampicillin | 100 µg/mL |
| Chloramphenicol | 34 µg/mL |
| Tetracyclin | 12.5 µg/mL |

### *4.2.1 Gateway cloning*

The gene of interest (GOI) was amplified with indicated primers (Table 13) subsequently checked by an agarosegel for the appropriate size and thereupon precipitated with PEG400. The product was internalised into pDONR207 by BP clonase overnight at 25 °C in a water bath. After successful transformation of the recombinant plasmid it was amplified with

*Escherichia coli* (*E.* coli) XL1 Blue cells, with the appropriate supplied Luria – Bertani (LB) medium (LB-medium: 0,5% (w/v) Bacto™ yeast extract (Roth), 1% Bacto™ tryptone (BD Biosciences), 1% (w/v) KCl; for solid 1% of Bacto™ Agar (BD Biosciences)) with the appropriate antibiotic resistence of the backbone plasmid (Table 3, Table 4). Before continuing, the proper gene sequence was confirmed by Sanger-sequencing after extracting the Plasmid with miniprep of liquid cultures (GeneElute™ Plasmid Miniprep Kit, Sigma Aldrich) following the manufacturer's instructions. After that, the pDONR207 with the GOI was used to recombine with the plasmid backbone containing the required tag (Table 4) (Karimi et al., 2002) with the help of the LR clonase. After 1 h on 25 °C in a water bath, the reaction was transformed into *E. coli* XL1 Blue cells and selected on appropriate LB medium.

**Table 4. Gateway constructs used in this study.**

| plasmid name | stock name | backbone plasmid | comments |
|---|---|---|---|
| RLP44-RFP | pSW49 | pK7RWG2 | Wolf lab |
| RLP44-ECD-mcherry | pSW295 | pK2GW7 | Wolf lab |
| PSKR1-GFP | pSW763 | pH7WGF2 | Ladwig et al., 2015 |
| mGFP-Lti6b | pSW250 | pK7WGF2 | Wolf lab |
| BAK1-HA | pSW73 | pGWB14 | Wolf lab |
| BRI1-RFP | pSW504 | pB7RWG2 | Wolf lab |
| mRFP-Lti6b | pSW246 | pUBN-RFP-Dest | Maizel lab |
| RLP44-GFP | pSW48 | pK7FWG2 | Wolf lab |
| RLP44ECD | pSW841 | pK7RWG2 | this study |
| RLP44ECD_clusterI | pSW836 | pK7RWG2 | this study |
| RLP44ECD_clusterII | pSW837 | pK7RWG2 | this study |
| RLP44ECD_clusterIII | pSW838 | pK7RWG2 | this study |
| RLP44ECD_clusterIV | pSW839 | pK7RWG2 | this study |

### *4.2.2 GreenGate cloning*

The idea is based on the generation of entry modules, six of different kinds, which can be combined flexible, but due to determined sticky ends, the sequence was set. All constructs were generated according to Lampropoulos et al., 2013.

#### 4.2.2.1 Generation of entry vectors

GOI was amplified with indicated primers (Table 13) and Q5® High-Fidelity DNA Polymerase (NEB) and checked on an agarosegel for the correct size. After subsequent purification (GeneJet GEL Extraction Kit, ThermoFisher), the product was digested with

*Eco31I* (ThermoFisher) before column-purification as already described. Empty entry vectors were separately digested with the same restriction enzyme and also purified. Ligation of both products was performed by Sticky-end Ligase Master Mix (NEB) following the manufacturer's instructions. After ligation reaction, mixture was transformed in *E. coli* XL1 Blue and cultivated in selective LB medium with appropriate antibiotic supply. The backbone (pGGA000 or pGGC000) for the entry vectors carries the Amp-resistance gene (Table 3). Positive colonies were confirmed by single colony PCR and sequenced after further amplification of the plasmid. For generation of different modules, appropriate primer overhangs have to be considered to maintain the proper order of modules in the destination vector. In accordance to that, specific initial vectors were used for building the promoter (pGGA000) or the GOI (pGGC000). Special care has to be taken, if the GOI has internal *Eco31I* restriction sites. Those recognition sites have to be removed by site directed mutagenesis before creation of the entry modules. The *BRI1* gene had three internal *Eco31I* cuttings sites which were silently mutated (Table 6/Table 13). *BRI1cnu3* was cloned with SW1297 and SW1298 from genomic DNA of a *bri1*$^{cnu3}$ plant. *BRI1cnu4* was cloned with SW1299 and SW1255 from genomic DNA of a *bri1*$^{cnu4}$ plant (Table 6/Table 13).

#### 4.2.2.2 Generation of destination vectors

A mixture of 1.5 µL of each of the six modules (A – F) (Table 6) and 1 µL of the destination vector (pGGZ001), 2 µL 10x buffer, 1.5 µL 10 nM ATP, 1 µL T4 DNA ligase, 1 µL *Eco31I* were added to run the GreenGate reaction (Table 5) to create final GreenGate constructs (Table 7) (Lampropoulos et al., 2013).

**Table 5. GreenGate reaction program.**

| temperature (°C) | duration (min) | number of cycles |
|---|---|---|
| 37 | 2 | |
| 16 | 2 | }30 |
| 50 | 5 | 1 |
| 80 | 5 | 1 |

**Table 6. Entry modules used for GreenGate constructs.**

| name | details | source of plasmid | PCR template | primers | mutagenesis |
|---|---|---|---|---|---|
| pSW299 | RLP44 (at3g49750) promoter | this study | *Arabidopsis* genomic DNA | SW1149/SW1150 | |
| pSW334 | RLP44 (at3g49750) CDS | Wolf lab | *Arabidopsis* cDNA | SW1179/SW1205 | |
| pSW182 | B-Dummy | Lampropoulos et al., 2013 | | | |
| pSW393 | pMAS::SulfR::tMAS | Lampropoulos et al., 2013 | | | |
| pSW184 | D-Dummy | Lampropoulos et al., 2013 | | | |
| pSW186 | UBQ10 terminator | Lampropoulos et al., 2013 | | | |
| pSW319 | pMAS::BastaR::tMAS | Lampropoulos et al., 2013 | | | |
| pSW183 | GFP | Lampropoulos et al., 2013 | | | |
| pSW379 | BRI1(AT4G39400) promoter | this study | *Arabidopsis* genomic DNA | SW1280/SW1281 | |
| pSW380 | BRI1(AT4G39400) CDS | this study | *Arabidopsis* genomic DNA | SW1254/SW1255 | SW1316/SW1317/SW1296/ SW1297/SW1298/SW1299 |
| pSW391 | BRI1cnu3 | this study | pSW380/genomic DNA | SW1254/SW1255 | SW1316/SW1317/SW1296/ SW1297/SW1298/SW1299 |
| pSW381 | BRI1cnu4 | this study | pSW380/genomic DNA | SW1254/SW1255 | SW1316/SW1317/SW1296/ SW1297/SW1298/SW1299 |
| pSW419 | BRI1cnu3,4 | this study | pSW380/genomic DNA | SW1254/SW1255 | SW1316/SW1317/SW1296/ SW1297/SW1298/SW1299 |
| pSW453 | p35S (mutated Eco311I)::D-AlaR::t35S | Lampropoulos et al., 2013 | | | |
| pGGZ001 | destination vector | Lampropoulos et al., 2013 | | | |
| pSW620 | GAGA-GFP | Wolf lab | | | |
| pSW759 | RLP44-clusterI | this study | pSW334 | SW1179/SW1205 | SW1809/SW1820/SW1811/SW1812 |
| pSW760 | RLP44-cluster_II | this study | pSW334 | SW1179/SW1205 | SW1813/SW1814/SW1815/SW1816 |
| pSW762 | RLP44-cluster_IV | this study | pSW334 | SW1179/SW1205 | SW1817/SW1818 |
| pSW944 | GAGAGA-mTurquoise | Grossmann Lab / pPD0021 | | | SW1819/SW1819/SW1820/SW1821 |

**Table 7. Assembled final GreenGate constructs in this sudy.**

| | pRLP44:RLP44-GFP | |
|---|---|---|
| **pSW362** | **construct** | **stock name** |
| A-module | pRLP44 | pSW299 |
| B-module | B-Dummy | pGGB003 |
| C-module | RLP44 | pSW334 |
| D-module | GFP | pSW182 |
| E-module | tUBQ10 | pGGE009 |
| F-Module | Basta$^{R}$ | pGGF001 |
| Destination vector | | pGGZ001 |

| | pBRI1:BRI1 | |
|---|---|---|
| **pSW388** | **construct** | **stock name** |
| A-module | pBRI1 | pSW379 |
| B-module | B-Dummy | pGGB003 |
| C-module | BRI1 | pSW380 |
| D-module | D-Dummy | pGGD002 |
| E-module | tUBQ10 | pGGE009 |
| F-Module | Basta$^{R}$ | pGGF001 |
| Destination vector | | pGGZ001 |

| | pRLP44:RLP44-GAGA-GFP | |
|---|---|---|
| **pSW731** | **construct** | **stock name** |
| A-module | pRLP44 | pSW299 |
| B-module | B-Dummy | pGGB003 |
| C-module | RLP44 | pSW334 |
| D-module | GAGA-GFP | pSW620 |
| E-module | tUBQ10 | pGGE009 |
| F-Module | Sulf$^{R}$ | pGGF006 |
| Destination vector | | pGGZ001 |

| | pBRI1:BRI1cnu3 | |
|---|---|---|
| **pSW389** | **construct** | **stock name** |
| A-module | pBRI1 | pSW379 |
| B-module | B-Dummy | pGGB003 |
| C-module | BRI1cnu3 | pSW391 |
| D-module | D-Dummy | pGGD002 |
| E-module | tUBQ10 | pGGE009 |
| F-Module | Basta$^{R}$ | pGGF001 |
| Destination vector | | pGGZ001 |

| | 35S:RLP44ECD-mTurquoise | |
|---|---|---|
| **pSW945** | **construct** | **stock name** |
| A-module | pRLP44 | pSW299 |
| B-module | B-Dummy | pGGB003 |
| C-module | RLP44_BTMD | pSW870 |
| D-module | pPD0021 | pSW944 |
| E-module | tUBQ10 | pGGE009 |
| F-Module | Sulf$^{R}$ | pGGF006 |
| Destination vector | | pGGZ001 |

| | pBRI1:BRI1cnu4 | |
|---|---|---|
| **pSW390** | **construct** | **stock name** |
| A-module | pBRI1 | pSW379 |
| B-module | B-Dummy | pGGB003 |
| C-module | BRI1cnu4 | pSW381 |
| D-module | tUBQ10 | pGGE009 |
| E-module | tUBQ10 | pGGE009 |
| F-Module | Basta$^{R}$ | pGGF001 |
| Destination vector | | pGGZ001 |

| | 35S:RLP44ClusterI-GAGA-GFP | |
|---|---|---|
| **pSW844** | **construct** | **stock name** |
| A-module | pRLP44 | pSW299 |
| B-module | B-Dummy | pGGB003 |
| C-module | RLP44clusterI | pSW759 |
| D-module | GAGA-GFP | pSW620 |

| | pBRI1:BR1cnu3,4 | |
|---|---|---|
| **pSW427** | **construct** | **stock name** |
| A-module | pBRI1 | pSW379 |
| B-module | B-Dummy | pGGB003 |
| C-module | BRI1cnu3,4 | pSW419 |
| D-module | D-Dummy | pGGD002 |

| | | |
|---|---|---|
| E-module | tUBQ10 | pGGE009 |
| F-Module | Sulf$^R$ | pGGF006 |
| Destination vector | | pGGZ001 |

| | | |
|---|---|---|
| E-module | tUBQ10 | pGGE009 |
| F-Module | Basta$^R$ | pGGF001 |
| Destination vector | | pGGZ001 |

| | 35S:RLP44ClusterII-GAGA-GFP | |
|---|---|---|
| **pSW845** | **construct** | **stock name** |
| A-module | pRLP44 | pSW299 |
| B-module | B-Dummy | pGGB003 |
| C-module | RLP44cluster_II | pSW760 |
| D-module | GAGA-GFP | pSW620 |
| E-module | tUBQ10 | pGGE009 |
| F-Module | Sulf$^R$ | pGGF006 |
| Destination vector | | pGGZ001 |

| | pBRI1:BRI1-GFP | |
|---|---|---|
| **pSW420** | **construct** | **stock name** |
| A-module | pBRI1 | pSW379 |
| B-module | B-Dummy | pGGB003 |
| C-module | BRI1 | pSW380 |
| D-module | GFP | pGGD001 |
| E-module | tUBQ10 | pGGE009 |
| F-Module | Basta$^R$ | pGGF001 |
| Destination vector | | pGGZ001 |

| | 35S:RLP44ClusterIV-GAGA-GFP | |
|---|---|---|
| **pSW846** | **construct** | **stock name** |
| A-module | pRLP44 | pSW299 |
| B-module | B-Dummy | pGGB003 |
| C-module | RLP44cluster_IV | pSW762 |
| D-module | GAGA-GFP | pSW620 |
| E-module | tUBQ10 | pGGE009 |
| F-Module | Sulf$^R$ | pGGF006 |
| Destination vector | | pGGZ001 |

| | pBRI1:BRI1cnu3-GFP | |
|---|---|---|
| **pSW421** | **construct** | **stock name** |
| A-module | pBRI1 | pSW379 |
| B-module | B-Dummy | pGGB003 |
| C-module | BRI1cnu3 | pSW391 |
| D-module | GFP | pGGD001 |
| E-module | tUBQ10 | pGGE009 |
| F-Module | Basta$^R$ | pGGF001 |
| Destination vector | | pGGZ001 |

| | pBRI1:BRI1cnu3,4-GFP | |
|---|---|---|
| **pSW423** | **construct** | **stock name** |
| A-module | pBRI1 | pSW379 |
| B-module | B-Dummy | pGGB003 |
| C-module | BRI1cnu3,4 | pSW419 |
| D-module | GFP | pGGD001 |
| E-module | tUBQ10 | pGGE009 |
| F-Module | Basta$^R$ | pGGF001 |
| Destination vector | | pGGZ001 |

| | pBRI1:BRI1cnu4-GFP | |
|---|---|---|
| **pSW422** | **construct** | **stock name** |
| A-module | pBRI1 | pSW379 |
| B-module | B-Dummy | pGGB003 |
| C-module | BRI1cnu4 | pSW381 |
| D-module | GFP | pGGD001 |
| E-module | tUBQ10 | pGGE009 |
| F-Module | Basta$^R$ | pGGF001 |
| Destination vector | | pGGZ001 |

After the GreenGate reaction, *E. coli* XL1 Blue were transformed with 5 µL of the mixture. Insertion of the construct was confirmed by colony PCR and constructs were used to transform *Agrobacterium tumefaciens* strain ASE (pSOUP$^+$).

### *4.2.3 Transformation of Escherichia coli and Agrobacterium tumefaciens*

The strain *E. coli* XL-1 Blue was used for both cloning systems. Chemically competent cells were transformed with the required plasmid by heat-shock at 42 °C for 45 sec. and afterwards incubated around 2-4 hours at 37 °C.

For constructs assembled by Gateway, *Agrobacterium tumefaciens* strain C58C1 was used. Electro competent cells were transformed by electroporation with the required plasmid in an electroporator and subsequently incubated at 28 °C for 2-4 hours.

For selection of positive agrobacteria clones, rifampicin, carbenicillin and the antibiotic of the resistance backbone plasmid needed to be added (Table 4). The concentrations for antibiotics were used according to Table 3.

For constructs built by GreenGate, *Agrobacterium tumefaciens* strain ASE pSOUP$^{+}$ was used. Chemically competent cells were transformed with the needed plasmid by freezing in liquid nitrogen, afterwards put on 37 °C before the cells were incubated at 28 °C for 3-4 hours. For selection of positive agrobacteria clones, spectinomycin, kanamycin, tetracylin and for those constructs (Table 7) in pGGZ001 backbone, spectinomycin were used. The concentrations for antibiotics were used according to Table 3.

### *4.2.4 Plant transformation and stable transgenic line selection*

To generate stable lines, the background has to be chosen appropriate to the hypothesis. Plants were grown for about 4 weeks and the first inflorescences were trimmed to induce more growth. Right before dipping of the plants, siliques were removed.

Agrobacteria with the desired plasmid were spread on selective plates and incubated for one night at 28 °C. Two nights before plant transformation, agrobacteria were amplified to two fresh selective LB-plates and incubated for two nights at 28 °C.

To each plate, 15 mL fresh LB medium was added and agrobacteria were resuspended in this in total 30 mL. Agrobacteria suspension was mixed with 120 mL 5% sucrose and 0.03 silwet L-77 (Lehle Seeds). Plants were dipped carefully with all inflorescences in the solution. Transformed plants were covered with a lid and kept wet and without light for one day. To increase the transformation efficiency, the procedure was repeated after 7 days (Clough and Bent 1998).

T1 plants were selected according to the selection marker and around 40 T1 plants were selected and propagated. Subsequently, approximately 20 T2 seeds were plated on the appropriate ½ MS selection medium to check for single integration lines. ¼ of the offspring should not survive, 8 plants of the surviving plants of each single integration line were selected and T3 seeds collected. If all offspring survives, the stable T3 seeds were ready to use for experiments. *Arabidopsis* lines used in this study are listed in Table 8.

**Table 8. *Arabidopsis* lines used in this study.**

| genotype | reference |
|---|---|
| mGFP-Lti6b | Cutler et al., 2000 |
| Col-0 (Columbia-0) | *Arabidopsis* biological resource centre |
| RLP44ECD-mCherry (Col-0) | This study |
| RLP44ECD-mCherry (*rlp44$^{cnu2}$*) | This study |
| RLP44ECD-mCherry (*cnu2*) | Wolf lab |
| RLP44ECD-mCherry(PMEIox) | This study |
| PMEIox | Wolf et al., 2012 |
| *cnu1* | Wolf et al., 2012 |
| *cnu2* | Wolf et al., 2014 |
| *cnu3* | This study |
| *cnu4* | This study |
| *bri1$^{cnu1}$* | Wolf et al., 2012 |
| *rlp44$^{cnu2}$* | Wolf et al., 2014 |
| *bri1$^{cnu3}$* | This study |
| *bri1$^{cnu4}$* | This study |
| secRFP | Zheng 2005 |
| FH107 | Martinière et al., 2011 |
| pRLp44:RLP44-GAGA-GFP (*cnu2*) | Borja Garnelo Gómez 2017 |
| pRLP44:RLP44-clusterII-GAGA-GFP (*cnu2*) | This study |
| pRLP44:RLP44-GFP (*rlp44$^{cnu2}$*) | This study |
| pBRI1:BRI1-GFP (*cnu3*) | This study |
| pBRI1:BRI1-GFP (*cnu4*) | This study |
| *rlp44-3* | Wolf et al., 2014 / SAIL_596_E12 |
| *bri1-301* | Li and Nam 2002 |
| pBRI1:BRI1 (*bri1-301*) | This study |
| pBRI1:BRI1cnu3 (*bri1-301*) | This study |
| pBRI1:BRI1cnu4 (*bri1-301*) | This study |
| pBRI1:BRI1cnu3,4 (*bri1-301*) | This study |
| *bri1-null* | Jaillais et al., 2011 / GK_134E10 |
| pBRI1:BRI1-GFP (*bri1-null*) | This study |
| pBRI1:BRI1-GFPcnu3 (*bri1-null*) | This study |
| pBRI1:BRI1-GFPcnu4 (*bri1-null)* | This study |
| pBRI1:BRI1-GFPcnu3,4 (*bri1-null*) | This study |
| *cpd* | Szekeres et al., 1996 |
| *dwf4-102* | Nakamoto et al., 2006 / SALK_020761 |
| BZR1-1D | Wang et al., 2002 |
| *bes1-D* | Yin et al., 2002 |
| *bin2-1* | Li and Nam 2002 |
| RLP44-RFP | Wolf et al., 2014 |
| RLP44-RFP (*bri1$^{cnu4}$*) | This study |
| mRFP-Lti6B | This study |

| | |
|---|---|
| *rlp44*$^{cnu2}$ *bri1*$^{cnu4}$ #50 | This study |
| *rlp44*$^{cnu2}$ *bri1*$^{cnu4}$ #79 | This study |
| *pskr1-3 pskr2-1* | Kutschmar et al., 2009 |
| *pskr1-2 psyr1r1* | Mosher and Kemmerling 2013 |
| *tpst-1* | Komori et al., 2009 |
| PSKR1ox | Kutschmar et al., 2009 |
| *rlp44*$^{cnu2}$ *pskr1-3* | This study |
| *rlp44*$^{cnu2}$ *pskr1-3 pskr2-1* | This study |
| PSKR1ox (*bri1*$^{cnu4}$) | This study |
| PSKR1ox (*rlp44*$^{cnu2}$) | This study |

## 4.3 Genomic DNA extraction and genotyping

### *4.3.1 gDNA extraction*

Genomic DNA (gDNA) extraction protocol was adapted from Edwards et al., 1991. gDNA was extracted from a preferable young plant and a single leaf was harvested in a 2 mL reaction tube together with a glass ball. After shock-freezing in liquid nitrogen the sample was homogenized with the help of a tissue homogenizer (QIAGEN). 250 µL of gDNA extraction buffer (150 nM Tris pH = 8, 250 mM NaCl, 25 mM EDTA, 0.5% SDS) was added to the homogenized tissue and mixed. After spinning down in a table top microcentrifuge at full speed for 15 min at room temperature, 150 µL of the supernatant was mixed with 150 µL isopropanol. This mixture was centrifuged for 10 min. Afterwards, the DNA pellet was washed with 500 µL of 70% Ethanol and centrifuged for 10 min. Supernatant was removed carefully and the pellet air-dried before dissolving in 40 µL TlowE buffer (10 mM Tris-HCL (pH = 8), 0.5 mM EDTA).

### *4.3.2 Genotyping*

Cleaved amplified polymorphic sequences (CAPS) are helpful tool to genotype mutant lines based on point mutations. CAPS primers were used to amplify the sequence with PCR and subsequent restriction with the appropriate restriction enzyme revealed the genotypes of *rlp44*$^{cnu2}$ (Wolf et al., 2014)*, bri1*$^{cnu3}$*, bri1*$^{cnu4}$*, bri1-301* (Li and Nam 2002). Primers and restriction enzymes are listed in Table 11.

Different t-DNA insertion lines were used in this study. For genotyping it was necessary to take a t-DNA specific primer. All used primer sequences are listed in Table 11. For *bri1-null* (GK_134E10) (Jaillais et al., 2011), SW1378 + SW1379 for the wildtype allele and SW1378 + SW1377 for the t-DNA, were used. Both *pskr* mutant lines are SALK lines, for

*pskr1-2* SW1745 + SW1746 for the wildtype allele and SW1745 +SW230 for the t-DNA. For *pskr2-1* SW1747 + SW1748 were combined for the wildtype and SW14747+SW230 for the t-DNA.

*rlp44-3* is a SAIL line. For the wildtype allele, SW425+SW326 were used, and for the t-DNA SW425+SW390 were used (Table 11)

## 4.4 Microscopic analysis

Confocal laser scanning microscopy of plant material was performed on a TCS SP5 inverted confocal microscope (Leica) or before on a LSM 510 Meta confocal scanning microscope (Zeiss). Used laser lines for excitation and emission wavelengths are depicted in Table 9. Images were analysed and processed with ImageJ (https://imagej.nih.gov/ij/).

**Table 9. Excitation and emission wavelengths used in this study.**

| fluorophore | excitation [nm] | emission [nm] |
|---|---|---|
| mTurquoise | 458 | 490-525 |
| GFP | 488 | 480-530 |
| RFP | 543 | 560-610 |
| mCherry | 543 | 560-610 |
| Propidium iodide | 543 | 560-610 |
| FM4-64 | 543 | 670-750 |
| Basic fuchsin | 514 | 420-480 |
| Calcofluore | 405 | 420-480 |

### *4.4.1 Fm4-64 staining*

1 µM FM4-64 was added to liquid ½ MS medium and seedlings were stained for 15 min for subsequent imaging. Microscope settings were used according toTable 9.

### *4.4.2 Basic fuchsin staining*

*Arabidopsis* seedlings were stained with basic fuchsin for the standard protocol for estimating the vasculature on 6 dag. Seedlings were first fixed in methanol (Honeywell) for 1-4 hours at room temperature. Methanol was removed and seedlings incubated in 10% (w/v) NaOH for 2-4 hours at 65 °C. Next step after removing the NaOH was the staining in 0.01% basic fuchsin solution in water (1% stock prepared in 100% Ethanol) for five minutes. Afterwards seedlings were destained with 70% Ethanol for 10 min and seedlings

can be stored in 50% V/V) Glycerol at 4°C. Seedlings were mounted in 50% Glycerol and sealed with polish for long-term storage. Xylem was counted below the hypocotyl. Secondary wall thickenings were also visible in the transmitted light channel. Microscope settings were used according to Table 9.

### *4.4.3 Calcofluor White staining*

For total vascular cell number assessment, roots were additionally to the basic fuchsin staining incubated with 100 µg/mL calcofluor white to stain the cellulose in the cell walls (Sigma-Aldrich, Fluorescence Brightener 28). The used stock solution was 20 mg/mL in water. Microscope settings were used according to Table 9.

### *4.4.4 Propidium iodide staining*

Roots were incubated in 10 µg/mL propidium iodide dissolved in water for about 10 min, subsequently mounted in the same solution and directly imaged. Microscope settings were used according to Table 9.

### *4.4.5 Plasmolysis*

The plasmolysis was always performed with 3-5 weeks old plants. Leaf disks were cut out and incubated in 0.6 M sorbitol solution for at least 10 min. Microscope settings were used according to Table 9.

## 4.5 RNA extraction and quantitative Real-Time PCR

### *4.5.1 RNA extraction and reverse transcription*

RNA was isolated derived from max. 100 mg *Arabidopsis* seedling tissue, liquid nitrogen frozen plant material was homogenized with the help of TissuelyserII (Qiagen). RNA was extracted with the help of RNA purification kit (Roboklon) following the manufacturer's instructions. DNase digestion directly on the column was included, with the recommended enzyme from Roboklon. After obtaining the RNA concentrations with the Nanodrop, 1 µg of RNA was used for cDNA synthesis. Therefore, 1 µg RNA in 5.75 µL RNase free water was mixed with 0.625 µL 10 mM dNTPs (Sigma-Aldrich), 0.625 µL 40 µM oligo dT primer (eurofines). This mix was incubated for 5 min on 65 °C and subsequently hold on

ice for another 5 min before adding a mixture of 2 µL 5 x Reverse Transcriptase buffer (Roboklon), 0.25 µL Ribolock RNase inhibitor 40 u/µL (ThermoFisher), 0.5 µL 100 mM DTT (Rokoblon) and 0.25 µL AMV Reverse Transkriptase (Roboklon) was added and hold for 1 hour at 42 °C. The reaction was stopped with putting the mixture to 85 °CX for 5 min. Afterwards the cDNA was stored at -20 °C and is was diluted 1:40 in $H_20$ before it was used for quantitative RT-PCR.

### *4.5.2 Quantitative Real-Time-PCR*

The diluted cDNA was added to a mixture of 1.5 µL 10x PCR reaction buffer (Sigma-Aldrich), 0.2 µL 50 mM MgCl2 (Sigma-Aldrich) , 0.3 µL 10 mM dNTPs (Sigma-Aldrich) , 0.05 µL 100 µM of each primer, 0,15 µL 1:400 diluted SYBR Green I nucleic acid gel stain (Sigma-Aldrich), 0.3 µL Jump Start Polymerase (Sigma-Aldrich) and 7.45 µL water. The used primers are listed in Table 12. The reactions were run in Rotor-Gene Q 2plex (Qiagen) and the raw data was analysed with the 75 Rotor-Gene Q 2plex software. Obtained $C_T$ values were analysed according the $2^{-\Delta\Delta C\,T}$ method and normalized to the appropriate mock condition (Muller et al., 2002).

## 4.6 Co-immunoprecipitation (Co-IP) and western blotting

Co-IP were performed either in stable transgenic *Arabidopsis* lines or in transiently overexpressing *N. benthamiana* leaves. For the latter, an agroinfiltration with the investigated proteins has to happen before Co-IP.

**Step 1:** First, agrobacteria main cultures with the proteins to investigate were grown overnight and centrifuged – the bacteria pellet is pelleted for 30 min at 3000 rpm and resuspended in water. Agrobacteria were starved for 1-3 hours at gentle agitation at room temperature. The $OD_{600}$ was measured and adjusted to 0.5. The cultures were mixed according the experimental outline and infiltrate in *N. benthamiana* leaves. Plants were incubated for two days before harvesting.

Transgene expressing *Arabidopsis* lines were plated on standard ½ MS plates and whole seedling plant material was harvested after 7-9 dag.

**Step 2**: Plant material was frozen in liquid nitrogen and grinded using mortar and pestle. Extraction buffer 1:2 was added. (100 mM Tris-HCl (pH 8.0), 150 mM NaCl, 10% (v/v)

Glycerol, 5 mM EDTA (Sigma-Aldrich), 2% (v/v) Igepal CA-630 (Sigma-Aldrich). Added fresh: 5 mM DTT (Sigma-Aldrich), 1% (v/v) Protease Inhibitor Cocktail (Bimake)

**Step 3**: Sample with extraction buffer was centrifuged at 4 °C at 13000 rom for 15 min. 60 µL aliquot of the supernatant was directly boiled in 20 µL 4x SDS-PAGE sample buffer (Roti®- Load 1, Carl Roth) and kept as input sample and the remaining supernatant was incubated with 15 µL of equilibrated slurry anti-tag MicroBeads (Chromotek GFP-Trap® or RFP-Trap®) for 2 hours at 4 °C in a table-top rotator. Subsequently, beads were washed, i.e. spun down at lowest possible speed, removing old buffer, adding fresh buffer and repeated for three times. After washing steps, the beads were boiled at 95 °C for 5-10 min in 30 µL 2x sample buffer (Roti®- Load 1, Carl Roth). Samples were either directly used for SDS-PAGE or stored at 4 °C.

SDS-polyacrylamid-gelelectrophorese (PAGE) gels were prepared freshly according the respective protein size. For BRI1/PSKR1, 7% acrylamide resolving gel was used, 12% acrylamide for RLP44 (resolving gel buffer: 1.5 M Tris-HCl pH 8.6). For the stacking gel, 4.5% acrylamide were always used (stacking gel buffer: 0.5 M Tris-HCl pH 6.8). SDS-PAGE were run in BioRad chambers in running buffer (25 mM Tris, 0.19 M Glycine, 0.35 mM SDS) at 100/200 V. The same amount of protein was loaded from the SDS-PAGE and after Western blotting, the PVDF membrane (Immonlion-P, Millipoe) was incubated with the indicated antibodies. Before incubation with the antibody, the membrane was blocked for at least 1 hour with 5% BSA in 1 x TBST blocking solution (20 nM Tris-base pH 7.4, 150 mM NaCl, 0.05% Tween). Primary antibodies, mouse monoclonal anti-GFP (1:10.000) (Biolegend), rabbit polyclonal anti-RFP (1:10000) (Karin Schumacher), rabbit polyclonal anti-BRI1 (1:5000) (Bojar et al., 2014), mouse monoclonal anti-HA (1:5000) (F-7, SantaCruz Biotechnology), rabbit polyclonal anti-BAK1 (1:5000) (Bojar et al., 2014), were diluted in 3% BSA and incubated with the membrane overnight at 4 °C on a shaker. Subsequently, membranes were washed 8 x 5 min with 1 X TBST and afterwards they were incubated with the secondary antibodies, goat polyclonal anti-rabbit coupled to horseradish peroxidase conjugate (1:10000) (ThermoFisher) or rabbit polyclonal anti-mouse coupled to horseradish peroxidase conjugate (1:10000) (Sigma-Aldrich) diluted in in 3% BSA for 1 hour on agitation at room temperature. Afterwards, membranes were washed 8 x 5 min before imaging with an ECL imaging device (INTAS). For chemiluminescent reaction,

either SuperSignal™ west pico chemiluminescent substrate (ThermoFisher) or the SuperSignal™ west femto chemiluminescent substrate (ThermoFisher) was used.

## 4.7 FRET-FLIM

### *4.7.1 FRET-FLIM cloning*

For the Foerster Resonance Energy Transfer, 2in1 vectors in a Gateway system were used (Hecker et al., 2015). For this, the GOI was cloned into specific entry vectors, pDONR221-P1P4 and pDONR221-P3P2 (Table 13). Subsequently both to be tested GOIs were combined into one backbone plasmid (Table 10).

**Table 10. Constructs used for FRET-FLIM in this study.**

| plasmid name | stock name | backbone plasmid | comments |
|---|---|---|---|
| PSKR1-GFP | pSW763 | pH7WGF2 | Ladwig et al., 2015 |
| RLP44-RFP | pSW49 | pK7RGW2 | Wolf et al. 2014 |
| FLS2-RLP44 | pSW583 | pFRETtc-2in1-CC | this study |
| BRI1WT-RLP44 | pSW579 | pFRETtc-2in1-CC | this study |

### *4.7.2 FRET-FLIM measurements*

FRET-FLIM measurements were performed by Dr. Friederike Wanke and Nina Glöckner according to Ladwig et al., 2015.

## 4.8 Glycan array

### *4.8.1 Recombinant protein*

The recombinant protein RLP44_StrepII-tag_9xHis-tag: 250ul á 1.7mg/ml (stored in 150mM NaCl, 20mM citrate pH = 5 ) was provided by Dr. Ulrich Hohmann and produced according to Hohmann et al., 2018.

### *4.8.2 AGATA 1.0 glycan arrays*

AGATA 1.0 glycan arrays were provided by Prof. William Willats. Please refer to the appendix for composition details of the glycan array.

### *4.8.3 Self-produced glycan arrays*

Pectins with different degree in demethylesterification were dissolved to a 0.75% solution in water. Therefore, the amount was first dissolved in 8 mL water, warmed up to 40 °C and stirred for 10 min. After dissolving of the powder, the amount was adjusted to 10 mL.
Used pectins: pectin from citrus fruit (SIGMA – P-9135), pectin esterified from citrus fruit 10% (SIGMA-P9561), pectin esterified potassium salt from citrus fruit 40% (SIGMA-P9436), pectin, esterified potassium salt from citrus fruit 70% (SIGMA-P9311), and polygalacturonic acid (Megazyme 30402).
Solutions were centrifuged to remove possible undissolved pectin resides, and subsequently 1 µL of the solution was immobilized on a Nitrocellulose Blotting Membrane (Amersham ™ Protran™ -10600002). After drying, the membranes were kept at 4 °C.

### *4.8.4 Performing glycan arrays*

The used recombinant protein was stored in 150mM NaCl, 20mM citrate pH = 5. To maintain constant conditions, we first blocked the arrays for 1 hour with 5% BSA in citrate buffer, followed by overnight incubation at 4 °C of 10 µg RLP44 on one array. Afterwards, arrays were washed 5 times with citrate buffer with PBS and were incubated subsequently for 1 hour at room temperature in PBS, 0.1% Tween diluted 1:5000 Strep-Tactin® HRP Conjugate (iba). Afterwards 5 times washing with PBS 0.1% Tween, and additional incubation for 2 hours, imaging was performed with SuperSignal™ west femto chemiluminescent substrate (ThermoFisher Scientific) using an ECL imaging device (INTAS). The picture was quantified with ImageJ (https://imagej.nih.gov/ij/).

## 4.9 Statistical analysis

The number of samples is always denoted in the legend of the respective figure. The significance of the difference between samples was either calculated by One-way ANOVA, Two-way ANOVA with subsequent Tukey's post hoc test, or by Student's t-test. Xylem cells quantification was evaluated with Mann-Whitney U-test or Kruskal-Wallis modified U-test and Dunn's post hoc test with Benjamini-Hochberg correction. Asterisks indicate significance with *$p < 0.05$, **$p < 0.01$, and ***$p < 0.001$.

## 4.10 Primers used in this study

**Table 11. Primers used in this study for genotyping.**

| primer name | stock name | sequence (5'-3') | gene | special remark |
|---|---|---|---|---|
| rlp44_CAPS_F | SW502 | AATCTACAAACTCTCACTCAC | At4G49750 | HinfI |
| rlp44_CAPS_R | SW504 | CTGACCGGATAATTCGTTATC | At4G49750 | HinfI |
| bri1-301_CAPS_F | SW1426 | GGTTTGGAGATGTTTACAAAG | At4G39400 | Sau3AI |
| bri1-301_CAPS_R | SW1427 | AAAATCCGGTGAATCCGTTG | At3G39400 | Sau3AI |
| bri1cnu3_CAPS_R | SW1120 | TCGATTCCTGATGAGGTAGGTG | At4G39400 | Cfr42I |
| bri1cnu3_CAPS_R | SW1121 | AAGATCCGCAAACGTGAGCTTC | At4G39400 | Cfr42I |
| bri1cnu4_CAPS_F | SW1158 | TCAGGAGCTCATGTATGTCA | At4G39400 | BseL1 |
| bri1cnu4_CAPS_R | SW1159 | TCCAATTGGTGTTGTTAGCAG | At4G39400 | BseL1 |
| rlp44-3_SAIL_596_E12_F | SW425 | acctcacttctgctaaaacgc | At4G49750 | |
| rlp44-3SAIL_596_E12_R | SW426 | AGACCTAATTGCTGCGGAATC | At4G49750 | |
| LB3_Sail | SW390 | ATAACCAATCTCGATACAC | | SAIL insertion |
| GK-134E10_F | SW1378 | TAGCGGAAACAAAATCAGTGG | At4G39400 | |
| GK-134E10_R | SW1379 | TCGTTCCATTGAAGAGATTGG | At4G39400 | |
| GK-o8409 | SW1377 | ATATTGACCATCATACTCATTGC | | GABI-KAT insertion |
| pskr1-3_SALK_008585_F | SW1745 | CTCGCTTTCTGGTATGACGAG | At2G02220 | |
| pskr1-3_SALK_008585_R | SW1746 | TCCGAAACTATACACATCGCC | At2G02220 | |
| pskr2-1_SALK_203857_F | SW1747 | TTCTTAGACTGTTTGGCTCGG | At2G22942 | |
| pskr2-1_SALK_203857_R | SW1748 | GCGTTACAAACATGCAACAAG | At2G22942 | |
| LBb1.3_Salk | SW230 | ATTTTGCCGATTTCGGAAC | | SALK insertion |

**Table 12. Primers for quantitative Real-Time PCR.**

| primer name | stock name | sequence (5'-3') | gene |
|---|---|---|---|
| Clath_F | SW801 | tcgattgcttggtttggaagat | At1G10730 |
| Clath_R | SW802 | gcacttagcgtggactctgtttgc | At1G10730 |
| RLP44_F | SW612 | TCAGATTCCGCAGCAATTAG | At4G49750 |
| RLP44_R | SW613 | TCCTGCAACGGATAACCATA | At4G49750 |
| DWF4_F | SW803 | caacagcaaaacaacggagcg | At3G50660 |
| DWF4_R | SW804 | tctgaaccagcacatagccttg | At3G50660 |
| SAUR15_F | SW618 | AAGAGGATTCATGGCGGTCTATG | At4G38850 |
| SAUR15_R | SW619 | GTATTGTTAAGCCGCCCATTGG | At4G38850 |

**Table 13. Primers used in this study for cloning**

| primer name | stock name | sequence (5'-3') | gene |
|---|---|---|---|
| BRI1_GGC_F | SW1254 | AACAGGTCTCAGGCTCATGAAGACTTTTTCAAGCTTCT | At4G39400 |
| BRI1_GGC_R | SW1255 | AACAGGTCTCACTGATAATTTTCCTTCAGGAACTTC | At4G39400 |
| BRI1_GGC_1R-new2 | SW1316 | AACAGGTCTCaATCACACGCGCCGGAGAGAAAGTCAG | At4G39400 |
| BRI1_GGC_2F-new2 | SW1317 | aacaGGTCTCaTGATACACTCACTGGaCTCGATCTCTCTGGA | At4G39400 |
| BRI1_GGC_2Rnew | SW1296 | aacaGGTCTCaGAGtCCAGGATTGTTCAAGAA | At4G39400 |
| BRI1_GGC_3Fnew | SW1297 | aacaGGTCTCaACTCTGTGGTTATCCTCTT | At4G39400 |
| BRI1_GGC_3Rnew | SW1298 | aacaggTCTCaGGCCTCCTTCCATGAGATCT | At4G39400 |
| BRI1_GGC_4Fnew | SW1299 | aacaGGTCTCaGgCCAGCGTCCCTTGCTGGT | At4G39400 |
| RLP44BTMD-C1_47_L | SW1809 | AACAGGTCTCaCgcTAACTGGACAAACTCCGTCT | At3G49750 |

| | | | |
|---|---|---|---|
| RLP44BTMD-C1_47_R | SW1810 | AACAGGTCTCaAgcGAGATTACTCGCCGGATCTT | At3G49750 |
| RLP44BTMD-C1_77_L | SW1811 | AACAGGTCTCaCGCACTCTCACTCACAAACCTCTC | At3G49750 |
| RLP44BTMD-C1_77_R | SW1812 | AACAGGTCTCaTGCgtagattcttccgttgttac | At3G49750 |
| RLP44BTMD-C2_146_L | SW1813 | AACAGGTCTCaTGCCTTAAACGTAATCGATCTCCAC | At3G49750 |
| RLP44BTMD-c2_147_R | SW1814 | AACAGGTCTCaGGCAGCGCAAAGAGCGAGCTGC | At3G49750 |
| RLP44BTMD-C2_170_L | SW1815 | AACAGGTCTCaGGCGCTC TCG GCG TTT GAT GTG TC | At3G49750 |
| RLP44BTMD-C2_170_R | SW1816 | AACAGGTCTCaCGCCGCTAATAGACCTAATTGCTGC | At3G49750 |
| RLP44BTMD-C3_192_198_L | SW1817 | AACAGGTCTCaTGCGACTGGGAATTTCCCGGCGTTTAACGCGAGTTCGTTTATA | At3G49750 |
| RLP44BTMD-C3_192_198_R | SW1818 | AACAGGTCTCaCGCCGGGAAATTCCCAGTCGCATTCGACAAATACGTCGGAAT | At3G49750 |
| RLP44BTMD-C4_180_L | SW1819 | AACAGGTCTCaCGCACTT TCCGGTCAGATTCCGAC | At3G49750 |
| RLP44BTMD:-C4_180_R | SW1820 | AACAGGTCTCaTGCGTTATTCGACACATCAAACGC | At3G49750 |
| RLP44BTMD-C4_208_L | SW1821 | AACAGGTCTCaTGCAGGATTGTATGGTTATCCGTTGC | At3G49750 |
| RLP44BTMD-C4_208_R | SW1822 | AACAGGTCTCaTGCATTCCCTATAAACGAACTCGC | At3G49750 |
| GGC_44BTMD_oStop_R | SW1875 | AACAGGTCTCActgaTTTACTCTTCATCATCATCTC | At3G49750 |
| RLP44_GWoStop_R | SW374 | GGGGACCACTTTGTACAAGAAAGCTGGGTaGTAATCAGGCATAGATTGACT | at3g49750 |
| RLP44_GW_L | SW372 | GGGGACAAGTTTGTACAAAAAAGCAGGCTATGACAAGGAGTCACCGGTTAC | At3G49750 |
| RLP44_GGP_Rneu | SW1205 | AACAGGTCTCACTGAGTAATCAGGCATAGATTGAC | at3g49750 |
| RLP44_GGP_F | SW1179 | AACAGGTCTCAGGCTCAATGACAAGGAGTCACCGGTTA | At3G49750 |
| GGC_44BTMD_oStop_R | SW1875 | AACAGGTCTCActgaTTTACTCTTCATCATCATCTC | At3G49750 |
| BRI1_attB4_R o spacer | SW1416 | GGGGACAACTTTGTATAGAAAAGTTGGGTGTAATTTTCCTTCAGGAACTTCTT | At4G39400 |
| BRI1_attB1_L +ta | SW1417 | GGGGACAAGTTTGTACAAAAAAGCAGGCTtaATGAAGACTTTTTCAAGCTTCTT | At4G39400 |
| FLS2_attB4_R o spacer | SW1418 | GGGGACAACTTTGTATAGAAAAGTTGGGTGAACTTCTCGATCCTCGTTACG | At5G46330.1 |
| FLS2_attB1_F +ta | SW1419 | GGGGACAAGTTTGTACAAAAAAGCAGGCTtaATGAAGTTACTCTCAAAGAC | At5G46330.1 |
| RLP44_attb3_F +ta | SW1420 | GGGGACAACTTTGTATAATAAAGTTGtaATGACAAGGAGTCACCGGTTAC | AT3G49750 |
| RLP44_GW_CD_F | SW1437 | GGGGACAAGTTTGTACAAAAAAGCAGGCTATGTGTTTATGGTTGAGG | At3G49750 |
| RLP44_GW_CD_R | SW1438 | GGGGACCACTTTGTACAAGAAAGCTGGGTtGTAATCAGGCATAGATTG | At3G49750 |
| pRLP44_F | SW1149 | AACAGGTCT**C**AACCTtttgcgatatttttggctgtc | At3G49750 |
| pRLP44_R | SW1150 | AACAGGTCTCATGTTttttaaattttagagaggtttc | At3G49750 |
| BRI1prom_GGA_F | SW1280 | AACAGGTCTCAACCTgatcttccttctttatttg | At4G39400 |
| BRI1prom_GGA_R | SW1281 | AACAGGTCTCATGTTttctcaagagtttgtgagag | At4G39400 |

# 5 Bibliography


Albert, Isabell et al. 2015. "An RLP23–SOBIR1–BAK1 Complex Mediates NLP-Triggered Immunity." *Nature Plants* 1(10):15140.

Amano, Yukari, Hiroko Tsubouchi, Hidefumi Shinohara, Mari Ogawa, and Yoshikatsu Matsubayashi. 2007. "Tyrosine-Sulfated Glycopeptide Involved in Cellular Proliferation and Expansion in Arabidopsis." *Proceedings of the National Academy of Sciences of the United States of America* 104(46):18333–38.

Asami, Tadao et al. 2001. "Selective Interaction of Triazole Derivatives with DWF4, a Cytochrome P450 Monooxygenase of the Brassinosteroid Biosynthetic Pathway, Correlates with Brassinosteroid Deficiency in Planta." *Journal of Biological Chemistry* 276(28):25687–91.

Atmodjo, Melani A., Zhangying Hao, and Debra Mohnen. 2013. "Evolving Views of Pectin Biosynthesis." *Annual Review of Plant Biology* 64(1):747–79.

Baum, Stuart F., Joseph G. Dubrovsky, and Thomas L. Rost. 2002. "Apical Organization and Maturation of the Cortex and Vascular Cylinder in Arabidopsis Thaliana (Brassicaceae) Roots." *American Journal of Botany* 89(6):908–20.

Belkhadir, Youssef and Yvon Jaillais. 2015. "Tansley Review The Molecular Circuitry of Brassinosteroid Signaling." *New Phytologist*.

Bella, J., K. L. Hindle, P. A. McEwan, and S. C. Lovell. 2008. "The Leucine-Rich Repeat Structure." *Cellular and Molecular Life Sciences* 65(15):2307–33.

Van den Berg, Claudia, Viola Willemsen, Willem Hage, Peter Weisbeek, and Ben Scheres. 1995. "Cell Fate in the Arabidopsis Root Meristem Determined by Directional Signalling." *Nature* 378(6552):62–65.

Bishopp, Anthony et al. 2011. "A Mutually Inhibitory Interaction between Auxin and Cytokinin Specifies Vascular Pattern in Roots." *Current Biology* 21(11):917–26.

Boisson-Dernier, Aurélien et al. 2013. "ANXUR Receptor-Like Kinases Coordinate Cell Wall Integrity with Growth at the Pollen Tube Tip Via NADPH Oxidases." *PLoS Biology* 11(11).

Boisson-Dernier, Aurélien, Sharon A. Kessler, and Ueli Grossniklaus. 2011. "The Walls Have Ears: The Role of Plant CrRLK1Ls in Sensing and Transducing Extracellular Signals." *Journal of Experimental Botany* 62(5):1581–91.

Bojar, Daniel et al. 2014. "Crystal Structures of the Phosphorylated BRI1 Kinase Domain and Implications for Brassinosteroid Signal Initiation." *Plant Journal* 78(1):31–43.

Borja Garnelo Gómez. 2017. "Phosphorylation of RLP44: Shifting between Subcellular Localization and Receptor Complexes." *PhD Thesis* (November).

Brand, Ulrike, Jennifer C. Fletcher, Martin Hobe, Elliot M. Meyerowitz, and Rüdiger Simon. 2000. "Dependence of Stem Cell Fate in Arabidopsis on a Feedback Loop Regulated by CLV3 Activity." *Science* 289(July):617–19.

Caffall, Kerry Hosmer and Debra Mohnen. 2009. "The Structure, Function, and Biosynthesis of Plant Cell Wall Pectic Polysaccharides." *Carbohydrate Research* 344(14):1879–1900.

Caño-Delgado, Ana et al. 2004. "BRL1 and BRL3 Are Novel Brassinosteroid Receptors That Function in Vascular Differentiation in Arabidopsis." *Development (Cambridge, England)* 131(21):5341–51.

Caño-Delgado, Ana, Ji-Young Lee, and Taku Demura. 2010. "Regulatory Mechanisms for Specification and Patterning of Plant Vascular Tissues." *Annual Review of Cell and Developmental Biology* 26(1):605–37.

Carlsbecker, Annelie et al. 2010. "Cell Signalling by microRNA165/6 Directs Gene Dose-Dependent Root Cell Fate." *Nature* 465(7296):316–21.

Carpin, S. et al. 2001. "Identification of a Ca(2+)-Pectate Binding Site on an Apoplastic Peroxidase." *The Plant Cell* 13(3):511–20.

Cavalier, David M. et al. 2008. "Disrupting Two Arabidopsis Thaliana Xylosyltransferase Genes Results in Plants Deficient in Xyloglucan, a Major Primary Cell Wall Component." *The Plant Cell* 20(June):1519–37.

Chen, Jia et al. 2016. "FERONIA Interacts with ABI2-Type Phosphatases to Facilitate Signaling Cross-Talk between Abscisic Acid and RALF Peptide in *Arabidopsis*." *Proceedings of the National Academy of Sciences* 113(37):E5519–27.

Cheung, Alice Y. and Hen Ming Wu. 2011. "THESEUS 1, FERONIA and Relatives: A Family of Cell Wall-Sensing Receptor Kinases?" *Current Opinion in Plant Biology* 14(6):632–41.

Chinchilla, Delphine et al. 2007. “A Flagellin-Induced Complex of the Receptor FLS2 and BAK1 Initiates Plant Defence.” *Nature* 448(7152):497–500.

Chinchilla, Delphine, Libo Shan, Ping He, Sacco de Vries, and Birgit Kemmerling. 2009. “One for All: The Receptor-Associated Kinase BAK1.” *Trends in Plant Science* 14(10):535–41.

Clark, Steven E., Robert W. Williams, and Elliot M. Meyerowitz. 1997. “The CLAVATA1 Gene Encodes a Putative Receptor Kinase That Controls Shoot and Floral Meristem Size in Arabidopsis.” *Cell* 89(1):575–85.

Clough, Steven J. and Andrew F. Bent. 1998. “Floral Dip: A Simplified Method for Agrobacterium-Mediated Transformation of *Arabidopsis Thaliana*.” *Plant Journal* 16(6):735–43.

Clouse, Steven D. 1996. “Molecular Genetic Studies Confirm the Role of Brassinosteroids in Plant Growth and Development.” *Plant Journal* 10(1):1–8.

Cosgrove, Daniel J. 2005. “Growth of the Plant Cell Wall.” *Nature Reviews. Molecular Cell Biology* 6(November):850–61.

Cutler, S. R., D. W. Ehrhardt, J. S. Griffitts, and C. R. Somerville. 2000. “Random GFP::cDNA Fusions Enable Visualization of Subcellular Structures in Cells of Arabidopsis at a High Frequency.” *Proceedings of the National Academy of Sciences* 97(7):3718–23.

Czyzewicz, Nathan, Kun Yue, Tom Beeckman, and Ive De Smet. 2013. “Message in a Bottle: Small Signalling Peptide Outputs during Growth and Development.” *Journal of Experimental Botany* 64(17):5281–96.

Decreux, Annabelle and Johan Messiaen. 2005. “Wall-Associated Kinase WAK1 Interacts with Cell Wall Pectins in a Calcium-Induced Conformation.” *Plant and Cell Physiology* 46(2):268–78.

Derbyshire, Paul, Maureen C. McCann, and Keith Roberts. 2007. “Restricted Cell Elongation in Arabidopsis Hypocotyls Is Associated with a Reduced Average Pectin Esterification Level.” *BMC Plant Biology* 7:1–12.

Deslauriers, Stephen D. and Paul B. Larsen. 2010. “FERONIA Is a Key Modulator of Brassinosteroid and Ethylene Responsiveness in Arabidopsis Hypocotyls.” *Molecular Plant* 3(3):626–40.

Doblas, Verónica G. et al. 2017. “Root Diffusion Barrier Control by a Vasculature-Derived Peptide Binding to the SGN3 Receptor.” 284(January):280–84.

Dolan, L. et al. 1993. “Cellular Organisation of the Arabidopsis Thaliana Root.” *Development* 119(1):71–84.

Donner, T. J., I. Sherr, and E. Scarpella. 2009. “Regulation of Preprocambial Cell State Acquisition by Auxin Signaling in Arabidopsis Leaves.” *Development* 136(19):3235–46.

Edwards, K., C. Johnstone, and C. Thompson. 1991. “A Simple and Rapid Method for the Preparation of Plant Genomic DNA for PCR Analysis.” *Nucleic Acids Research* 19(6):1349.

Feng, Wei, Daniel Kita, Alexis Peaucelle, Heather N. Cartwright, et al. 2018. “The FERONIA Receptor Kinase Maintains Cell-Wall Integrity during Salt Stress through Ca 2+ Signaling.” *Current Biology* 1–10.

Feng, Wei, Daniel Kita, Alexis Peaucelle, and Hen-ming Wu. 2018. “The FERONIA Receptor Kinase Maintains Cell-Wall Integrity during Salt Stress through Ca 2 + Signaling Article The FERONIA Receptor Kinase Maintains Cell-Wall Integrity during Salt Stress through Ca 2 + Signaling.” 666–75.

Francis, K. E., S. Y. Lam, and G. P. Copenhaver. 2006. “Separation of Arabidopsis Pollen Tetrads Is Regulated by QUARTET1, a Pectin Methylesterase Gene.” *Plant Physiology* 142(3):1004–13.

Friedrichsen, D. M., C. a Joazeiro, J. Li, T. Hunter, and J. Chory. 2000. “Brassinosteroid-Insensitive-1 Is a Ubiquitously Expressed Leucine-Rich Repeat Receptor Serine/threonine Kinase.” *Plant Physiology* 123(4):1247–56.

Friml, Jiří et al. 2003. “Efflux-Dependent Auxin Gradients Establish the Apical-Basal Axis of Arabidopsis.” *Nature* 426(6963):147–53.

Fukuda, Hiroo. 1997. “Tracheary Element Differentiation.” 9(July):3–7.

Gampala, Srinivas S. et al. 2007. “An Essential Role for 14-3-3 Proteins in Brassinosteroid Signal Transduction in Arabidopsis.” *Developmental Cell* 13(2):177–89.

Goda, H. 2004. “Comprehensive Comparison of Auxin-Regulated and Brassinosteroid-Regulated Genes in Arabidopsis.” *Plant Physiology* 134(4):1555–73.

Gómez-Gómez, Lourdes, Georg Felix, and Thomas Boller. 1999. “A Single Locus Determines Sensitivity to Bacterial Flagellin in Arabidopsis Thaliana.” *Plant Journal* 18(3):277–84.

Gonneau, Martine et al. 2018. “Receptor Kinase THESEUS1 Is a Rapid Alkalinisation Factor 34 Receptor in Arabidopsis.” *Curr Biol* in press:1–7.

Grabov, a et al. 2005. “Morphometric Analysis of Root Shape.” *The New Phytologist* 165(2):641–51.

Grove, Michael D. et al. 1979. “Brassinolide, a Plant Growth-Promoting Steroid Isolated from Brassica Napus Pollen [12].” *Nature* 281(5728):216–17.

Gust, Andrea A. and Georg Felix. 2014. “Receptor like Proteins Associate with SOBIR1-Type of Adaptors to Form Bimolecular Receptor Kinases.” *Current Opinion in Plant Biology* 21:104–11.

Gutierrez, Ryan, Jelmer J. Lindeboom, Alex R. Paredez, A. M. C. Emons, and David W. Ehrhardt. 2009. “Arabidopsis Cortical Microtubules Position Cellulose Synthase Delivery to the Plasma Membrane and Interact with Cellulose Synthase Trafficking Compartments.” *Nature Cell Biology* 11(7):797–806.

Han, Zhifu, Yadong Sun, and Jijie Chai. 2014. “Structural Insight into the Activation of Plant Receptor Kinases.” *Current Opinion in Plant Biology* 20:55–63.

Hanus, Jaroslav and Karim Mazeau. 2006. “The Xyloglucan–Cellulose Assembly at the Atomic Scale.” *Biopolymers* (80):9–30.

Hardtke, Christian S. and Thomas Berleth. 1998. “The Arabidopsis Gene MONOPTEROS Encodes a Transcription Factor Mediating Embryo Axis Formation and Vascular Development.” *EMBO Journal* 17(5):1405–11.

Hartmann, Jens et al. 2013. “Phytosulfokine Control of Growth Occurs in the Epidermis , Is Likely to Be Non-Cell Autonomous and Is Dependent on Brassinosteroids.” 579–90.

Hartmann, Jens, Cornelia Fischer, Petra Dietrich, and Margret Sauter. 2014. “Kinase Activity and Calmodulin Binding Are Essential for Growth Signaling by the Phytosulfokine Receptor PSKR1.” 192–202.

Hartwig, Thomas et al. 2012. “Propiconazole Is a Specific and Accessible Brassinosteroid (BR) Biosynthesis Inhibitor for Arabidopsis and Maize.” *PLoS ONE* 7(5):1–11.

Haruta, Miyoshi, Grzegorz Sabat, Kelly Stecker, Benjamin B. Minkoff, and Michael R. Sussman. 2014. “A Peptide Hormone and Its Receptor.” *Science* 343(January):408–11.

He, J. X., J. M. Gendron, Y. Yang, J. Li, and Z. Y. Wang. 2002. “The GSK3-like Kinase BIN2 Phosphorylates and Destabilizes BZR1, a Positive Regulator of the Brassinosteroid Signaling Pathway in Arabidopsis.” *Proceedings of the National Academy of Sciences* 99(15):10185–90.

He, Zheng Hui, Masaaki Fujiki, and Bruce D. Kohorn. 1996. “A Cell Wall-Associated, Receptor-like Protein Kinase.” *Journal of Biological Chemistry* 271(33):19789–93.

Hecker, Andreas et al. 2015. “Binary 2in1 Vectors Improve in Planta (Co)localization and Dynamic Protein Interaction Studies.” *Plant Physiology* 168(3):776–87.

Helariutta, Yrjo et al. 2000. “The SHORT-ROOT Gene Controls Radial Patterning of the Arabidopsis Root through Radial Signaling.” *Cell* 101(5):555–67.

Hématy, Kian et al. 2007. “A Receptor-like Kinase Mediates the Response of Arabidopsis Cells to the Inhibition of Cellulose Synthesis.” *Current Biology : CB* 17:922–31.

Heyman, J. et al. 2013. “ERF115 Controls Root Quiescent Center Cell Division and Stem Cell Replenishment.” *Science* 342(6160):860–63.

Hirakawa, Y. et al. 2008. “Non-Cell-Autonomous Control of Vascular Stem Cell Fate by a CLE Peptide/receptor System.” *Proceedings of the National Academy of Sciences* 105(39):15208–13.

Hohmann, Ulrich et al. 2018. “Mechanistic Basis for the Activation of Plant Membrane Receptor Kinases by SERK-Family Coreceptors.” *Proceedings of the National Academy of Sciences* 201714972.

Holzwart, Eleonore et al. 2018. “Integration of Brassinosteroid and Phytosulfokine Signalling Controls Vascular Cell Fate in the Arabidopsis Root.” *bioRxiv*.

Hothorn, Michael et al. 2011. “Structural Basis of Steroid Hormone Perception by the Receptor Kinase BRI1.” *Nature* 474(7352):467–72.

Huck, N. 2003. “The Arabidopsis Mutant Feronia Disrupts the Female Gametophytic Control of Pollen Tube Reception.” *Development* 130(10):2149–59.

Huerta, Apolonio Ignacio. 2016. “The Receptor-like Protein , RLP44 , Regulates Root Xylem Differentiation through a yet Unknown Signaling Pathway and Mediates Differential Phosphorylation of BAK1-BRI1 Complexes.”

Hypocotyl, Arabidopsis, Alexis Peaucelle, and Raymond Wightman. 2015. “The Control of Growth Symmetry Breaking in the Report The Control of Growth Symmetry Breaking in the Arabidopsis Hypocotyl.” 1746–52.

Ibañes, Marta, Norma Fàbregas, Joanne Chory, and Ana I. Caño-Delgado. 2009. “Brassinosteroid Signaling and Auxin Transport Are Required to Establish the Periodic Pattern of Arabidopsis Shoot Vascular

Bundles." *Proceedings of the National Academy of Sciences of the United States of America* 106(32):13630–35.

Igarashi, Daisuke, Kenichi Tsuda, and Fumiaki Katagiri. 2012. "The Peptide Growth Factor, Phytosulfokine, Attenuates Pattern-Triggered Immunity." *Plant Journal* 71(2):194–204.

Iwasaki, T. .. and H. Shibaok. 1991. "Brassinosteroids Act as Regulators of Trachery Element Differentiation in Isolated Zinna Mesophyll Cells." *Plant Cell Physiology* 32(July):1004–7.

Jaillais, Y., Y. Belkhadir, E. Balsemao-Pires, J. L. Dangl, and J. Chory. 2011. "Extracellular Leucine-Rich Repeats as a Platform for Receptor/coreceptor Complex Formation." *Proceedings of the National Academy of Sciences* 108(20):8503–7.

Jaillais, Yvon et al. 2011. "Tyrosine Phosphorylation Controls Brassinosteroid Receptor Activation by Triggering Membrane Release of Its Kinase Inhibitor." *Genes & Development* 25(3):232–37.

Jendretzki, Arne, Janina Wittland, Sabrina Wilk, Andrea Straede, and Jürgen J. Heinisch. 2011. "How Do I Begin? Sensing Extracellular Stress to Maintain Yeast Cell Wall Integrity." *European Journal of Cell Biology* 90(9):740–44.

Jones, D. A., C. M. Thomas, Hammond-Kossack K.E., P. J. Balint-Kurti, and J. D. G. Jones. 1994. "Isolation of the Cf-9 Gene for Resistance to Cladosporum Fulvum by Transposon Tagging." *Science* 266(November):789–93.

Jürgens, G. et al. 2001. "Apical-Basal Pattern Formation in Arabidopsis Embryogenesis." *The EMBO Journal* 20(14):3609–16.

Kang, Yeon Hee, Alice Breda, and Christian S. Hardtke. 2017. "Brassinosteroid Signaling Directs Formative Cell Divisions and Protophloem Differentiation in *Arabidopsis* Root Meristems." *Development* 144(2):272–80.

Karimi, M., D. Inze, and A. Depicker. 2002. "{GATEWAY} Vectors for \textit{Agrobacterium}-Mediated Plant Transformation." *Trends in Plant Science* 7(5):193–95.

Kessler, S. A., H. Lindner, D. S. Jones, and U. Grossniklaus. 2015. "Functional Analysis of Related CrRLK1L Receptor-like Kinases in Pollen Tube Reception." *EMBO Reports* 16(1):107–15.

Kidner, Catherine, Venkatesan Sundaresan, Keith Roberts, and Liam Dolan. 2000. "Clonal Analysis of the Arabidopsis Root Con ® Rms That Position , Not Lineage , Determines Cell Fate."

Kim, Tae-Wuk and Zhi-Yong Wang. 2010. "Brassinosteroid Signal Transduction from Receptor Kinases to Transcription Factors." *Annual Review of Plant Biology* 61(1):681–704.

Kim, Tae Wuk et al. 2009. "Brassinosteroid Signal Transduction from Cell-Surface Receptor Kinases to Nuclear Transcription Factors." *Nature Cell Biology* 11(10):1254–60.

Kim, Tae Wuk, Shenheng Guan, Alma L. Burlingame, and Zhi Yong Wang. 2011. "The CDG1 Kinase Mediates Brassinosteroid Signal Transduction from BRI1 Receptor Kinase to BSU1 Phosphatase and GSK3-like Kinase BIN2." *Molecular Cell* 43(4):561–71.

Kobe, Bostjan and Johann Deisenhofer. 1994. "The Leucine-Rich Repeat: A Versatile Binding Motif." *Trends in Biochemical Sciences* 19(10):415–21.

Kock, Christian, Yves F. Dufrï¿½ne, and Jï¿½rgen J. Heinisch. 2015. "Up against the Wall: Is Yeast Cell Wall Integrity Ensured by Mechanosensing in Plasma Membrane Microdomains?" *Applied and Environmental Microbiology* 81(3):806–11.

Kolbeck, Andreas. 2015. "Cell Wall Integrity Signal Propagation: Localisation and Tunrover of Receptor-Like Protein (RLP)44."

Komori, R., Y. Amano, M. Ogawa-Ohnishi, and Y. Matsubayashi. 2009. "Identification of Tyrosylprotein Sulfotransferase in Arabidopsis." *Proc Natl Acad Sci U S A* 106(35):15067–72.

Kondo, Yuki et al. 2014. "Plant GSK3 Proteins Regulate Xylem Cell Differentiation Downstream of TDIF-TDR Signalling." *Nature Communications* 5:1–11.

Kondo, Yuki, Takashi Fujita, Munetaka Sugiyama, and Hiroo Fukuda. 2015. "A Novel System for Xylem Cell Differentiation in Arabidopsis Thaliana." *Molecular Plant* 8(4):612–21.

Kubo, Minoru et al. 2005. "Transcription Switches for Protoxylem and Metaxylem Vessel Formation." *Genes and Development* 19(16):1855–60.

Kumar, Manoj, Liam Campbell, and Simon Turner. 2016. "Secondary Cell Walls: Biosynthesis and Manipulation." *Journal of Experimental Botany* 67(2):515–31.

Kutschmar, A. et al. 2009. "PSK-Alpha Promotes Root Growth in Arabidopsis." *New Phytol* 181(4):820–31.

Ladwig, Friederike et al. 2015. "Phytosulfokine Regulates Growth in Arabidopsis through a Response Module at the Plasma Membrane That Includes CYCLIC NUCLEOTIDE-GATED CHANNEL17, H+-

ATPase, and BAK1." *The Plant Cell* 27(6):1718–29.
Lampropoulos, Athanasios et al. 2013. "GreenGate - A Novel, Versatile, and Efficient Cloning System for Plant Transgenesis." *PLoS ONE* 8(12).
Lang, Ingeborg, Stefan Sassmann, Brigitte Schmidt, and George Komis. 2014. "Plasmolysis: Loss of Turgor and Beyond." *Plants* 3(4):583–93.
Laurenzio, Laura Di et al. 1996. "The SCARECROW Gene Regulates an Asymmetric Cell Division That Is Essential for Generating the Radial Organization of the Arabidopsis Root." 86:423–33.
Lee, Jin Suk et al. 2012. "Direct Interaction of Ligand – Receptor Pairs Specifying Stomatal Patterning." *Genes & Development* 7:126–36.
Levesque-Tremblay, Gabriel, Jerome Pelloux, Siobhan A. Braybrook, and Kerstin Müller. 2015. "Tuning of Pectin Methylesterification: Consequences for Cell Wall Biomechanics and Development." *Planta* 242(4):791–811.
Li, J. and J. Chory. 1997. "A Putative Leucine-Rich Repeat Receptor Kinase Involved in Brassinosteroid Signal Transduction." *Cell* 90(5):929–38.
Li, J., P. Nagpal, V. Vitart, T. C. McMorris, and J. Chory. 1996. "A Role for Brassinosteroids in Light-Dependant Development of Arabidopsis." *Science* 272(April):398–401.
Li, J., K. H. Nam, D. Vafeados, and J. Chory. 2001. "BIN2, a New Brassinosteroid-Insensitive Locus in Arabidopsis." *Plant Physiology* 127(1):14–22.
Li, Jia et al. 2002. "BAK1, an Arabidopsis LRR Receptor-like Protein Kinase, Interacts with BRI1 and Modulates Brassinosteroid Signaling." *Cell* 110(2):213–22.
Li, Jianming and Kyoung Hee Nam. 2002. "Regulation of Brassinosteroid Signaling by a GSK3 / SHAGGY-Like Kinase." *Science* 295(2002):1299–1301.
Liebrand, Thomas W. H. et al. 2013. "Receptor-like Kinase SOBIR1/EVR Interacts with Receptor-like Proteins in Plant Immunity against Fungal Infection." *Proceedings of the National Academy of Sciences* 110(32):13228–13228.
Liebrand, Thomas W. H., Harrold A. van den Burg, and Matthieu H. A. J. Joosten. 2014. "Two for All: Receptor-Associated Kinases SOBIR1 and BAK1." *Trends in Plant Science* 19(2):123–32.
Lin, Wenwei, Wenxin Tang, Charles Anderson, and Zhenbiao Yang. 2018. "FERONIA's Sensing of Cell Wall Pectin Activates ROP GTPase Signaling in Arabidopsis." *bioRxiv*.
Liners, F., J. F. Thibault, and P. Van Cutsem. 1992. "Influence of the Degree of Polymerization of Oligogalacturonates and of Esterification Pattern of Pectin on Their Recognition by Monoclonal Antibodies." *Plant Physiology* 99(3):1099–1104.
Liu, Qingquan, Le Luo, and Luqing Zheng. 2018. "Lignins: Biosynthesis and Biological Functions in Plants." *International Journal of Molecular Sciences* 19(2).
Lucas, William J. et al. 2013. "The Plant Vascular System: Evolution, Development and Functions." *Journal of Integrative Plant Biology* 55(4):294–388.
Ma, Xiyu, Guangyuan Xu, Ping He, and Libo Shan. 2016. "SERKing Coreceptors for Receptors." *Trends in Plant Science* 21(12):1017–33.
Mähönen, Ari Pekka et al. 2006. "Cytokinin Signaling and Its Inhibitor AHP6 Regulate Cell Fate during Vascular Development." *Science* 311(5757):94–98.
Mandava. 1988. "Plant Growth-Promoting Brassinosteroids."
Mao, Dandan et al. 2015. "FERONIA Receptor Kinase Interacts with S-Adenosylmethionine Synthetase and Suppresses S-Adenosylmethionine Production and Ethylene Biosynthesis in Arabidopsis." *Plant Cell and Environment* 38(12):2566–74.
Martinière, Alexandre, Philippe Gayral, Chris Hawes, and John Runions. 2011. "Building Bridges: Formin1 of Arabidopsis Forms a Connection between the Cell Wall and the Actin Cytoskeleton." *Plant Journal* 66(2):354–65.
Matsubayashi, Y. 2006. "Disruption and Overexpression of Arabidopsis Phytosulfokine Receptor Gene Affects Cellular Longevity and Potential for Growth." *Plant Physiology* 142(1):45–53.
Matsubayashi, Y. and Y. Sakagami. 1996. "Phytosulfokine, Sulfated Peptides That Induce the Proliferation of Single Mesophyll Cells of Asparagus Officinalis L." *Proceedings of the National Academy of Sciences of the United States of America* 93(15):7623–27.
Matsubayashi, Yoshikatsu. 2011. "Post-Translational Modifications in Secreted Peptide Hormones in Plants." *Plant and Cell Physiology* 52(1):5–13.
Matsubayashi, Yoshikatsu. 2014. "Posttranslationally Modified Small-Peptide Signals in Plants." *Annual*

*Review of Plant Biology* 65(1):385–413.
Matsubayashi, Yoshikatsu, Leiko Takagi, Naomi Omura, Akiko Morita, and Youji Sakagami. 1999. "The Endogenous Sulfated Pentapeptide Phytosulfokine- ␣ Stimulates Tracheary Element Differentiation of Isolated Mesophyll Cells of Zinnia 1." 120(August):1043–48.
Matsuzaki, Yo, Mari Ogawa-Ohnishi, Ayaka Mori, and Yoshikatsu Matsubayashi. 2010a. "Secreted Peptide Signals Required for Maintenance of Root Stem Cell Niche in <em>Arabidopsis</em>" *Science* 329(5995):1065 LP-1067.
Matsuzaki, Yo, Mari Ogawa-Ohnishi, Ayaka Mori, and Yoshikatsu Matsubayashi. 2010b. "Secreted Peptide Signals Required for Maintenance of Root Stem Cell Niche in Arabidopsis." *Science (New York, N.Y.)* 329(5995):1065–67.
McFarlane, Heather E., Anett Döring, and Staffan Persson. 2014. "The Cell Biology of Cellulose Synthesis." *Annual Review of Plant Biology* 65(1):69–94.
Mendel, Melanie. 2017. "The Role of Protein Interactions in RLP44 Function." (December).
Miyazaki, Saori et al. 2009. "ANXUR1 and 2, Sister Genes to FERONIA/SIRENE, Are Male Factors for Coordinated Fertilization." *Current Biology* 19(15):1327–31.
Mosher, Stephen and Birgit Kemmerling. 2013. "PSKR1 and PSY1R-Mediated Regulation of Plant Defense Responses." *Plant Signaling & Behavior* 8(5):e24119.
Motose, H. et al. 2009. "Involvement of Phytosulfokine in the Attenuation of Stress Response during the Transdifferentiation of Zinnia Mesophyll Cells into Tracheary Elements." *Plant Physiology* 150(1):437–47.
Muller, Patrick Y., André R. Miserez, and Zuzana Dobbie. 2002. "Processing of Gene Expression Data Generated by Quantitative Real-Time RT-PCR." *Bioinformatics, Biocomputing* 32(6).
Muller, R., A. Bleckmann, and R. Simon. 2008. "The Receptor Kinase CORYNE of Arabidopsis Transmits the Stem Cell-Limiting Signal CLAVATA3 Independently of CLAVATA1." *The Plant Cell Online* 20(4):934–46.
Murphy, Evan, Stephanie Smith, and Ive De Smet. 2012. "Small Signaling Peptides in Arabidopsis Development: How Cells Communicate Over a Short Distance." *The Plant Cell* 24(8):3198–3217.
Nakamoto, D. 2006. "Inhibition of Brassinosteroid Biosynthesis by Either a dwarf4 Mutation or a Brassinosteroid Biosynthesis Inhibitor Rescues Defects in Tropic Responses of Hypocotyls in the Arabidopsis Mutant Nonphototropic Hypocotyl 4." *Plant Physiology* 141(2):456–64.
Nakayama, Takuya et al. 2017. "A Peptide Hormone Required for Casparian Strip Diffusion Barrier Formation in *Arabidopsis* Roots." *Science* 355(6322):284–86.
Noguchi, Takahiro et al. 1999. "Brassinosteroid-Insensitive Dwarf Mutants of Arabidopsis Accumulate Brassinosteroids." *Plant Physiology* 121(3):743–52.
Oh, Man-Ho et al. 2009. "Tyrosine Phosphorylation of the BRI1 Receptor Kinase Emerges as a Component of Brassinosteroid Signaling in Arabidopsis." *Pnas* 106(2):658–663.
Ohashi-Ito, K. and D. C. Bergmann. 2007. "Regulation of the Arabidopsis Root Vascular Initial Population by LONESOME HIGHWAY." *Development* 134(16):2959–68.
Ohashi-Ito, K., M. Oguchi, M. Kojima, H. Sakakibara, and H. Fukuda. 2013. "Auxin-Associated Initiation of Vascular Cell Differentiation by LONESOME HIGHWAY." *Development* 140(4):765–69.
Ohashi-Ito, Kyoko, Yoshihisa Oda, and Hiroo Fukuda. 2010. "Arabidopsis VASCULAR-RELATED NAC-DOMAIN6 Directly Regulates the Genes That Govern Programmed Cell Death and Secondary Wall Formation during Xylem Differentiation." *The Plant Cell* 22(10):3461–73.
Pauly, Markus, Peter Albersheim, Alan Darvill, and William S. York. 1999. "Molecular Domains of the Cellulose / Xyloglucan Network in the Cell Walls of Higher Plants." 20.
Peaucelle, Alexis et al. 2008. "Arabidopsis Phyllotaxis Is Controlled by the Methyl-Esterification Status of Cell-Wall Pectins." *Current Biology* 18:1943–48.
Peaucelle, Alexis et al. 2011. "Pectin-Induced Changes in Cell Wall Mechanics Underlie Organ Initiation in Arabidopsis." *Current Biology* 21:1720–26.
Pelletier, Sandra et al. 2010. "A Role for Pectin de-Methylesterification in a Developmentally Regulated Growth Acceleration in Dark-Grown Arabidopsis Hypocotyls." *New Phytologist* 188(3):726–39.
Pelloux, Jérôme, Christine Rustérucci, and Ewa J. Mellerowicz. 2007. "New Insights into Pectin Methylesterase Structure and Function." *Trends in Plant Science* 12(6):267–77.
Penel, Claude and Hubert Greppin. 1994. "Binding of Plant Isoperoxidases to Pectin in the Presence of Calcium." *FEBS Letters* 343(1):51–55.

Qi, Jiyan et al. 2017. “Mechanical Regulation of Organ Asymmetry in Leaves.” *Nature Plants* 3(9):724–33.
Ridley, Brent L., Malcolm A. O’Neill, and Debra Mohnen. 2001. *Pectins: Structure, Biosynthesis, and Oligogalacturonide-Related Signaling*. Vol. 57.
Rodicio, Rosaura and Jürgen J. Heinisch. 2010. “Together We Are Strong—cell Wall Integrity Sensors in Yeasts.” *Yeast (Chichester, England)* 26(10):545–51.
De Rybel, Bert et al. 2013. “A bHLH Complex Controls Embryonic Vascular Tissue Establishment and Indeterminate Growth in Arabidopsis.” *Developmental Cell* 24(4):426–37.
Rybel, Bert De et al. 2009. “Chemical Inhibition of a Subset of Arabidopsis Thaliana GSK3-like Kinases Activates Brassinosteroid Signaling.” 594–604.
De Rybel, Bert, Ari Pekka Mähönen, Yrjö Helariutta, and Dolf Weijers. 2015. “Plant Vascular Development: From Early Specification to Differentiation.” *Nature Reviews Molecular Cell Biology*.
Santiago, Julia et al. 2016. “Mechanistic Insight into a Peptide Hormone Signaling Complex Mediating Floral Organ Abscission.” *eLife* 5(April 2016):1–19.
Santiago, Julia, Christine Henzler, and Michael Hothorn. 2013. “Molevular Mechanism for Plant Steroid Receptor Activation by Somatic Embryogenesis Co-Receptor Kinases.” 889(2013).
Sattelmacher, B. 2001. “The Apoplast and Its Significance for Plant Mineral Nutrition.” *New Phytologist* 149(2):167–92.
Sauter, Margret. 2015. “Phytosulfokine Peptide Signalling.” 66(17):5161–69.
Scavetta, R. D. et al. 1999. “Structure of a Plant Cell Wall Fragment Complexed to Pectate Lyase C.” *The Plant Cell* 11(6):1081–92.
Scheller, Henrik Vibe and Peter Ulvskov. 2010. “Hemicelluloses.”
Scheres, Ben et al. 1994. “Embryonic Origin of the Arabidopsis Primary Root and Root Meristem Initials.” *Development* 2487:2475–87.
Schlereth, Alexandra et al. 2010. “MONOPTEROS Controls Embryonic Root Initiation by Regulating a Mobile Transcription Factor.” *Nature* 464(7290):913–16.
Schuetz, Mathias, Rebecca Smith, and Brian Ellis. 2012. “Xylem Tissue Specification, Patterning, and Differentiation Methylation and Chromatin Patterning Mechanisms.” *Journal of Experimental Botany* 64(2):695–709.
Shen, Yunping and Andrew C. Diener. 2013. “Arabidopsis Thaliana RESISTANCE TO FUSARIUM OXYSPORUM 2 Implicates Tyrosine-Sulfated Peptide Signaling in Susceptibility and Resistance to Root Infection.” *PLoS Genetics* 9(5).
Shinohara, Hidefumi, Mari Ogawa, Youji Sakagami, and Yoshikatsu Matsubayashi. 2007. “Identification of Ligand Binding Site of Phytosulfokine Receptor by on-Column Photoaffinity Labeling.” *Journal of Biological Chemistry* 282(1):124–31.
Shiu, S. H. and A. B. Bleecker. 2001. “Receptor-like Kinases from Arabidopsis Form a Monophyletic Gene Family Related to Animal Receptor Kinases.” *Proceedings of the National Academy of Sciences* 98(19):10763–68.
Smakowska-luzan, Elwira et al. 2018. “An Extracellular Network of Arabidopsis Leucine-Rich Repeat Receptor Kinases.” *Nature Publishing Group* 1–22.
De Smet, Stefanie, Ann Cuypers, Jaco Vangronsveld, and Tony Remans. 2015. “Gene Networks Involved in Hormonal Control of Root Development in Arabidopsis Thaliana: A Framework for Studying Its Disturbance by Metal Stress.” *International Journal of Molecular Sciences* 16(8):19195–224.
Somerville, Chris. 2006. “Cellulose Synthesis in Higher Plants.” *Annual Review of Cell and Developmental Biology* 22(1):53–78.
Song, Wen, Zhifu Han, Jizong Wang, Guangzhong Lin, and Jijie Chai. 2017. “Structural Insights into Ligand Recognition and Activation of Plant Receptor Kinases.” *Current Opinion in Structural Biology* 43:18–27.
Spadoni, S. et al. 2006. “Polygalacturonase-Inhibiting Protein Interacts with Pectin through a Binding Site Formed by Four Clustered Residues of Arginine and Lysine.” *Plant Physiology* 141(2):557–64.
Sreeramulu, Shivakumar et al. 2013. “BSKs Are Partially Redundant Positive Regulators of Brassinosteroid Signaling in Arabidopsis.” *Plant Journal* 74(6):905–19.
Srivastava, Renu, Jian Xiang Liu, and Stephen H. Howell. 2008. “Proteolytic Processing of a Precursor Protein for a Growth-Promoting Peptide by a Subtilisin Serine Protease in Arabidopsis.” *Plant Journal* 56(2):219–27.
Stewart Gillmor, C., Patricia Poindexter, Justin Lorieau, Monica M. Palcic, and Chris Somerville. 2002. “α-

Glucosidase I Is Required for Cellulose Biosynthesis and Morphogenesis in Arabidopsis." *Journal of Cell Biology* 156(6):1003–13.

Stührwohldt, Nils, Renate I. Dahlke, Bianka Steffens, Amanda Johnson, and Margret Sauter. 2011. "Phytosulfokine-α Controls Hypocotyl Length and Cell Expansion in Arabidopsis Thaliana through Phytosulfokine Receptor 1." *PLoS ONE* 6(6).

Sun, Yadong et al. 2013. "Structure Reveals That BAK1 as a Co-Receptor Recognizes the BRI1-Bound Brassinolide." *Cell Research* 23(11):1326–29.

Sun, Yu et al. 2010. "Integration of Brassinosteroid Signal Transduction with the Transcription Network for Plant Growth Regulation in Arabidopsis." *Dev Cell* 19(5):765–77.

Szekeres, Miklós et al. 1996. "Brassinosteroids Rescue the Deficiency of CYP90, a Cytochrome P450, Controlling Cell Elongation and de-Etiolation in Arabidopsis." *Cell* 85(2):171–82.

Takeda, T. et al. 2002. "Suppression and Acceleration of Cell Elongation by Integration of Xyloglucans in Pea Stem Segments." *Proceedings of the National Academy of Sciences* 99(13):9055–60.

Tavormina, Patrizia, Barbara De Coninck, Natalia Nikonorova, Ive De Smet, and Bruno P. A. Cammue. 2015. "The Plant Peptidome: An Expanding Repertoire of Structural Features and Biological Functions." *The Plant Cell* 27(8):2095–2118.

Thomas, Schallus et al. 2010. "Malectin: A Novel Carbohydrate-Binding Protein of the Endoplasmic Reticulum and a Candidate Player in the Early Steps of Protein N-Glycosylation." *Seikagaku* 82(4):327–31.

Turner, Simon, Patrick Gallois, and David Brown. 2007. "Tracheary Element Differentiation." *Plant Biotechnology Reports* 8(1):58-407–33.

Ursache, Robertas, Shunsuke Miyashima, Qingguo Chen, Anne Vatén, and Keiji Nakajima. 2014. "Tryptophan-Dependent Auxin Biosynthesis Is Required for HD-ZIP III-Mediated Xylem Patterning." 1250–59.

Verbelen, Jean-Pierre, Tienne De Cnodder, Jie Le, Kris Vissenberg, and František Baluška. 2006. "The Root Apex of Arabidopsis Thaliana Consists of Four Distinct Zones of Growth Activities." 1(6):296–304.

Vert, Grégory and Joanne Chory. 2006. "Downstream Nuclear Events in Brassinosteroid Signalling." *Nature* 441(7089):96–100.

Vragović, Kristina et al. 2015. "Translatome Analyses Capture of Opposing Tissue-Specific Brassinosteroid Signals Orchestrating Root Meristem Differentiation." *Proceedings of the National Academy of Sciences of the United States of America* 112(3):923–28.

Wagner, T. A. 2001. "Wall-Associated Kinases Are Expressed throughout Plant Development and Are Required for Cell Expansion." *The Plant Cell Online* 13(2):303–18.

Wakabayashi, Kazuyuki, Takayuki Hoson, and Donald J. Huber. 2003. "Methyl de-Esterification as a Major Factor Regulating the Extent of Pectin Depolymerization during Fruit Ripening: A Comparison of the Action of Avocado (Persea Americana) and Tomato (Lycopersicon Esculentum) Polygalacturonases." *Journal of Plant Physiology* 160(6):667–73.

Wang, G. et al. 2008. "A Genome-Wide Functional Investigation into the Roles of Receptor-Like Proteins in Arabidopsis." *Plant Physiology* 147(2):503–17.

Wang, Jizong et al. 2015. "Allosteric Receptor Activation by the Plant Peptide Hormone Phytosulfokine." *Nature* 525(7568):265–68.

Wang, Xuelu and Joanne Chory. 2006. "Brassinoteroids Regulate Dissociation of BKI1, a Negative Regulator of BRI1 Signaling, from the Plasma Membrane." *Science* 313(5790):1118–22.

Wang, Z. Y., H. Seto, S. Fujioka, S. Yoshida, and J. Chory. 2001. "BRI1 Is a Critical Component of a Plasma-Membrane Receptor for Plant Steroids." *Nature* 410(6826):380–83.

Wang, Zhi Xin et al. 2014. "Structural Insights into the Negative Regulation of BRI1 Signaling by BRI1-Interacting Protein BKI1." *Cell Research* 24(11):1328–41.

Wang, Zhi Yong et al. 2002. "Nuclear-Localized BZR1 Mediates Brassinosteroid-Induced Growth and Feedback Suppression of Brassinosteroid Biosynthesis." *Developmental Cell* 2(4):505–13.

Wenqiang Tang. 2008. "BSKs Mediate Signal Tranduction from the Receptor Kinase BRI1 in Arabidopsis." *Science* 2(July):557–61.

Wolf, Sebastian et al. 2014. "A Receptor-like Protein Mediates the Response to Pectin Modification by Activating Brassinosteroid Signaling." *Proceedings of the National Academy of Sciences* 111(42):15261–66.

Wolf, Sebastian and Steffen Greiner. 2012. "Growth Control by Cell Wall Pectins." *Protoplasma*

249(SUPPL.2):169–75.
Wolf, Sebastian, Kian Hématy, and Herman Höfte. 2012. “Growth Control and Cell Wall Signaling in Plants.” *Annual Review of Plant Biology* 63(December 2011):381–407.
Wolf, Sebastian, Grégory Mouille, and Jérome Pelloux. 2009. “Homogalacturonan Methyl-Esterification and Plant Development.” *Molecular Plant* 2(5):851–60.
Wolf, Sebastian, Jozef Mravec, Steffen Greiner, Grégory Mouille, and Herman Höfte. 2012. “Plant Cell Wall Homeostasis Is Mediated by Brassinosteroid Feedback Signaling.” *Current Biology* 22:1732–37.
Xiao, Chaowen and Charles T. Anderson. 2013. “Roles of Pectin in Biomass Yield and Processing for Biofuels.” *Frontiers in Plant Science* 4(March):1–7.
Yamaguchi, Masatoshi et al. 2011. “VASCULAR-RELATED NAC-DOMAIN 7 Directly Regulates the Expression of a Broad Range of Genes for Xylem Vessel Formation.” *Plant Journal* 66(4):579–90.
Yamamoto, R. et al. 2001. “Brassinosteroid Levels Increase Drastically prior to Morphogenesis of Tracheary Elements.” *Plant Physiology* 125(2):556–63.
Yamamoto, R., T. Demura, and H. Fukuda. 1997. “Brassinosteroids Induce Entry into the Final Stage of Tracheary Element Differentiation in Cultured Zinnia Cells.” *Plant & Cell Physiology* 38(8):980–83.
Yin, Yanhai et al. 2002. “BES1 Accumulates in the Nucleus in Response to Brassinosteroids to Regulate Gene Expression and Promote Stem Elongation.” *Cell* 109(2):181–91.
Yokota, Takao. 1997. “The Structure, Biosynthesis and Function of Brassinosteroids.” *Trends in Plant Science* 2(4):137–43.
Zamil, M. S. and A. Geitmann. 2017. “The Middle Lamella - More than a Glue.” *Physical Biology* 14(1).
Zhang, Heqiao, Xiaoya Lin, et al. 2016. “SERK Family Receptor-Like Kinases Function as a Co-Receptor with PXY for Plant Vascular Development.” *Molecular Plant*.
Zhang, Heqiao, Zhifu Han, Wen Song, and Jijie Chai. 2016. “Structural Insight into Recognition of Plant Peptide Hormones by Receptors.” *Molecular Plant* 9(11):1454–63.
Zhang, W. et al. 2013. “Arabidopsis RECEPTOR-LIKE PROTEIN30 and Receptor-Like Kinase SUPPRESSOR OF BIR1-1/EVERSHED Mediate Innate Immunity to Necrotrophic Fungi.” *The Plant Cell* 25(10):4227–41.
Zheng, H. 2005. “A Rab-E GTPase Mutant Acts Downstream of the Rab-D Subclass in Biosynthetic Membrane Traffic to the Plasma Membrane in Tobacco Leaf Epidermis.” *The Plant Cell Online* 17(7):2020–36.
Zhou, Jing, Xu Wang, Jung-youn Lee, and Ji-young Lee. 2013. “Cell-to-Cell Movement of Two Interacting AT-Hook Factors in Arabidopsis Root Vascular Tissue Patterning.” 25(January):187–201.
Zipfel, Cyril et al. 2006. “Perception of the Bacterial PAMP EF-Tu by the Receptor EFR Restricts Agrobacterium-Mediated Transformation.” *Cell* 125(4):749–60.

# List of abbreviations

| | |
|---|---|
| AA | *amino acid* |
| AHL | *AT HOOK MOTIF NUCLEAR LOCALIZED* |
| AHP6 | *ARABIDOPSIS HISTIDINE PHOSPHOTRANSFER PROTEIN 6* |
| BAK1 | *BRI-ASSOCIATED KINASE 1* |
| BES1 | *BRI1 EMS SUPPRESSOR 1* |
| *bes-1D* | *BRI1 EMS SUPPRESSOR dominant* |
| BIN2 | *BRI1 INSENSITIVE 2* |
| *bin2-1* | *BRASSINOSTEROID-INSENSITIVE2-1* |
| BKI1 | *BRI1 KINASE INHIBITOR 1* |
| BL | *Brassinolide* |
| BR | *Brassinostreroid* |
| BRI1 | *BR INSENSITIVE 1* |
| BRL | *BRI1 LIKE* |
| BSKs | *BRI1 SUBSTRATE KINASES* |
| BSU1 | *BRI1 SUPPRESSOR* |
| BZR1 | *BRASSINAZOLE RESISTENT 1* |
| CD | *cytosolic domain* |
| CDG1 | *CONSTITUTIVE DIFFERENTIAL GROWTH1* |
| CDL | *CDG-LIKE* |
| CESA | *cellulose synthase* |
| CIF | *casparian strip formation integrity factor* |
| *cnu2* | *comfortably numb 2* |
| Co-IP | *Co-immunoprecipitation* |
| Col-0 | *Columbia-0* |
| *cpd* | *constitutive photomorphogenic dwarf* |
| CRN | *CORYNE* |
| CSC | *CESA complexes* |
| CW | *cell wall* |
| dag | *days after germination* |

| | |
|---|---|
| DET2 | *de-etiolated 2* |
| DM | *degree of demethylesterification* |
| ECD | *extracellular domain* |
| EDTA | *ethylenediaminetetraacetic acid* |
| EMS | *ethyl methanesulfonate* |
| ERF115 | *ETHYLEN RESPONSE FACTOR 115* |
| FER | *FERONIA* |
| FM4-64 | *(N-(3-triethylammoniumpropyl)-4-(6-(4-(diethylamino)* |
| gDNA | genomic DNA |
| GSK3 | *glycogen synthase kinase 3* |
| HG | *homogalacturonan* |
| ID | *island domain* |
| LB | *Luria – Bertani* |
| LHW | *LONESOME HIGHWAY* |
| LOG4 | *LONELY GUY 4* |
| LRRs | *leucine rich repeat regions* |
| Lti6B | *Low temperature induced protein 6B* |
| MS | *Murashige & Skroog* |
| *N. benthamiana* | *Nicotiana benthamiana* |
| PCR | *polymerase chain reaction* |
| PGA | *polygalacturonic acid* |
| PGIP | *polygalacturonase-inhibiting protein* |
| PM | *plasma membrane* |
| PME | *PECTIN METHYLESTERASE* |
| PMEIox | *PECTIN METHYLESTERASE INHIBITOR 5 OVEREXPRESSING* |
| PPZ | *propiconazol* |

| | |
|---|---|
| PSK | *PHYTOSULFPOKINE* |
| PSKR | *PSK RECEPTOR* |
| RALF | *RAPID ALKALINIZATION FACTOR* |
| RAM | *root apical meristem* |
| RGF | *root growth factor* |
| RLCK | *receptor like cytoplasmic kinase* |
| RLK | *receptor-like kinases* |
| RLP44 | *RECEPTOR-LIKE PROTEIN44* |
| *S. cerevisiae* | *Saccharomyces cerevisiae* |
| SAM | *shoot apical meristem* |
| SCW | *secondary cell wall* |
| SDS | *sodium dodecyl sulfate* |
| secRFP | *secreted red-fluorescent protein* |
| SERK | *SOMATIC EMBRYOGENESIS RECEPTOR KINASE* |
| SERK1 | *SOMATIC EMBRYOGENESIS RECEPTOR-LIKE KINASE 1* |
| SHR | *SHORTROOT* |
| TFs | *transcription factors* |
| THE1 | *THESEUS1* |
| TMD | *transmembrane domain* |
| TMO | *TAGET OF MONOPTEROS* |
| TPST | *tyrosylprotein sulfotransferase* |
| VND | *VASCULAR RELATED NAC DOMAIN* |
| WAKs | *wall associated kinases* |

# 6 Appendix

## Sample list Agata 1.0

**# Sample**

1 Mannan (ivory nut)
2 Galactomannan (carob)
3 Glucomannan (konjac)
4 Xylan (beechwood)
5 Xylan (Aspen)
6 Arabinoxylan (wheat)
7 Xyloglucan Tamarind seed
8 MLG Lichenan, β-glucan (1→3),(1→4)-β-D-glucan
9 β-glucan (Yeast), (1→6),(1→3)-β-D-glucan
10 β-glucan (oat), (1→3),(1→4)-β-D-glucan
11 β-glucan (Barley flour), (1→3),(1→4)-β-D-glucan
12 β-1,3-glucan (Euglena gracilis) (β-1→3-Glucan)
13 Pachyman
14 Pullulan
15 Laminarin
16 Carboxymethyl Cellulose
17 Ethyl cellulose
18 2-hydroxyethyl cellulose
19 Methyl cellulose
20 Carboxymethyl Cellulose 4M
21 Arabinogalactan, type II (AGP)
22 Locust bean gum, Galactomannan rich gum
23 Locust bean gum from Ceratonia siliqua seeds
24 Locust bean gum, Galactomannan rich gum
25 Gum Guar, Galactomannan rich gum
26 Gum guaic (tree resin)
27 Karaya gum
28 Tragacanth gum
29 Ghatti gum
30 Xanthan Rhodigel, 80
31 Gum arabic, Glycoproteins
32 Lime pectin DE: 81% (E81)
33 Lime pectin DE: 15% (B15)
34 Lime pectin DE: 15% (B34)
35 Lime pectin DE: 43% (B43)
36 Lime pectin DE: 64% (B64)
37 Lime pectin DE: 71% (B71)
38 Lime pectin DE: 11% (F11)
39 Lime pectin DE: 31% (F43)
40 Lime pectin DE: 76% (F76)
41 Lime pectin DE: 16% (P16)
42 Lime pectin DE: 46% (P53)
43 Lime pectin DE: 76% (P76)
44 Pectin with DE 1% & DA 0%, basic hydrolysis of SBP6230
45 Pectin with DE 9% & DA 15%, basic hydrolysis of SBP6230
46 Pectin with DE 25% & DA 16%, basic hydrolysis of SBP6230
47 Pectin with DE 31% & DA 24%, basic hydrolysis of SBP6230
48 Pectin with DE 46% & DA 26%, basic hydrolysis of SBP6230
49 Pectin with DE 53% & DA 26%, basic hydrolysis of SBP6230
50 Sugar beet Pectin
51 Linear Arabinan
52 Pectic galactan, (1-->4)-β-D-galactose polymer
53 RGI (soy bean)
54 RGI (potato)
55 RGI (citrus)
56 Polygalacturonic acid from citrus pectin (Danisco)
57 Lemon pectin
58 Apple pectin
59 Pectin (CP Kelco)
60 Esterified citrus pectin (Sigma)
61 Polygalacturonic acid from citrus pectin (Megazymes)
62 Galactan, potato
63 RGI potato de-galactanated saponified
64 RGI apple native saponified
65 RGI apple de-arabinanase saponified
66 RGI potato de-galactanated+arabinanased saponified
67 RGI potato de-arabinanase saponified
68 Modified hairy regions from apple RGI
69 Arabinan-depleted RG-I from sugar-beet
70 Modified hairy regions from sugar-beet RGI
71 Pectin, Base/PME, short deesterified blocks, DM 49
72 Pectin, Base/PME, short deesterified blocks, DM 56
73 Pectin, Base/PME, short deesterified blocks, DM 63
74 Pectin, Base, random deesterified blocks, DM 20
75 Pectin, Base, random deesterified blocks, DM 40
76 Pectin, Base, random deesterified blocks, DM 69
77 Pectin, Base, random deesterified blocks, DM 82
78 Pectin, Base, random deesterified blocks, DM 96
79 Pectin, Plant PME, big deesterified blocks, DM 14
80 Pectin, Plant PME, big deesterified blocks, DM 36
81 Pectin, Plant PME, big deesterified blocks, DM 75
82 Feruloylated pectin
83 Amylose (potato)
84 Amylopectin (potato)

**AGATA 1.0 Layout**

| 1 | 2 | 3 | 4 | 5 | 6 | 7 | 8 | 9 | 10 | 11 | 12 | |
|---|---|---|---|---|---|---|---|---|---|---|---|---|
| Ink | B | B | B | B | B | B | B | B | B | B | Ink | 1 |
| Ink | B | B | B | B | B | B | B | B | B | B | Ink | 2 |
| Ink | B | B | B | B | B | B | B | B | B | B | Ink | 3 |
| Ink | Ink | Ink | Ink | Ink | Ink | Ink | Ink | Ink | Ink | Ink | Ink | 4 |
| 1a | 2a | 3a | 4a | 5a | 6a | 7a | 8a | 9a | 10a | 11a | 12a | 5 |
| 1b | 2b | 3b | 4b | 5b | 6b | 7b | 8b | 9b | 10b | 11b | 12b | 6 |
| 1c | 2c | 3c | 4c | 5c | 6c | 7c | 8c | 9c | 10c | 11c | 12c | 7 |
| 1d | 2d | 3d | 4d | 5d | 6d | 7d | 8d | 9d | 10d | 11d | 12d | 8 |
| 13a | 14a | 15a | 16a | 17a | 18a | 19a | 20a | 21a | 22a | 23a | 24a | 9 |
| 13b | 14b | 15b | 16b | 17b | 18b | 19b | 20b | 21b | 22b | 23b | 24b | 10 |
| 13c | 14c | 15c | 16c | 17c | 18c | 19c | 20c | 21c | 22c | 23c | 24c | 11 |
| 13d | 14d | 15d | 16d | 17d | 18d | 19d | 20d | 21d | 22d | 23d | 24d | 12 |
| 25a | 26a | 27a | 28a | 29a | 30a | 31a | 32a | 33a | 34a | 35a | 36a | 13 |
| 25b | 26b | 27b | 28b | 29b | 30b | 31b | 32b | 33b | 34b | 35b | 36b | 14 |
| 25c | 26c | 27c | 28c | 29c | 30c | 31c | 32c | 33c | 34c | 35c | 36c | 15 |
| 25d | 26d | 27d | 28d | 29d | 30d | 31d | 32d | 33d | 34d | 35d | 36d | 16 |
| 37a | 38a | 39a | 40a | 41a | 42a | 43a | 44a | 45a | 46a | 47a | 48a | 17 |
| 37b | 38b | 39b | 40b | 41b | 42b | 43b | 44b | 45b | 46b | 47b | 48b | 18 |
| 37c | 38c | 39c | 40c | 41c | 42c | 43c | 44c | 45c | 46c | 47c | 48c | 19 |
| 37d | 38d | 39d | 40d | 41d | 42d | 43d | 44d | 45d | 46d | 47d | 48d | 20 |
| 49a | 50a | 51a | 52a | 53a | 54a | 55a | 56a | 57a | 58a | 59a | 60a | 21 |
| 49b | 50b | 51b | 52b | 53b | 54b | 55b | 56b | 57b | 58b | 59b | 60b | 22 |
| 49c | 50c | 51c | 52c | 53c | 54c | 55c | 56c | 57c | 58c | 59c | 60c | 23 |
| 49d | 50d | 51d | 52d | 53d | 54d | 55d | 56d | 57d | 58d | 59d | 60d | 24 |
| 61a | 62a | 63a | 64a | 65a | 66a | 67a | 68a | 69a | 70a | 71a | 72a | 25 |
| 61b | 62b | 63b | 64b | 65b | 66b | 67b | 68b | 69b | 70b | 71b | 72b | 26 |
| 61c | 62c | 63c | 64c | 65c | 66c | 67c | 68c | 69c | 70c | 71c | 72c | 27 |
| 61d | 62d | 63d | 64d | 65d | 66d | 67d | 68d | 69d | 70d | 71d | 72d | 28 |
| 73a | 74a | 75a | 76a | 77a | 78a | 79a | 80a | 81a | 82a | 83a | 84a | 29 |
| 73b | 74b | 75b | 76b | 77b | 78b | 79b | 80b | 81b | 82b | 83b | 84b | 30 |
| 73c | 74c | 75c | 76c | 77c | 78c | 79c | 80c | 81c | 82c | 83c | 84c | 31 |
| 73d | 74d | 75d | 76d | 77d | 78d | 79d | 80d | 81d | 82d | 83d | 84d | 32 |
| Ink | Ink | Ink | Ink | B | B | B | B | Ink | Ink | Ink | Ink | 33 |

**Dilutions of sample**

a: 1mg/mL

b: 0,2 mg/mL

c: 0,04 mg/mL

d: 0,008mg/mL

**Abbreviations**

B = buffer

**Notes**

Sample #7 (Xyloglucan Tamarind seed) has in dilution a had some spill over in dilution a of sample #4-6 and #8-10. When this is seen, the results around sample #7 will look like below:

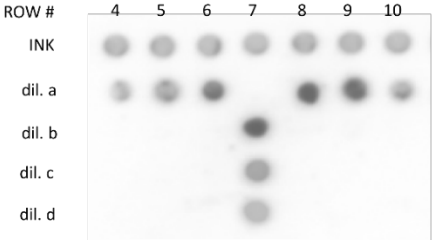


**Figure 40. AGATA 1.0 Layout.** Plan depicts the arrangement of the spotted oligosaccharides listed in the sample list AGATA 1.0

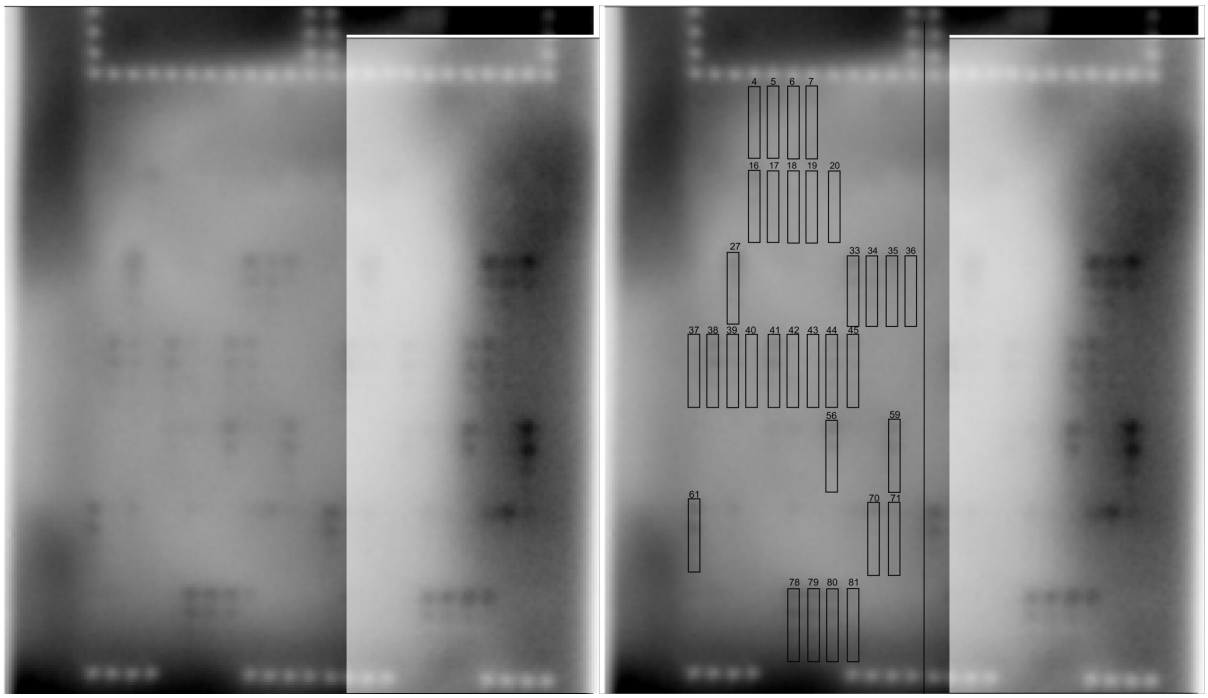


**Figure 41. AGAT1.0 Glycan array raw data after probing with RLP44ECD-StrepII–tagged recombinant protein.** The left and right glycan array are showing the very same experiment - in the right glycan array the quantified spots are marked with a black box and labelled with the corresponding number according to the AGAT1 sample list.

# 7 Acknowledgements

First of all I would like to thank my supervisor Dr. Sebastian Wolf. Thanks Sebo that you hired me as a technician and gave me the opportunity to keep my project and do my PhD. Without you and the cnus I would definitely not be here.

Thank you to my PhD committee members, to Prof. Dr. Karin Schumacher, special thanks goes to Prof. Dr. Julia Santiago Cuellar for coming the long way from Lausanne, and also thanks to Jun.-Prof. Dr. Steffen Lemke. I could not keep all my TAC members for the PhD defense, but I am thankful for the guidance within the last years and discussions in my TACs, thank you to Prof. Dr .Jan Lohmann and Prof. Dr. Thomas Greb.

I was really looking forward to write this part of the thesis and now I am sitting here and besides the PIs I don't really know how to start. Five years past by and I got to know amazing people, who don't only changed my point of view concerning science, they also changed me. Thank you for the awesome time!

To the entire AG Wolf: thanks for being the best colleagues I could have imagined. I really enjoyed working with you and I consider you more than colleagues! We were able to make the best out of a working day, even if it was working on the weekends or on a public holiday! Borja, I guess, finally we are close! I will miss your happiness, motivation, constructive discussions, and your drama!!! You were always there, scientifically and even more important personally I really appreciate your friendship! Thank you so much! Zhenni, tomato, I am happy that our friendship developed in the last years. Balcony beers, or in between working beers we can do it! Anka, it was always fun working with you, to go to sports, organize events and I am happy to be around a bit longer! And of course Hannah, especially the writing would have been super sad without you! Also thanks to all the students, I supervised during all those years. It was a nice experience and I also learned a lot! Thanks to the whole 2nd floor for this nice working environment, and special thanks to Ines for controlling everything!

Jana and Denis, thanks so much for the friendship behind the science! Endless coffee breaks, discussions about everything was always a pleasure with you! Thanks for keep reminding me for the storyline! I tend to get lost!

Görkem, Upendo, Zaida, Rachel thanks for being around in the lab and without you, the breaks would have been boring and less cookie intense! Special thanks to the running girls, for the nice runs we did and keeping us motivated to go to the military guy!
Running and complaining fits totally and helped me a lot – thanks Falco for sharing this moments! And of course Raina for always being ready to celebrate!
Also Maizel people, Andrea, Paola, Amaya, Zhauxue, Michi, and Lotte: Thanks for being around and always part of each event! People left, and everything will change – but I am super happy, that I was here at the right time!
Nina, Vadir und Theresa – thanks for the breaks, the discussions in the plant room and also the nice time at beer hours or at movings. ;)
Not forget about INF360 and AG Rausch where everything started! Thank you everyone there ☺ I also made new friend there – Sanja – thank you for being the most honest person I know. I miss our lunch breaks! Thanks to Heike for teaching me most of the techniques and being always there for questions. Thanks to Katja, without you this thesis would not be the same – I really owe you something! Tanja for always having an open ear and Angelika for helping with everything. And thanks to Philippe for always trying to keep me away from work :p , skating was always fun!
I also want to say thank Frederik, for calming me down and reminding me that I will finish this. Thank you so much for proof-reading this thesis!
Meine Mädels! Alle – Nadine M., Nadine E., Tabea, Miri, Caro und Maria danke für eure jahrelange Freundschaft – ihr habt immer so viel Verständnis für alles aufgebracht und mich unterstützt und motiviert. Ohne euch wäre ich schon oft untergegangen.
Danke an meine Familie, einfach an alle – auch wenn ihr oft nicht nachvollziehen konntet warum ich das eigentlich mache (glaubt mir – ich konnte es auch oft nicht!!). Ihr habt jede Entscheidung akzeptiert und noch mehr, ihr habt mich immer unterstützt. Mama und Papa, einfach Danke für alles! Auch an meine Brüder, Eugen und Arthur, ihr musstet mir schon immer helfen, sei es mich irgendwo abholen oder mir Physik erklären – danke – aber bald bitte nur noch Frau Dr. Holzwart! ☺ Jeannine, Ella und Ilvy – euch gehört auch gedankt! Ich bin froh, dass ich euch hab! <3